2011-03-24

Dissecting Signaling Pathways that Regulate Axonal Guidance Effects of Sonic Hedgehog: A Dissertation

Daorong Guo
University of Massachusetts Medical School

A Dissertation Presented

By

DAORONG GUO

Submitted to the Faculty of the

University of Massachusetts Graduate School of Biomedical Sciences, Worcester

in partial fulfillment of the requirements for the degree of

DOCTOR OF PHILOSOPHY

(March 24th, 2011)

INTERDISCIPLINARY GRADUATE PROGRAM

DISSECTING SIGNALING PATHWAYS THAT REGULATE AXONAL GUIDANCE EFFECTS OF SONIC HEDGEHOG

A Dissertation Presented By

Daorong Guo

The signatures of the Dissertation Defense Committee signifies completion and approval as to style and content of the Dissertation

Zheng-Zheng Bao, P.D., Thesis Advisor

Ingolf Bach, Ph.D., Member of Committee

Alonzo Ross, Ph.D., Member of Committee

Elizabeth Ryder, Ph.D., Member of Committee

Charles Sagerström, Ph.D., Member of Committee

The signature of the Chair of the Committee signifies that the written dissertation meets the requirements of the Dissertation Committee

Stephen Doxsey, Ph.D. Chair of Committee

The signature of the Dean of the Graduate School of Biomedical Sciences signifies that the student has met all graduation requirements of the School

Anthony Carruthers, Ph.D.
Dean of the Graduate School of Biomedical Sciences

Interdisciplinary Graduate Program

March 24, 2011

Copyright Notice

Acknowledgements

I am heartily thankful to my mentor, Dr. Zheng-zheng Bao, whose invaluable encouragement, guidance and support enabled me to finish my degree. I am grateful for the opportunity to begin, extend and finish my science project in her lab. This thesis would not have been possible unless close cooperation between she and me.

I would like to extend my gratitude to my advisory committee for consistently keeping me on track. I would like to thank Dr. Stephen Doxey for serving as committee chair. I would also like to thank Dr. Charles Sagerstrom, Dr. Alonzo Ross and Dr. Ingolf Bach for their advice and support during these years. I would like to thank Dr. Elizabeth Ryder for serving as my external committee member and for taking the time to read through my thesis.

It is a great pleasure to thank my lab members Mary Chau, Adrianne Kolpak, Jun Jiang and Dong Han for their friendship, scientific assistance and moral support. I would like to thank Adrianne Kolpak for establishing the system. I am indebted to Dong Han whose abundant knowledge helps me finish the project at the later stage.

I am especially grateful to my parents Changhe Li, Baixiang Guo and elder brother Daoqiang Guo for providing a loving environment for me. Their visits made my life abroad much easier. Lastly, I would like to express my deepest gratitude to my wife, Yuan-yuan Ma. She has always been my sun-shine, my joy and my destination.

Abstract

During development, axons respond to a variety of guidance cues in the environment to navigate to the proper targets. Sonic hedgehog (Shh), a classical morphogen, has been shown to function as a guidance factor that directly acts on the growth cones of various types of axons. We previously found that Shh affects retinal ganglion cell (RGC) axonal growth and navigation in a concentration-dependent manner. However, the signaling pathways that mediate such events are still unclear.

In this thesis, we show that high concentrations of Shh induce growth cone collapse and repulsive turning of the chick RGC through rapid increase of Ca^{2+} in the growth cone, and specific activation of PKCα and Rho signaling pathways. We further found that integrin linked kinase (ILK) acts as an immediate downstream effector of PKCα. PKCα directly phosphorylates ILK in vitro at two previously unidentified sites threonine-173 and -181. Inhibition of PKCα, Rho, and ILK by pharmacological inhibitors and/or dominant-negative approaches abolished the negative effects of high-concentration of Shh. We provide evidence that Rho likely functions downstream of PKC and suggest that PKC, Rho and ILK may cooperatively mediate the negative effects of high concentrations of Shh. Furthermore, retroviral expression of dominant-negative constructs of PKCα (DN-PKCα) and ILK-double mutants (ILK-DM) resulted in misguidance of RGC axons at the optic chiasm in vivo. These results demonstrate that new signaling pathways composed of PKCα, Rho, and ILK play an important role in Shh-induced axonal chemorepulsion.

In contrast, we show that attractive axonal turning in response to low concentrations of Shh is independent of PKCα, but requires the activity of cyclic nucleotides cAMP. Taken together, our results suggest that the opposing effects of Shh on axon guidance are mediated by different signaling pathways.

Table of Contents

List of Figures

List of Abbreviations

BDNF	b ain-derived neurotrop ic factor
BMP	bone morphogenetic proteins
Boc	Bi-directional Cdon-binding protein
cAMP	cyclic Adenosine Monophosphate
Cdo	cell adhension molecule-related/downregulated by oncogenes
cGMP	cyclic guanosine monophosphate (cGMP)
CSPG	chonfroitin sulfate proteoglycan
DAG	diacylglycerols
DCC	Deleted in Colorectal Cancer
Dhh	Desert hedgehog
DN-PKCα	Dominant-negative PKCα
DRG	Dorsal root ganglion
ERK	mitogen-activated protein kinase kinase/extracellular
FLIP	Focal laser-induced photolysis
Gas1	growth arrect-specific 1
GSK3β	glycogen synthase kinase 3 beta
GST	glutathione S-transferase
ip	Hedgehog interacting protein
Ihh	Indian hedgehog
ILK	Integrin linked kinase
ILKAP	ILK-associated protein

ILK-DM	Integrin linked kinase double mutants
IP3	inositol-1,4,5-trisphosphate
LDL	low-density lipoprotein
LPA	lysophosphatidic acid
MAG	Myelin-associated glycoprotein
MLC	myosin light chain
MLCK	myosin light chain kinase
NGF	Nerve growth factor
PAK	p21-activated kinase
PH	pleckstrin homology
PI3K	Phosphoinositide 3-Kinase.
PINCH	particularly interesting new cysteine-histidine protein
PIP2	phosphoinositol-4,5-bisphosphate
PIP3	phosphatidylinositol 3,4,5-trisphosphate
PKA	Protein Kinase A
PKB	Protein kinase B
PKC	Protein Kinase C
PKD-1	Protein Kinse D-1
PMA	phobol 12-myristate 13-acetate
Ptc	Patched
RGC	Retinal Ganglion Cells
Rho-GAP	GTPase acting proteins
Rho-GEF	guanine nucleotide exchange factors

ROCK	Rho-associated protein kinase
SFK	Src-family kinases
Shh	sonic hedgehog
Smo	Smothened
WASP	Wiskott-Aldrich Syndrome Protein

Chapter I. Introduction

Axon guidance

During embryonic development, growing axons of neurons follow precise pathways to find appropriate target cells. The axons are guided by a variety of attractive and repulsive guidance cues present in the extracellular environment. Attractive guidance cues induce axonal turning towards them, while repulsive guidance cues repel axons away or cause axon retraction. The guidance cues can either be diffusible or membrane-bound. Diffusible cues are secreted from the source of synthesis and generate a gradient, acting over a long distance (Kennedy et al., 2006). Membrane-bound cues positioned at a precise location act over short distance when axons encounter them (Klein, 2005). Establishing the accurate patterns of axon navigation is crucial to nervous system development, and understanding how axons make precise pathfinding decisions may suggest new strategies to promote axon regeneration after injury or disease (Engle, 2010) (Giger et al., 2010).

A palm-like structure termed the growth cone at the distal tip of the axon is considered as both a sensing unit to interpret the environmental signals, and a motor unit to steer the axon. Two major cytoskeleton components within the growth cone are actin filaments and microtubules, and they have been shown to be responsible for the motility of the growth cone (Dent and Gertler, 2003). Actin filaments are enriched in peripheral finger-like filopodia, whereas microtubules extended from the shaft of the axon are accumulated in the central domain of the growth cone. Guidance factors can interact with the receptors on the growth cone to initiate a series of signaling events,

Figure 1.1 Growth cone morphology and axon guidance.

A, The growth cone is separated into two regions: the peripheral domain and the central domain. The peripheral domain contains lamellipodia and filopodia, and is composed primarily of actin filaments (phalloidin staining in red). The central domain is located in the center of the growth cone and is composed primarily of microtubules (anti-tubulin staining in green). The central domain also contains many organelles and vesicles of various sizes. ***B,*** The axons are guided by a variety of attractive and repulsive guidance cues presented in the extracellular environment. Attractive guidance cues induce axonal turning towards the cues, while repulsive guidance cues repel axon away from the cues.

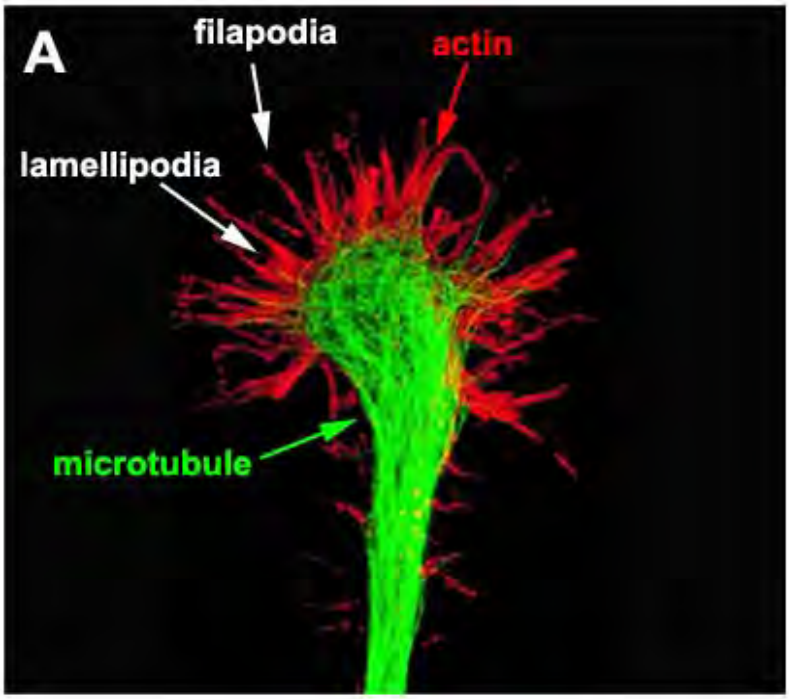
A
filapodia
actin
lamellipodia
microtubule

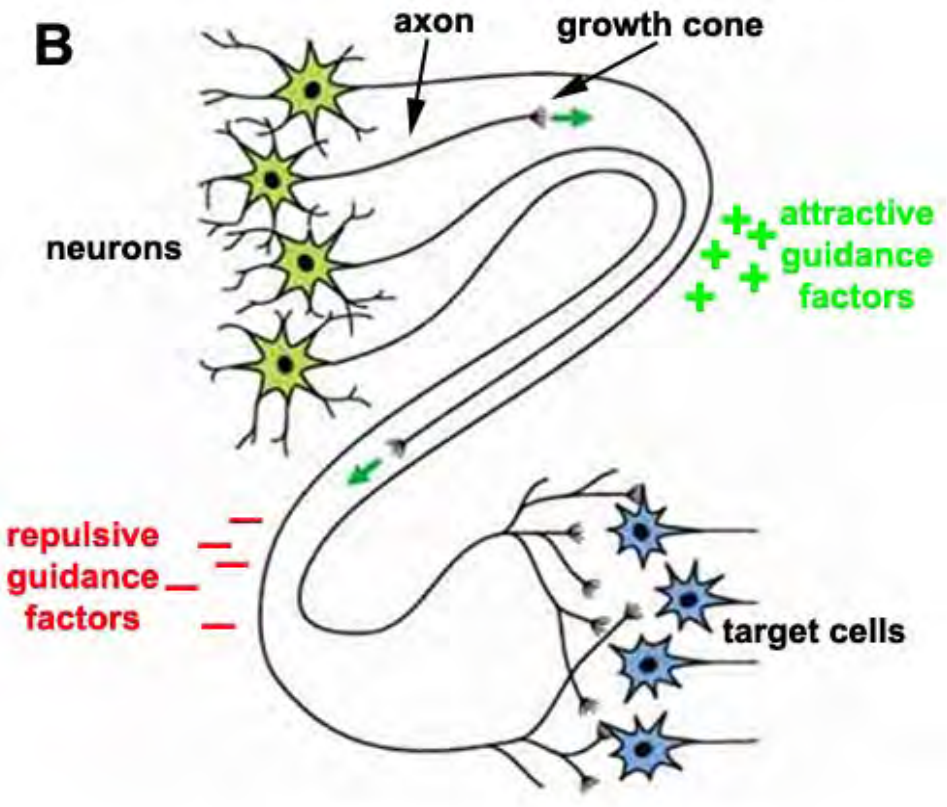
B
axon
growth cone
neurons
attractive
guidance
factors
repulsive
guidance
factors
target cells

leading to cytoskeleton rearrangement and subsequent movement of the growth cones (Dent and Gertler, 2003). The mechanisms of axon guidance have been well-studied in several conserved families of guidance factors including Slits, Ephrins, Netrins and Semaphorins (Chilton, 2006). Though these guidance factors have distinct signaling pathways, they share some common components and features to mobilize the growth cone (O'Donnell et al., 2009). Ca^{2+}, cyclic nucleotides and Rho-GTPases have been shown to regulate both chemoattraction and chemorepulsion of the guidance cues.

Due to the technical difficulties of manipulating Ca^{2+} concentration in vivo, the majority of experiments studying the roles of Ca^{2+} in axon guidance have been carried out on cultured neurons. In the resting state, growth cones maintain a baseline intracellular Ca^{2+} concentration. In vitro application of chemoattractants such as Netrins and BDNF (Brain-derived neurotrophic factor) from a point source leads to growth cone Ca^{2+} elevation towards the source of the chemoattractants (Song et al., 1997, Hong et al., 2000) . Chemorepellents such as MAG (Myelin-associated glycoprotein) can also increase the Ca^{2+} concentration facing the source of the chemorepellents (Henley et al., 2004). However, chemorepellents generally induce a small Ca^{2+} elevation locally while chemoattractants induce a larger Ca^{2+} elevation globally, suggesting the amplitude of Ca^{2+} gradients across the growth cones are responsible for the turning decisions (Gomez and Zheng, 2006). Elevation of Ca^{2+} occurs when Ca^{2+} channels on the plasma membrane or on intracellular stores open to allow Ca^{2+} to flow into the cytosol. Further analysis indicated that different guidance cues can activate different categories of Ca^{2+} channels, possibly contributing to the local vs global Ca^{2+} elevation (Gomez and Zheng, 2006,

Bashaw and Klein, 2010), though the identities of some channels still remain elusive. The repulsive turning is induced when chemorepellents are applied from a point source, but bath application of the chemorepellents generally causes growth cone collapse, and it has been suggested that this causes a substantial overall elevation of Ca^{2+} within the growth cone (Bolsover, 2005, Gomez and Zheng, 2006), though detailed comparison hasn't been performed. Therefore, it has been suggested that high and low Ca^{2+} elevation favor the negative effects of guidance cues, whereas moderate Ca^{2+} increase favors the positive effects of guidance cues.

Furthermore, Ca^{2+} alone, independent of guidance cue activation, can mediate growth cone turning. It has been found that high extracellular gradients of a Ca^{2+}-selective ionophore cause growth cone attraction, while low gradients of the ionophore cause growth cone repulsion in cultured *Xenopus* spinal neurons (Henley et al., 2004). Localized increase of Ca^{2+} by FLIP (focal laser-induced photolysis) is capable of inducing both attractive and repulsive turning, depending on the concentration of the extracellular Ca^{2+} (Zheng, 2000), further supporting the sole role of Ca^{2+} in axon guidance.

A number of proteins have been identified to act downstream and mediate the effects of Ca^{2+} elevation in a spatiotemporally restricted manner. These effectors include Ca^{2+} /calmodulin dependent kinases and phosphatases, Ca^{2+} -activated proteases, cyclic nucleotides and Rho GTPases (Gomez and Zheng, 2006). Among them, cyclic nucleotides and Rho GTPases have been given more attention as they show signaling

crosstalk with Ca^{2+}. For example, cyclic nucleotides can regulate Ca^{2+} concentration by controlling the activity of Ca^{2+} channels on the plasma membrane or on the ER. Conversely, Ca^{2+} can enhance the production of cyclic nucleotides through activation of soluble adenylyl cyclases and nitric oxide synthase (NOS) (Choi et al., 1992, Sculptoreanu et al., 1993).

Earlier studies showed that Netrin- or BDNF-mediated attraction of Xenopus spinal neurites can be converted to repulsion when cAMP signalling is blocked by the membrane-permeable cAMP antagonist or a specific protein kinase A (PKA) inhibitor (Ming et al., 1997, Song et al., 1997). Conversely, Sema III or MAG triggered repulsive turning of Xenopus spinal neurites can be converted to attraction by activation of cGMP or cAMP signaling, respectively. Moreover, Sema III-induced growth cone collapse of rat dorsal root ganglion (DRG) can also be inhibited by activation of the cGMP pathway (Song et al., 1998). Shh-induced growth cone collapse of chick RGC is accompanied by a decrease of cAMPs in the growth cone (Trousse et al., 2001). These evidences suggests that an increase of cyclic nucleotide activity favors positive guidance effects while a decrease of cyclic nucleotide activity favors negative guidance effects. By varying the ratio of the membrane-permeable cAMPs and cGMPs, later studies further indicated that the bi-directional turning decisions of growth cone to Netrin gradients is dependent on the relative ratio of cAMP and cGMP activities, with a high cAMP/cGMP ratio favors attraction, whereas a low cAMP/cGMP ratio favors repulsion (Nishiyama et al., 2003). Similar to Ca^{2+}, cyclic nucleotides alone can mediate growth cone turning, localized

increase of intracellular cAMP by focal photolysis of caged cAMP induces growth cone attraction (Guirland et al., 2003).

Rho-GTPases are another common signaling component shared by different axon guidance cues. The family includes Cdc42, Rac and Rho, whose roles have been extensively investigated in regulation of cytoskeleton dynamics and cell motility (Ridley, 2001). Regulated by upstream Rho-GEFs (guanine nucleotide exchange factors) and Rho-GAPs (GTPase activating proteins), Rho-GTPases cycle between GDP-bound inactive state and GTP-bound active state. Slits, Ephrins, Netrins and Semaphorins can all influence the activity of Rho-GTPases, but the activation degree of members of Rho-GTPases varies. For instance, Slits, which normally induce growth collapse and axon repulsion, increase Rac and Rho activity but decrease active Cdc42 levels (Wong et al., 2001, Fan et al., 2003). Netrins increase Rac and Cdc42 activity, but inhibit Rho activity when they induce axon attraction (Li et al., 2002, Gitai et al., 2003). In *Xenopus* spinal neurons, over-expression of dominant-negative Rac inhibits BDNF-induced attractive turning, whereas expression of dominant-negative Rho abolished LPA (lysophosphatidic acid)-induced repulsive turning (Yuan et al., 2003). Collectively, Rac/Cdc42 is generally associated with positive guidance effects but Rho with negative guidance effects.

The differential activations of Rho-GTPases are also the consequences of specific modulation of Rho-GEF or Rho-GAP immediately upstream of Cdc42, Rac or Rho. For instance, Slit-induced Rac activation is mediated through a conserved Rac-GAP (Vilse) (Lundstrom et al., 2004), whereas Netrins-induced activation of Rac/Cdc42 is attributed

to Trio-GEF (Briancon-Marjollet et al., 2008). Additionally, different receptors of the same guidance cue may recruit different GEFs to accomplish the opposite activation of Rho-GTPases members. Receptors of semaphorins, Plexin-B1 and Plexin-A1, bind to PDZ-RhoGEF and FARP2-GEF, resulting in activation of Rho and Rac respectively in different cellular contexts (Driessens et al., 2002, Toyofuku et al., 2005).

The downstream effectors of Rho such as ROCK (Rho-associated protein kinases) also play an important role in axon guidance. ROCK is a key regulator of actin organization.

A gradient of ROCK inhibitor Y-27632 is sufficient to induce attractive turning on *Xenopus* spinal neurons (Yuan et al., 2003). Inhibition of ROCK abolishes LPA-induced repulsive turning (Yuan et al., 2003), and blocks growth cone collapse induced by a group of guidance factors such as Ephrin-B2, -A5 or Semaphorin4A (Wahl et al., 2000, Yukawa et al., 2005, Petros et al., 2010), suggesting that Rho-ROCK signaling mainly mediates the negative effects of guidance cues.

More recently, classical morphogens such as Shh, BMPs (bone morphogenetic proteins), and Wnt family proteins, which determine the differentiation of various cell types within a tissue in a concentration-dependent manner, have been shown to mediate axon guidance (Sanchez-Camacho and Bovolenta, 2009). A good example of morphogen functioning as axon guidance cue is Wnt family proteins, which were originally characterized as secreted proteins from the roof plate of the developing spinal cord to determine different cell types within dorsal-ventral axis (Chizhikov and Millen, 2005). Recent studies showed that Wnt4 and Wnt7b are expressed in an anterior-posterior gradient within the

ventral spinal cord to attract ascending commissural axons after they cross the ventral midline (Lyuksyutova et al., 2003). Wnt1 and Wnt5a are expressed in an anterior-posterior gradient in the dorsal spinal cord and function as repellents for descending cortical motor axons (Liu et al., 2005). The attractive effect has been shown to be mediated by Wnt receptor Frizzled, whereas the repellent effect is mediated by another receptor, Ryk. BMPs and Shh have also been shown to mediate commissural axons navigation, with BMPs repelling commissural axons from the roof plate and Shh attracting these axons towards the floor plate (Butler and Dodd, 2003, Charron et al., 2003) . The detailed mechanism of Shh-induced axon guidance will be introduced in the following section.

Since actin filaments and microtubules are two major cytoskeletal components in the growth cones, a large body of research has focused on the mechanism by which guidance factors regulate the cytoskeletal rearrangement. However, an increasing number of reports have shown that endocytosis and exocytosis in the growth cone also play important roles in growth cone navigation (Tojima et al., 2007, Tojima et al., 2010, Kolpak et al., 2009). Experiments carried out in our lab have shown that negative guidance factors, such as Shh, can induce macropinocytosis in the growth cone, and inhibition of the macropinocytosis effectively abolished Shh-induced growth cone collapse and repulsive axon turning (Kolpak et al., 2009), suggesting that membrane trafficking events in response to guidance factors are critical for steering the growth cone.

Compared with clathrin- and caveolae- mediated endocytosis, macropinosomes are large vesicles with diameter from 0.2 μm to 1.0 μm, and can be easily labeled by fluid-phase endocytic markers such as dextran. The formation of the macropinosomes requires transient actin reorganization around the newly formed endocytic cup, as disassembly of actin filaments by cytochalasin D significantly reduced the formation of macropinosomes (Meier et al., 2002, Kolpak et al., 2009). The formation of the macropinosomes also requires several signaling components, including Rho-GTPases, p21-activated kinase, Src tyrosine kinase and PI3-kinase, though the requirement of these signaling components maybe cell-type specific (Swanson, 2008). For example, inhibition of PI3K signaling by wortmannin or LY294002 markedly decreased macropinocytosis in macrophages (Arali et al., 1996), but not in the growth cones of RGC cells (Kolpak et al., 2009). Dynamin, a small GTPase involved in the scission of newly formed vesicles from the membrane, is required for macropinocytosis as well. We previously showed that dynasore (a specific inhibitor of dynamin) and dynamin inhibitory peptide significantly decreased Shh-induced dextran uptake, suggesting that macropinocytosis in RGC axons requires the function of dynamin (Kolpak et al., 2009).

In summary, considerable progress has been made in defining the mechanisms of how guidance factors affect axon navigation. Studies from receptor level, second messenger level, cytoskeleton and membrane trafficking level provide abundant insight into the complex wiring specificity of axons, yet many questions remained unanswered. A better understanding of how the precise connectivity patterns of axon are established will shed light on many neural developmental disorders.

The retinotectal system

The eye is a light-sensing organ that receives and transmits visual information to the central nervous system (CNS). During development, a series of axon navigation events takes place to ensure that visual information is correctly relayed to the CNS targets. The mature retina is composed of six neuronal cell types and one glial cell type that are organized into different cellular layers with RGCs located at the vitreal side of the retina. RGCs are the only retinal neurons to project their axons out of the retina and into the brain. Due to its stereotypical projection, the navigation of RGC axons to their proper targets provides an ideal model system for studying axon guidance.

RGCs are the first cell type to differentiate during vertebrate retinogenesis. Their differentiation begins in the central region of the retina and gradually extends towards the periphery, thus forming a central to peripheral gradient of RGC differentiation. The progressive RGC differentiation is accompanied by the corresponding axonogenesis (Goldberg and Coulombre, 1972). All RGCs extend their axons towards the optic disc in the center where the RGC axons converge and exit the eye; therefore, axons emanating from more peripheral retina have to travel a longer distance to reach the exit point. The navigation of axons within the retina is called “intraretinal axon targeting”. To insure that RGC axons correctly project towards the optic disc, it has been found that a number of molecules are expressed in a gradient fashion within the retina to facilitate axon guidance. For example, chondroitin sulfate proteoglycans (CSPGs) (Brittis et al., 1992) and Zic3 (Zhang et al., 2004) are expressed high in the periphery but low in the retina center, acting as negative factors to repel axons towards the optic disc, while Shh is

Figure 1.2 The retinotectal system

A, Diagram of intraretinal axon pathfinding. A segment of retina is shown, with vitreal surface up. RGCs are located at the vitreal side of the retina and their axons project to the optic disc in a wave-like fashion beginning from the center of the retina. Coordinated effects of several positive factors (++++) and negative factors (-----) ensure axon projection to the optic disc. ***B,*** Diagram of RGC axons crossing at the chiasm of fish and bird. After RGC axons reach the optic disc (od), they converge and exit the eye to form the optic nerve (on). RGC axons further project towards the midline where they cross at the chiasm. In chick and fish, the entire axonal population from one eye projects contralaterally into the brain, whereas in higher vertebrate species, axons from temporal retina do not cross the midline but project ipsilaterally (not shown). Several negative guidance factors are expressed around the chiasm region to facilitate the local navigation process. N, nasal; T, temporal; V, ventral; D, dorsal; ot, optic tract; GCL, ganglion cell layer.

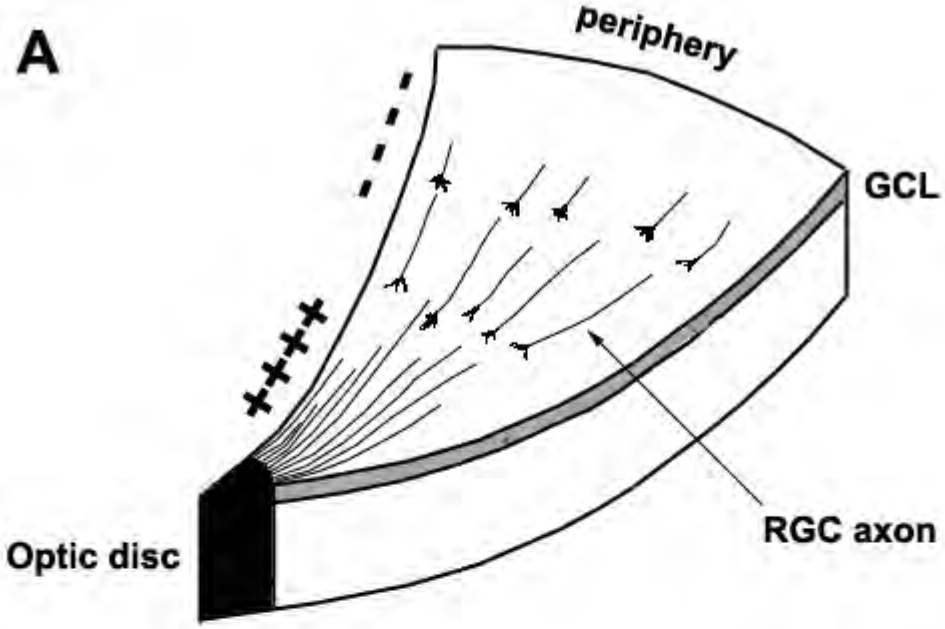
A
periphery
GCL
RGC axon
Optic disc

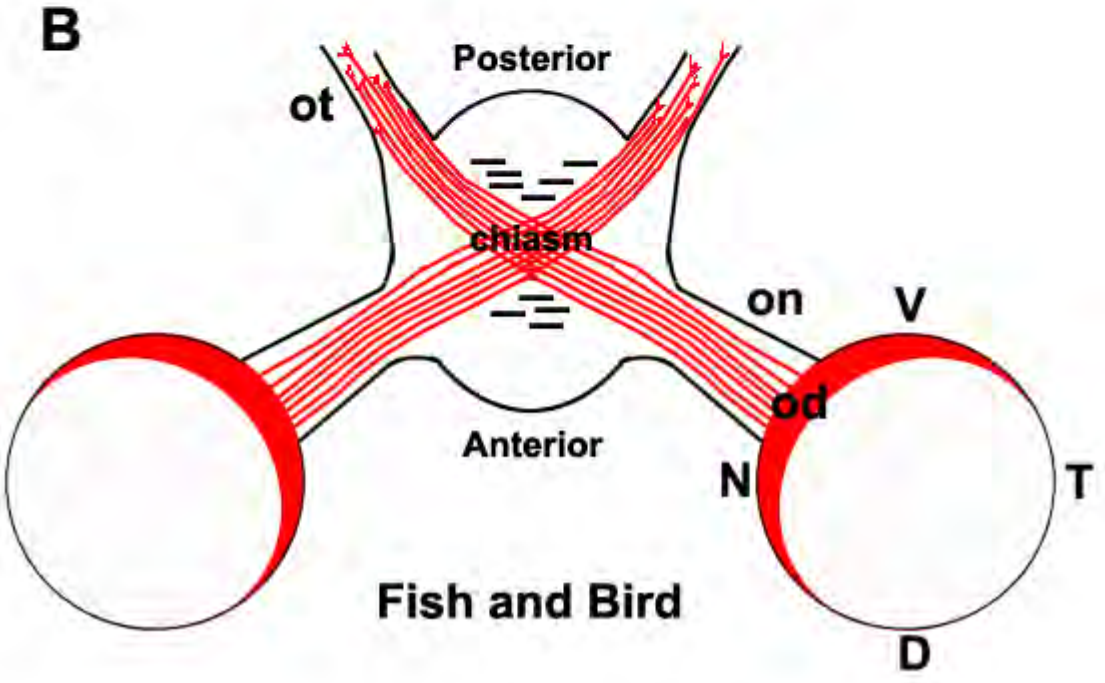
B
Posterior
ot
chiasm
on
V
od
Anterior
N
T
D
Fish and Bird

expressed low in the periphery and high in the center of retina, acting as a positive factor to attract axons to the optic disc (Kolpak et al., 2005). Peripheral axons that have to travel a longer distances to reach the retinal center can fasciculate with the pioneer axons ahead of them by expressing cell and substrate adhesion molecules such as L1, which exhibits homophilic binding activity (Van Vactor, 1998). To prevent centripetally growing axons extend to the opposite side of the retina after they reach the optic disc, studies from mice showed that axons from the dorsal retina encounter an increasing expression of EphB family protein at the ventral retina, which limits the bypass of axons at the optic disc (Birgbauer et al., 2000).

After RGC axons reach the optic disc, they exit the eye and form the optic nerve. The optic nerves from left and right eyes further project towards each other to meet at the ventral midline of the diencephalon, where they form an X-shaped intersection known as the optic chiasm. In higher vertebrate species, RGC axons originating from nasal retina cross the midline to project contralaterally, while axons from temporal retina do not cross the midline but project ipsilaterally to implement binocular vision. In fishes and birds, the entire axonal populations from one eye cross the midline to project contralaterally into the brain.

The mechanism determining whether RGC axons cross the midline has been explored in both mammals and non-mammalian vertebrates. The optic chiasm has been shown to be the source of several guidance factors, such as Slits, Ephrins, Semaphorins and Shh, which guide crossed or uncrossed axons. In mice, Slit1 and Slit2 are expressed in a complementary fashion near the chiasm, around the cross of the optic nerve. *Slit1/Slit2*

double knockouts mice show misprojected axons wandering before and after the chiasm. In vitro, both Slit proteins repel RGC axons (Plump et al., 2002). These data suggest that repulsion from Slit1/Slit2 limits the escape of axons from their normal path at the chiasm. For Ephrin family, ephrin-B2 is expressed in the radial glial cells located within the chiasm midline. Its receptor, EphB1, is exclusively expressed in the ventral-temporal retina, from where axons normally projects ipsilaterally. EphB1 knockout mice show significant reduction of ipsilateral projection, suggesting that chiasmatic ephrin-B2 is repulsive to ipsilateral but not contralateral projecting axons (Williams et al., 2003). However, in chick, ephrin-B expression is not detected at the ventral midline of the diencephalon. Since chick RGC axons only project contralaterally, it is possible that ephrin-B is not involved in the pathfinding for chick RGC axons.

Originally identified as a classical morphogen, Shh was recently shown to play an important role in restricting RGC axons projection at the chiasm (Trousse et al., 2001, Sanchez-Camacho and Bovolenta, 2008). In E2.5-E3 chick, when few RGCs have differentiated in the retina, Shh is expressed continuously in the entire ventral midline; at E5 and later, when newly formed axons reach the chiasm, Shh expression disappears from the chiasm but borders the anterior and posterior edges of the chiasm, suggesting that the spatio-temporal downregulation of Shh expression at the chiasm may be important for the correct navigation of axons (Trousse et al., 2001). This was confirmed by the fact that over-expression of Shh at the chiasm region resulted in prevention of RGC axons from reaching the region (Trousse et al., 2001). Conversely, loss of function study performed in mice, by neutralizing Shh protein at the chiasm region with anti-Shh antibody, leads to a widening of axon bundles at the chiasm and an increase of erroneous

axon projection into the ipsilateral tract and contralateral nerve (Sanchez-Camacho and Bovolenta, 2008). Collectively, these results indicate that upon arrival of RGC axons to the chiasm, Shh expression at the chiasm border restricts contralaterally projecting axons within the bundle. However, up to the present, no signaling mechanism of Shh involved in this process has been reported.

After RGC axons cross at the chiasm, they further project to the brain and eventually reach the superior colliculus in mammals or the optic tectum in non-mammalian vertebrates. Recent studies have shown that Ephrin and Wnt family proteins play important roles in the final axon navigation process (Flanagan, 2006).

The Sonic hedgehog signaling pathway and axon guidance

The hedgehog family includes three members in mammals: Sonic hedgehog (Shh), Desert hedgehog (Dhh) and Indian hedgehog (Ihh). Shh is the most extensively investigated member among the three. Synthesized as a 45kDa precursor protein, Shh protein undergoes autoproteolytical cleavage to generate a 19kDa N-terminal fragment (Shh-N) possessing signaling bioactivity, and a C-terminal fragment (Shh-C) possessing protease activity. Shh-N is then further modified by cholesterol modification at the C-terminus and palmitoylation at the N-terminus. These two modifications are believed to enhance the potency and diffusion of the protein (Nybakken and Perrimon, 2002) .

Though the *Hedgehog* gene was first identified in a screen of genes that control the segmentation pattern of *Drosophila melanogaster*, mammalian homologs of the

Hedgehog genes appear to play broad roles during embryonic development. The roles of Shh were extensively studied in the patterning of the neural tube. In the developing vertebrate neural tube, Shh is secreted from the notochord and floor plate at the ventral midline and spreads dorsally into the neural tube in a graded fashion to induce the differentiation of diverse cell types in the dorsal–ventral axis of the neural tube (Patten and Placzek, 2000). The effects of Shh on cell fate determination are mediated through a transcription-dependent signaling pathway, where binding of Shh to its receptor, Patched (Ptc), a 12-transmembrane protein, relieves the inhibition of Ptc on the co-receptor Smoothened (Smo), a serpentine protein resembling G-protein associated receptors. Activated Smo subsequently induces translocation of a family of Gli transcription factors into the nucleus where they regulate the expression of target genes.

The mechanism by which gradients of Shh specify distinct cell fates in the developing spinal cord is not fully understood. But it has been proposed that a negative feedback mechanism, involving target genes transcriptionally regulated by Shh, is responsible for the appropriate response of cells to graded Shh. For example, Ptc is not only the transducer of Shh signaling, but also a target of Shh signaling. The up-regulation of the *Ptc* gene and its subsequent increase of protein expression at the cell surface sequesters Shh ligand, limiting its spread in the tissues and the level of Shh signaling in the target field (Ribes and Briscoe, 2009).

Figure 1.3. The canonical sonic hedgehog signaling pathway.

The canonical Shh signaling pathway involves two transmembrane proteins, Ptc and Smo. In the absence of ligand, Ptc inhibits Smo via an unknown mechanism. In the presence of ligand, inhibition of Smo by Ptc is relieved, leading to translocation of Gli transcription factors into the nucleus where they activate the expression of target genes. The transcription-dependent pathway is mainly responsible for cell fate determination and tissue patterning.

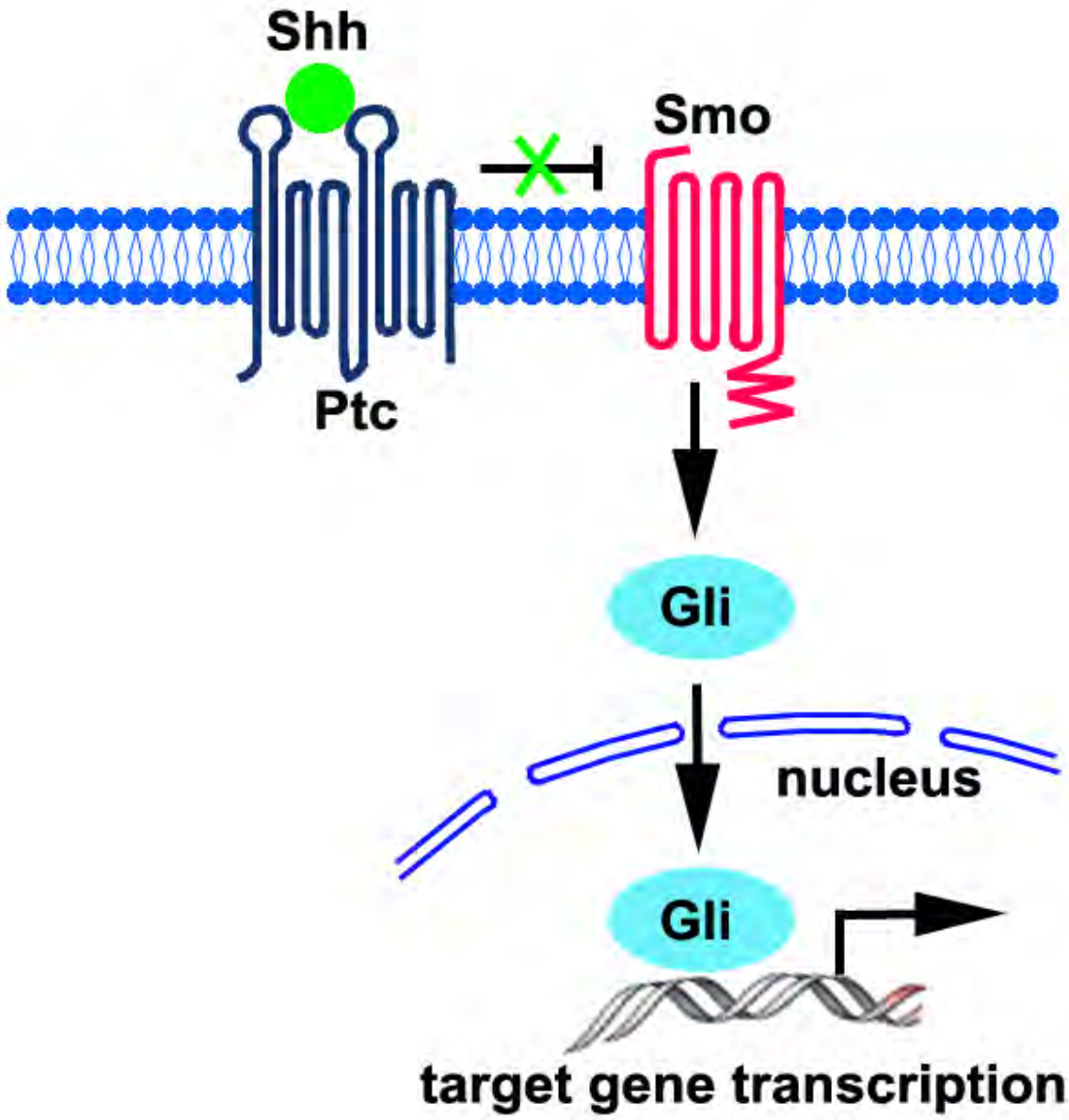
Shh
Smo
Ptc
Gli
nucleus
Gli
target gene transcription

More recently, Shh has been shown to act as a guidance factor to direct axonal projection. It plays important roles in the pathfinding of commissural axons towards the floor plate, along the longitudinal axis of the spinal cord, and in the guidance of retinal ganglion cell (RGC) axons toward the optic disc and at the optic chiasm (Trousse et al., 2001, Charron et al., 2003, Bourikas et al., 2005, Kolpak et al., 2005, Sanchez-Camacho and Bovolenta, 2008). The guidance effects of Shh occur through binding to different receptors and are independent of its canonical signaling pathway (Sanchez-Camacho and Bovolenta, 2009). In addition to Ptc, five new receptors have been found to directly bind to Shh. These receptors include Boc (Bi-directional Cdon-binding protein) (Tenzen et al., 2006), Cdo (Cell adhesion molecule-related/downregulated by oncogenes) (Tenzen et al., 2006), Hip (Hedgehog interacting protein) (Chuang and McMahon, 1999), Gas1 (Growth arrest-specific 1) (Allen et al., 2007) and megalin (McCarthy et al., 2002). Among these receptors, Boc and Hip have been shown to play roles in Shh-induced axon guidance.

In the developing neural tube of mice and rats, floor plate-derived Shh, in collaboration with netrin-1, can act as a chemoattractant to attract dorsal commissural axons towards the ventral midline (Charron et al., 2003). Boc and Cdo were investigated as candidate receptors of Shh in guiding commissural axons because their extracellular domains share a high degree of homology with those of other axon guidance receptors, such as Slit receptor Robo and netrin receptor Deleted in Colorectal Cancer (DCC). Both Cdo and Boc are expressed in the progenitors of commissural neurons at the dorsal neural tube, but Boc expression covers more ventrally and can be detected in differentiated commissural neurons when their axons approach the midline. Further analysis in mice

showed that genetic loss of *Boc*, but not *Cdo,* resulted in deviation of commissural axons trajectories in the neural tube, a phenotype similar to that of Smo knock-out mice, suggesting that Boc receptor is responsible for Shh-induced projection of commissural axons (Okada et al., 2006). Similar experiments carried out in zebrafish, where injection of antisense morpholinos against *Boc* also resulted in defects in the dorsoventrally projecting axons (Connor et al., 2005). Though Cdo knock-out mice exhibit holoprosencephaly, a developmental defect often associated with mutations in the Shh signaling pathway (Zhang et al., 2006), whether Cdo is involved in axon guidance is currently unknown.

The attractive effect of Shh on commissural axons is believed to be mediated through a non-canonical transcription-independent pathway. In vitro, dissociated rat commissural axons turn towards Shh gradients within minutes after the application of Shh, too quickly to attribute to a transcriptional effect. Furthermore, the attractive turning cannot be abolished by pre-treatment of transcription inhibitor actinomycin D or by repression of Gli-mediated transcription (Yam et al., 2009). However, the attractive turning seemed to require the activation of Src family kinases (SFKs) by Shh, as Shh treatment acutely increased the phosphorylation of SFKs in the growth cone of commissural axons, and the attractive turning is abolished by pre-treatment with PP2, a chemical inhibitor of SFKs, or by over-expressing a negative regulator of SFKs in the commissural neurons (Yam et al., 2009). Additionally, activation of SFKs by Shh required expression of Boc at the cell surface (Yam et al., 2009). However, Boc knock-out mice did not show obvious disruption of the spinal cord patterning. Taken together, these data suggest that the

Figure 1.4. The sonic hedgehog signaling and axon guidance in the neural tube.

In the developing neural tube, floor plate-derived Shh forms a ventral to dorsal gradient, and acts as a chemoattractant to attract dorsal commissural axons towards the ventral midline. This guidance activity of Shh (shown as "+") is dependent on Smo, Boc receptor and downstream SFKs in a transcription-independent manner. After reaching the floor plate, commissural axons across the midline, turn, and migrate anteriorly. Shh, expressed in a posterior to anterior gradient repels postcommissural axons to grow anteriorly. This repulsive effect of Shh (shown as "-") is dependent on Hip receptor alone. RP, roof plate; FP, floor plate; A, anterior; P, posterior; D, dorsal; V, ventral.

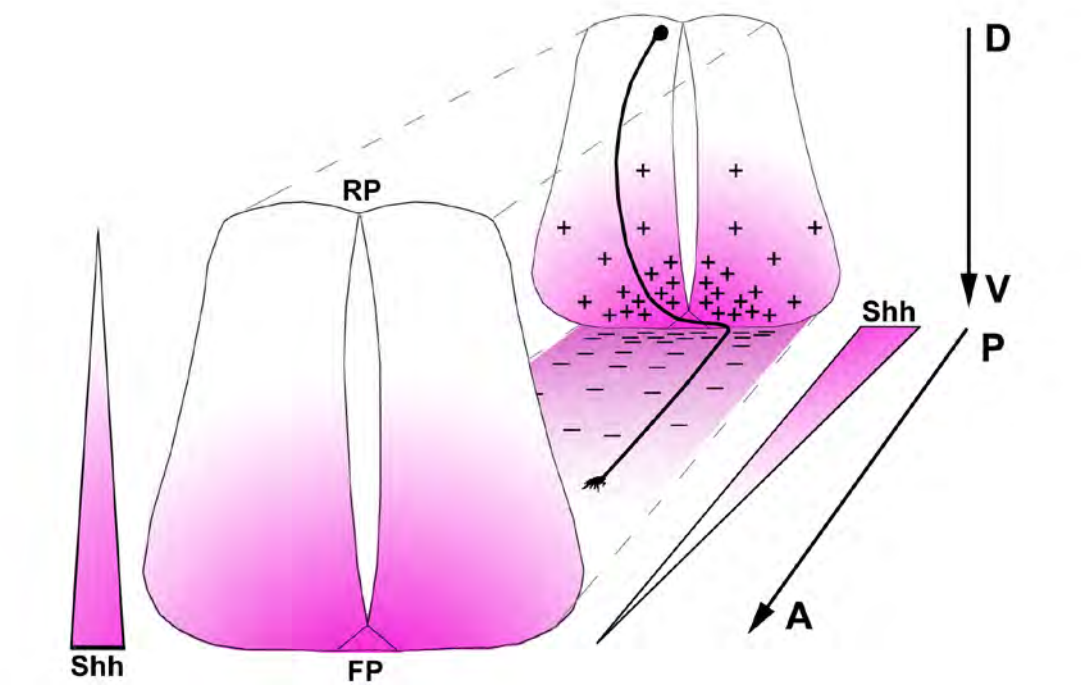
RP
D
V
P
Shh
A
Shh
FP

guidance activity of Shh on commissural axons is mediated by Boc receptor and downstream SFKs in a transcription-independent manner, and does not rely on cell fate changes within the spinal cord.

Gas1 is a glycosylphosphatidylinositol-linked membrane glycoprotein, initially identified through a screening of mouse somitic gene products that can directly bind to Shh (Lee et al., 2001). Gas1 is also expressed in the commissural axons and Gas1 null embryos exhibit aberrant axonal projection. But Gas1-mutants also exhibit defects in spinal cord patterning. Therefore, it is still unclear whether Gas1 directly mediates axon steering in response to Shh (Allen et al., 2007).

The role of the Hip receptor in Shh-induced axon guidance was investigated in chick spinal cord (Bourikas et al., 2005). Hip, but not Ptc and Smo, is expressed in the postcommissural axons after commissural axons cross the floor plate and navigate rostrally. Disruption of Shh function by anti-Shh antibody or RNAi interference resulted in abnormal projection of the postcommissural axons. RNAi knock-down of Hip, but not Ptc and Smo, caused similar phenotype as that of Shh knock-down, suggesting that Hip is required for Shh-mediated postcommissural axons navigation independent of the Ptc and Smo. In this system, Shh is considered as a negative guidance cue for postcommissural axons because over-expression of Shh in the spinal cord caused postcommissural axons to stop or turn away from the high level of Shh source. Again, knock-down of Hip did not change the patterning or cell differentiation within the spinal cord, suggesting that the repellent effect of Shh on postcommissural axons is direct (Bourikas et al., 2005). How

Hip mediates Shh-induced axon guidance is currently unclear as Hip is a type-1 transmembrane glycoprotein lacking an intracellular domain (Chuang and McMahon, 1999). It had been proposed that Hip may attenuate hedgehog signaling by competing with Ptc for Shh binding (Bosanac et al., 2009).

As described earlier, spatial-temporal regulation of Shh expression at the center of chiasm region may constrain RGC axons within the bundles, but the signaling mechanism mediating this response is still unclear. A recent study in mice showed that Boc is expressed in a subset of RGC cells whose axons project ipsilaterally and knock-down of Boc reduced the number of ipsilateral axons (Fabre et al., 2010). However, in chick and fish, all RGC axons navigate contralaterally, it remains to be determined if Boc is necessary for such process.

During the past several years, a large body of studies has shown that Shh can regulate a variety of cellular functions beyond axon guidance through new signaling pathways. For examples, PI3K/Akt signaling was demonstrated to be essential for Shh-dependent neural patterning (Riobo et al., 2006). ERK signaling can be activated by Shh to promote cell proliferation and differentiation in several cell types (Osawa et al., 2006, Elia et al., 2007). Through Rho signaling, Shh also modulates angiogenesis (Renault et al., 2010), epithelial morphogenesis (Kim et al., 2009) and cell migration (Renault et al., 2010). The effects of Shh on these cellular functions are largely independent of Gli-mediated transcription, suggesting the response of cells to Shh can be programmed through canonical and non-canonical signaling separately (Jenkins, 2009).

The Protein kinase C family

Protein kinase C (PKCs) is a family of serine/threonine kinases that plays a pivotal role in mediating G protein-coupled receptor and other growth factor-dependent cellular responses (Newton, 1995, Dempsey et al., 2000). PKC isoforms are classified into conventional PKCs (α, βI, βII, γ), novel PKCs (δ, ε, η, θ) and atypical PKCs (ζ, λ), mainly based on their differences in the regulatory domain and second messenger(Ca^{2+}) requirements (Steinberg, 2008). All PKCs contain a variable N-terminus regulatory domain and a highly conserved C-terminus kinase domain. The regulatory domain of all PKCs contains a C1 sub-domain, which functions as a phobol 12-myristate 13-acetate (PMA)/diacylglycerols (DAG) binding motif for conventional and novel PKCs. The C1 sub-domain of atypical PKCs is atypical, and it binds to PIP3 (phosphatidylinositol 3,4,5-trisphosphate), ceramide or PB1 domain containing proteins. Conventional and novel PKCs also have a C2 sub-domain, which contains recognition sites for acidic phospholipids. However, the C2 sub-domain of conventional PKCs binds to phospholipids in a Ca^{2+} -dependent manner, while novel PKCs do not. The structural differences determine that conventional PKCs require Ca^{2+} and PMA/DAG for their activation, novel PKCs only require PMA/DAG, and atypical PKCs require neither.

The traditional view of conventional PKC activation begins with external agonists binding to the corresponding receptors, which then leads to activation of phospholipase C (PLC). PLC cleaves phosphoinositol-4,5-bisphosphate (PIP2) into 1,2-diacylglycerol and inositol-1,4,5-trisphosphate (IP3). The IP3 binds to the ER-based Ca^{2+} channels which release Ca^{2+} into the cytoplasm where Ca^{2+} binds to the C2 sub-domain of the

Figure 1.5 The protein kinase C

A, Domain structure of protein kinase C isoforms. All PKCs contain an N-terminus regulatory domain and a C-terminus kinase domain. PMA/ DAG binds to the C1 sub-domain of the conventional and novel PKCs, while Ca^{2+} only binds to the C2 sub-domain of conventional PKCs. The structural differences determine that conventional PKCs require Ca^{2+} and PMA/DAG for their activation, whereas novel PKCs only require PMA/DAG. The catalytic domain of all PKCs contains three highly conserved phosphorylation sites that are critical for the catalytic activity of PKCs. ***B,*** The activation process of the conventional PKCs. Agonists-induced receptor activation lead to a series of signaling events that ultimately release Ca^{2+} from the ER to the cytoplasm. Binding of Ca^{2+} to the C2 domain of the PKC enhance its membrane affinity. Cytosolic PKC translocates to the plasma membrane where DAG binds to the C1 domain of PKC, fully activating the protein.

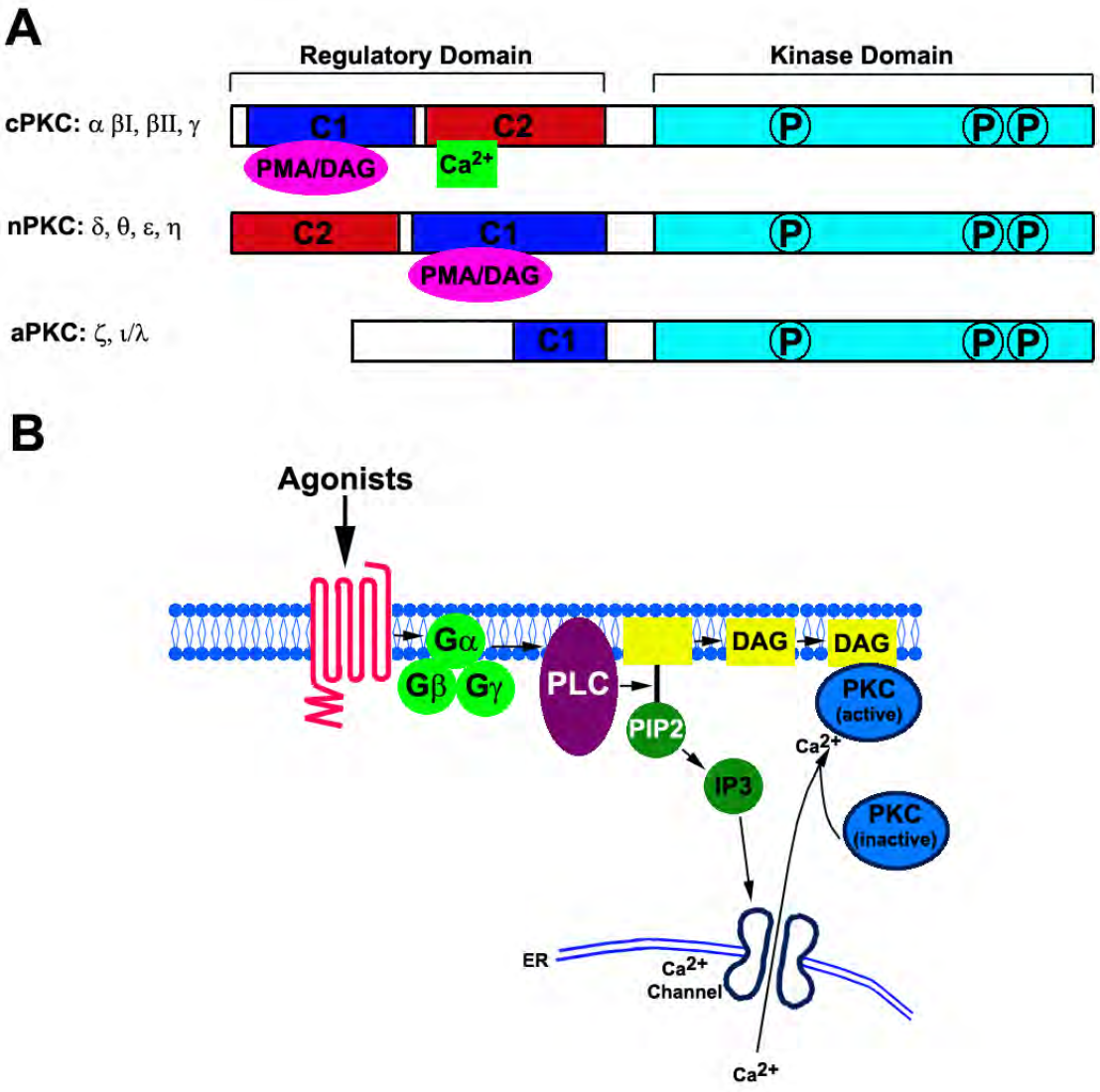
A
Regulatory Domain
Kinase Domain
cPKC: α βI, βII, γ
C1
C2
PMA/DAG
Ca2+
nPKC: δ, θ, ε, η
C2
C1
PMA/DAG
aPKC: ζ, ι/λ
C1
P
B
Agonists
Gα
Gβ
Gγ
PLC
DAG
DAG
PIP2
IP3
PKC
(active)
PKC
(inactive)
Ca2+
ER
Ca2+
Channel
Ca2+

conventional PKCs and increases the affinity of the PKCs with the plasma membrane. PKCs then translocate to the membrane where their C1 sub-domain interacts with membrane-bound DAG. PKC translocation to the plasma membrane has generally been considered as the hallmark of its activation.

The catalytic domains of all PKCs are highly conserved, and each catalytic domain contains three phosphorylation sites that are critical for the catalytic activity of PKCs. The first phosphorylation site of PKCs is a threonine residue (T497 in PKCα) within the activation loop. The kinase that is responsible for phosphorylation of this site is Protein Kinse D-1(PKD-1) and the phosphorylation of this residue is believed to stabilize the active conformation of the PKCs. Once threonine is phosphorylated, PKCs undergo two additional serine/threonine phosphorylations (T638/S657 in PKCα) in the V5 sub-domain. For conventional and novel PKCs, these phosphorylations steps are autophosphorylation events and are believed to mature and enhance the catalytic activity of this enzyme.

Because there is no convenient way to activate an individual isoform of PKC, PMA, which mimics the function of DAG, is widely used to evaluate the functions of PMA-sensitive PKCs, including conventional and novel PKCs. Emerging evidence indicates a general role of PKCs in axon guidance. When applied uniformly into neuronal cultures, PMA lead to growth cone collapse (Bonsall and Rehder, 1999, Zhou and Cohan, 2001); when pulsed from the side of the growth cones, PMA caused repulsive turning (Xiang et al., 2002, Kolpak et al., 2009). However, it is inconclusive from these experiments whether different PKC isoforms regulate the axonal repulsive effects synergistically or

individually. Studies focusing on physiologically relevant axon guidance proteins demonstrate that a PKC isoform-specific mechanism underlies the axonal guidance effects in response to different cues. For example, thrombin and protein tyrosine phosphatase μ (PTPμ)-induced growth cone collapse of rat dorsal root ganglion axons and chick RGC axons resulted from selective activation of novel PKCε and PKCδ, respectively (Mikule et al., 2003, Ensslen and Brady-Kalnay, 2004); while Wnt-mediated attractive guidance of rat commissural axons required atypical PKCζ (Wolf et al., 2008).

A novel PKCδ was shown to be specifically required for the transcriptional regulation of Gli and Ptc (Riobo et al., 2006a), suggesting a PKC isoform is involved in Shh canonical signaling pathway. We previously showed that PMA and Shh elicit similar negative guidance effects on chick RGC axons and the effects are likely to be transcription-independent. One of the major aims of our work is to identify which PKC isoform mediates Shh-induced axon guidance.

The Integrin-linked kinase

Integrin-linked kinase (ILK) was first identified in a yeast-two-hybrid screen as a direct binding protein to the cytoplasmic tail of β1 and β3 integrins (Hannigan et al., 1996). Since integrins are the major cell surface proteins that interact with the extracellular matrix and that themselves lack enzymatic activity, the finding of ILK as a kinase that directly binds to integrin drew a lot of attention. Indeed, it has been found that ILK plays many important roles in integrin-mediated cell adhesion, spreading, migration, and signaling (Hannigan et al., 2005). However, the function of ILK isn't restricted to

relaying integrin signaling. Increasing evidence has suggested that ILK can function independent of integrin (Vespa et al., 2003, Fielding et al., 2008, Fielding et al., 2011). For example, ILK co-localizes with several centrosomal and mitotic spindle proteins such as ch-TOG and RUVBL, and the protein complex plays an essential role in mitotic spindle assembly and mitosis (Fielding et al., 2008).

ILK is highly evolutionarily conserved and is composed of three structurally distinct domains: an N-terminal domain containing ankyrin repeats, a pleckstrin homology (PH)-like domain in the middle and a C-terminal putative serine/threonine kinase-like domain (Dedhar et al., 1999). The N-terminus of ILK consists of five ankyrin repeats, the first of which mediates direct interaction with PINCH (particularly interesting new cysteine-histidine protein), a family of LIM domain containing adaptor proteins that bind to ILK before the recruitment of the complex to focal adhesion sites. The N-terminus of ILK also directly binds to ILK-associated protein (ILKAP), a PP2C family phosphatase. PINCH and ILKAP may facilitate the ILK phosphorylation on downstream Akt and GS3Kβ (Fukuda et al., 2003, Kumar et al., 2004). The central PH-like domain of ILK has been shown to bind phosphatidylinositol-3,4,5-trisphosphate (PIP3) and is involved in growth factor-induced, PI3K-dependent activation of ILK (Delcommenne et al., 1998).

The C-terminus kinase-like domain exhibits significant sequence homology to Ser/Thr protein kinases, but lacks several critical residues required for eukaryotic protein kinase activity (Hanks et al., 1988). Since its discovery, the kinase activity of ILK has been subjected to debate and controversy. Recombinant ILK expressed in bacteria or purified

Figure 1.6 The integrin-linked kinase

ILK is composed of three domains: an N-terminal domain that binds PINCH and ILKAP, a PH-like domain in the middle that binds PIP3, and a C-terminal putative kinase-like domain that binds a variety of proteins including parvins and paxillin. ILK may possess kinase activity; several mutations (R211A, K220A and S343A) within the PH and kinase domain have been shown to abolish its kinase activity, but the conclusion remains controversial. ILK mainly functions as an “adaptor” to provide a platform for coupling integrin signaling to actin rearrangement.

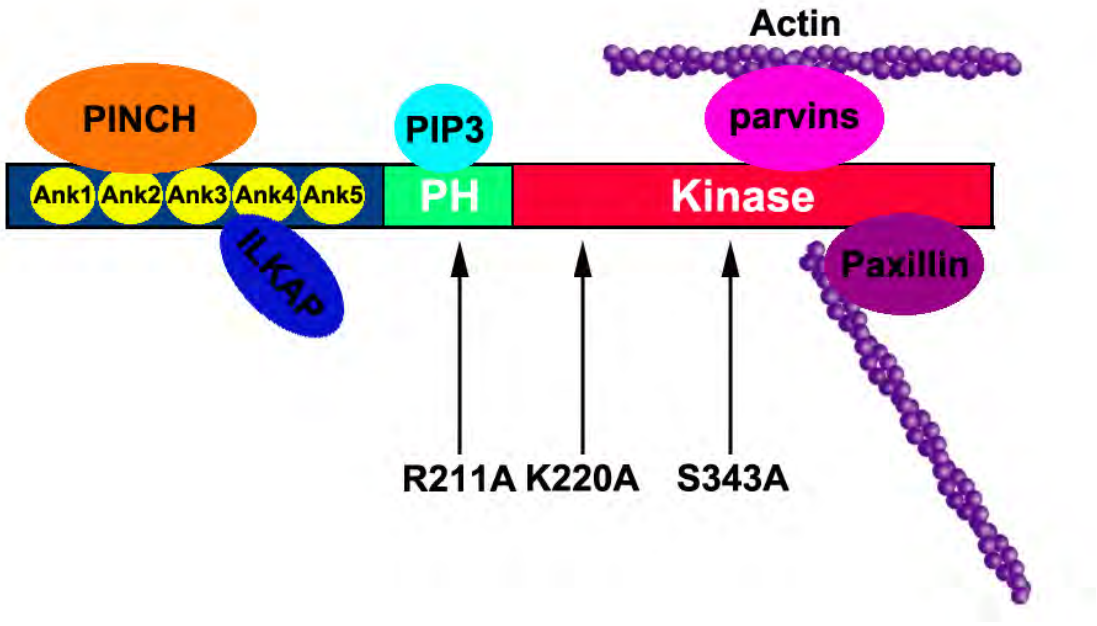
Actin
PINCH
PIP3
parvins
Ank1
Ank2
Ank3
Ank4
Ank5
PH
Kinase
ILKAP
Paxillin
R211A
K220A
S343A

ILK from cell extracts has been shown to phosphorylate a number of substrates in vitro, including the cytoplasmic tail of β1 and β3 integrin, AKT/PKB, GSK3β, myosin light chain (MLC), as well as the model substrate myelin basic protein (Hannigan et al., 1996, Delcommenne et al., 1998, Persad et al., 2001, Muranyi et al., 2002). Moreover, mutational analysis of ILK with R211A mutation in PIP3 binding site, K220A/M mutation in the putative ATP-binding site, and S343A mutation in the potential autophosphorylation site all result in catalytically inactive ILK in vitro (Persad et al., 2001, Filipenko et al., 2005). In the above studies, phosphorylation of AKT/PKB and GSK3β has been extensively used as readout of ILK kinase activity. However, evidence of ILK kinase activity in vivo is weak. Mice carrying the above point mutations do not show change of AKT/PKB or GSK3β phosphorylation (Lange et al., 2009). Deletion of the *ilk* gene in mouse chondrocytes (Grashoff et al., 2003) and keratinocytes (Sakai et al., 2003) do not change AKT/PKB or GSK3β phosphorylation level either. In *Drosophila melanogaster* and *Caenorhabditis elegans*, expressing inactive kinase ILK does not show any phenotype, but can fully rescue the phenotypes caused by deletion of the *ilk* gene (Zervas et al., 2001, Mackinnon et al., 2002), further suggesting the kinase activity of ILK probably does not exist in vivo. At present, there is no explanation to reconcile the conflicting observations. It could be that the catalytic activity of ILK is not general, rather species-specific, tissue-specific and cell-type specific.

In addition to the cytoplasmic tails of integrin, the C-terminal domain of ILK can bind to several actin-associated proteins such as parvin family proteins (α, β, and γ-parvin) and paxillin (Legate et al., 2006). These interactions link ILK signaling to the regulation of

the actin cytoskeleton. Inhibition of ILK activity causes disorganized actin cytoskeleton that results in defects in cell migration and cell adhesion (Sakai et al., 2003, Qian et al., 2005, Fan et al., 2009).

The study of ILK function in neuronal cells is limited. ILK protein is enriched in the growth cone of DRG and hippocampal neurons (Mills et al., 2003, Guo et al., 2007b). By using pharmacological inhibitor, siRNA knock-down, dominant-negative ILK and genetic deletion strategies, it has been shown that ILK is responsible for neurite outgrowth (Ishii et al., 2001, Mills et al., 2003), neuronal polarity formation (Guo et al., 2007b, Oinuma et al., 2007) and CNS myelination (Chun et al., 2003). However, whether ILK is involved in axon guidance is not clear.

Chapter II. Protein kinase Cα and integrin-linked kinase mediate negative axonal guidance effects of Sonic Hedgehog

ABSTRACT

In addition to its role as a morphogen, Sonic hedgehog (Shh) has also been shown to function as a guidance factor that directly acts on the growth cones of various types of axons. However, the noncanonical signaling pathways that mediate the guidance effects of Shh protein remain poorly understood. We demonstrate that a novel signaling pathway consisting of protein kinase Cα (PKCα) and integrin-linked kinase (ILK) mediates the negative guidance effects of high concentration of Shh on retinal ganglion cell (RGC) axons. Shh rapidly increased Ca^{2+} levels and activated PKCα and ILK in the growth cones of RGC axons. By in vitro kinase assay, PKCα was found to directly phosphorylate ILK on threonine-173 and -181. Inhibition of PKCα or expression of a mutant ILK with the PKCα phosphorylation sites mutated (ILK-DM), abolished Shh-induced macropinocytosis, growth cone collapse and repulsive axon turning. In vivo, expression of a dominant negative PKCα or ILK-DM disrupted RGC axon pathfinding at the optic chiasm but not the projection toward the optic disc, supporting that this signaling pathway plays a specific role in Shh-mediated negative guidance effects.

INTRODUCTION

Sonic hedgehog (Shh), a well characterized morphogen, has recently been shown to act as a guidance factor to direct axonal projection. Shh signaling plays important roles in the pathfinding of commissural axons towards the floor plate, along the longitudinal axis of the spinal cord, and in the guidance of retinal ganglion cell (RGC) axons toward the optic disc and at the optic chiasm (Trousse et al., 2001, Charron et al., 2003, Bourikas et al., 2005, Kolpak et al., 2005, Sanchez-Camacho and Bovolenta, 2008, Fabre et al., 2010). We previously demonstrated that Shh plays a dual role in chick RGC axon growth and guidance, acting as a positive factor at a lower concentration and as a negative factor at a higher concentration in vitro (Kolpak et al., 2005, Kolpak et al., 2009). Shh can act directly on the growth cones in a transcription-independent manner, causing growth cone collapse and repulsive axon turning of chick RGCs through Rho-GTPases (Kolpak et al., 2009), and inducing attractive axon turning of rat commissural neurons through the Src family kinase (Yam et al., 2009).

Protein kinase C (PKC) is a family of serine/threonine kinases that are classified into conventional PKCs (α, βI, βII, γ), novel PKCs (δ, ε, η, θ) and atypical PKCs (ζ, λ), based on their second messenger requirements (Steinberg, 2008). Conventional PKCs require Ca^{2+} and diacylglycerols (DAG) for activation, while novel PKCs require DAG only and atypical PKCs require neither. PKCδ was shown to be involved in the Shh canonical signaling cascade, required for the transcriptional regulation of Gli and Patched-1 (Riobo et al., 2006a). Activation of conventional and novel PKCs by phorbol myristate acetate (PMA) elicits repulsive axon turning of *Xenopus* spinal neurons and chick RGCs (Xiang

et al., 2002, Kolpak et al., 2009). However, the roles of specific PKC isoforms and their substrates in axon guidance are not completely understood.

Integrin-linked kinase (ILK), first identified in a yeast-two-hybrid screen as a direct binding protein to the cytoplasmic tail of β1 integrin, has been implicated in cancer cell growth and survival through modulation of downstream targets (Hannigan et al., 2005). By binding to PINCH, parvin and other proteins, ILK functions as an "adaptor" to provide a platform for coupling cell adhesion and growth factor signaling. In neurons, expression of dominant-negative constructs of ILK (E359K or S343A) inhibits neurite outgrowth (Ishii et al., 2001, Mills et al., 2003) and neuronal polarity determination (Guo et al., 2007). However, the role of ILK in axon guidance has not been reported.

Here, we demonstrate that a novel signaling pathway composed of PKCα and ILK mediates the negative effects of a high concentration of Shh on chick RGC axons. Shh rapidly increased Ca^{2+} levels, activated PKCα, leading to phosphorylation of ILK in the growth cones of RGC axons. Disruption of PKCα and ILK signaling pathway abolished the negative guidance effects of Shh on RGC axons and resulted in aberrant RGC axon pathfinding at the optic chiasm in vivo, demonstrating a critical role of this pathway in Shh-mediated axon guidance.

MATERIALS AND METHODS

Antibodies and constructs: Anti-PKCα, βI, δ, ζ, μ and anti-Phospho-PKCα (Ser657) were obtained from Santa Cruz Biotechnology. Anti-Phospho-PKC (pan), anti-Phospho-ILK (Thr173) and anti-integrin β1 $pTpT^{788/789}$ were purchased from Cell Signaling, Abgent and Invitrogen, respectively. Anti-GAP-43 and recombinant PKCα were from Millipore. Dominant-negative PKCα (Soh and Weinstein, 2003) and RCASBP-Y DV constructs were provided by Dr. B. Weinstein and Dr. W. Pavan through Addgene. pGEX-ILK-WT was a gift from Prof. Chuanyue Wu (Univ. of Pittsburgh). Mutations of ILK were generated by site-directed mutagenesis using QuikChange kit (Stratagene). To generate RCAS constructs, full length DN-PKCα and ILK-Double Mutants (ILK-DM) were first cloned in-frame into entry vector pENTR1A-GFP-N2 (a generous gift from Drs. E. Campeau and P. Kaufman, UMass. Med. Sch.)(Campeau et al., 2009), then a Gateway Cloning system (Invitrogen) was used to recombine target sequences into the retroviral vector RCASBP-Y DV. All constructs were verified by DNA sequencing. RCAS virus was prepared by transfection of a chicken fibroblast line, DF1 and concentrated by ultracentrifugation as described before (Chau et al., 2006).

Cell culture and time-lapse experiments: Fertilized White Leghorn eggs (Charles River Laboratories) were incubated in a moisturized 38°C incubator. Axon cultures were prepared as described previously (Kolpak et al., 2009). To prepare RCAS-virus infected RGC axon culture, RCAS viruses were microinjected into optic vesicles at E1.5 and then the embryos were returned to incubator until E6 or E7. P19 cells were differentiated into neuronal cells as previously described (Jones-Villeneuve et al., 1982).

Time-lapse experiments were performed on a Carl Zeiss Axiovert 200 microscope equipped with a 37°C heated stage. Time-lapse images were recorded for 30 minutes at 1-minute intervals. To study the effect of PKC on Shh-induced growth cone collapse, cultures were pre-incubated with 100 nM Gö6976 (EMD Biosciences) or 50 nM PKC_{β} inhibitor (EMD Biosciences) for 30 minutes before adding vehicle or Shh (recombinant Shh-N, R&D system). Growth cone collapse was scored by a loss of lamellipodia and decrease of filopodia number to three and less per growth cone.

Cell fractionation and immunoblotting: Dissected E6 retinas were incubated in media for 15 minutes and then treated with either vehicle or 3.0 μg/ml Shh for the time indicated. After washing twice with ice-cold PBS, retinal lysates were prepared in Buffer A (20 mM Tris-HCl, pH 7.5, 0.25 M sucrose, 2 mM EGTA, 2 mM EDTA, protease and phosphotase inhibitor cocktails) by first passing through a needle and then sonicating. The lysates were centrifuged at 100,000 g for 1 hour and the supernatant was designated as cytosolic fraction. The pellet was re-suspended with buffer A containing 1% TritonX-100 on ice for 30 min. Following centrifugation as before, the supernatant was collected as detergent-soluble fraction. The pellet was dissolved with buffer A containing 1% SDS and designated as detergent-insoluble fraction. Protein concentration was determined by Bio-Rad detergent compatible protein assay. Equal amounts of protein were loaded onto SDS-PAGE gel, and a standard western blot protocol was followed.

Immunoprecipitation assay: Differentiated P19 cells are treated with vehicle control or Shh (3.0ug/ml) for 5mins. Ice-cold PBS is used to stop the reaction. Cells are lysed in buffer and then incubated with anti-PKCα at 4 degree overnight

Protein purification and in vitro phosphorylation: E.coli strain BL21 (DE3) was used for expression of the glutathione S-transferase (GST) fusion proteins of ILK-WT and mutants. GST fusion proteins were purified by glutathione-agarose beads (Sigma) according to the manufacturer's instruction. For in vitro phosphorylation assay, purified recombinant PKCα (0.1 μg) (Millipore) and ILK (0.4 μg) were mixed in 20 μl of the reaction mixture (20 mM HEPES, pH 7.4, 10 mM $MgCl_2$, 1 mM $CaCl_2$, 2.5 μM ATP, 0.125 μg/ml phosphatidylserine, 200 nM PMA). After addition of 0.75 μl of [γ-^{32}P] ATP (10mCi/ml) (Perkin Elmer), the reaction mixture was incubated for 30 min at 30°C. Samples were analyzed on SDS-PAGE and then developed by Phosphoimager.

DiI labeling and immunofluorescent staining: RCAS viral stocks were microinjected into optic vesicles at E1.5 as described previously (Jin et al., 2003), and the embryos were returned to the incubator until E7. At E7, the lens and vitreous body of the right eyes were removed and a small amount of DiI (1 mg/ml) was injected into the optic disc with a fine glass micropipette. The embryos were then fixed with 4% paraformaldehyde at 37°C for 2 to 3 weeks. After that, the embryos were imbedded in 3% agarose and sectioned at 150 μm on a vibratome. Sections were mounted on coverslips and examined on a Nikon Eclipse E600 microscope or Leica TBS SP2 confocal microscope.

Immunocytochemistry staining was carried out similarly as described previously (Kolpak et al., 2009). Fluorescent images were acquired using a 63x objective on a Zeiss Axiovert 200 microscope. The background staining of the antibodies was determined by omitting the primary antibodies. For quantification of fluorescence signals using the Image J software, axons were randomly chosen throughout the coverslips and images were taken with a fixed exposure time (below saturation and with minimal background signal) for all samples. Because Shh reduced growth cone area, a segmented line tracing tool was used to draw a line in the center of the axon in Image J to measure the fluorescence intensity from the tip of the growth cone to the end of the shaft in the image. Mean fluorescent intensity along the line was recorded to compare the results. Because the exposure was set to minimize the background fluorescence level, the background signal was not significantly increased due to growth cone collapse, as shown in the experiment skipping the primary antibody. To quantify the colocalization of GAP43 and phospho-PKCα (Ser657), fluorescent images of the two channels were taken using a Leica TBS SP2 confocal microscope with fixed, unsaturated exposure settings. Quantification of colocalization were carried out as described previously (Jaskolski et al., 2005). Normalized mean deviation product (nMDP), index of correlation (I_{corr}), and the color map with cooler color representing less colocalization and hotter color representing stronger colocalization were generated using the Image J plugin software. Thirty paired images were measured in each condition.

Axon turning assay, dextran internalization and calcium imaging: Dextran uptake, axon turning assay and data analyses were carried out similarly as in our previous study

(Kolpak et al., 2009). For dextran internalization, RCAS-virus infected retinas were dissected at E6 or E7 and cultured overnight. The cultures were treated with 2.5 mg/ml 10K tetramethylrhodamine dextran (Invitrogen) with 3.0 μg/ml Shh or vehicle for 2 mins at 37°C, washed, and then fixed in 4% paraformaldehyde. GFP-positive axons were photographed and analyzed.

To study the effect of PKC on Shh-induced axonal turning, RGC cultures were pre-incubated with 5 nM Gö6976 (inhibiting PKCα) for 1 hour or 50 nM PKC$_\beta$ inhibitor for 30 minutes prior to the turning assays. For the experiments with the DN-PKCα and ILK-DM-expressing axons, RCAS-virus infected RGC cultures were prepared as above, and the turning assay was performed on GFP-positive axons.

For calcium imaging, RGC cultures were loaded with 5 μM Fluo-3 AM (Invitrogen) for 30 minutes, rinsed with media prior to imaging. Imaging was initiated 20 seconds before the pulsing of picospritzer delivering vehicle or Shh protein, with a similar setup as used in the turning assay above. Images were acquired at 1 frame/s with excitation wavelength at 488 nm. In some experiments, 5 μM cyclopamine (Toronto Research Chemicals) was added to the media 30 minutes before application of Shh.

RESULTS

As we and others previously showed (Trousse et al., 2001, Kolpak et al., 2009), minutes after the addition of Shh (2.5-3.0 μg/ml) into the culture media, chick RGC axons exhibited rapid growth cone collapse (67.0±2.3 % of total axons collapsed); a loss of lamellipodia and retrieval of filopodia occurred, followed by axon retraction (Fig. 2.1*A*). To explore the mechanism by which Shh induces growth cone collapse, pharmacological inhibitors to various signaling pathways were added prior to the addition of Shh in the culture, and the axonal response was recorded by time-lapse microscopy. Since several PKC isotypes (e.g. α, β, δ, ζ) have been shown to be expressed in RGC axons in mice and chick (Wu et al., 2003, Wong et al., 2004), specific inhibitors of PKC signaling were tested. Some of them, e.g. a PKCδ inhibitor Rottlerin, caused rapid growth cone collapse and axon retraction by themselves at the recommended concentrations precluding their use in the study of Shh signaling (data not shown). In contrast, Gö6976, a widely used inhibitor for PKCα and PKCβI at 100 nM concentration or lower, or a PKCβ-specific inhibitor, did not have any significant effect on RGC axons when added alone. Pre-treatment of Gö6976, however, abolished the effect of Shh on RGC axons. Growth cones did not collapse after addition of Shh (10.8±2.7 % of growth cones collapsed) (Fig. 2.1*B*), rather remained dynamic with motile lamellipodia and filopodia, and no significant axon retraction was observed. In contrast, the PKCβ-specific inhibitor did not block the Shh-induced growth cone collapse (67.1±12.2 % of axons collapsed) or axon retraction (Fig. 2.1*B*). These data suggest that PKCα may play a role in the growth cone collapse in response to Shh.

Figure 2.1. Shh-induced growth cone collapse is blocked by inhibition of PKCα. Time-lapse microscopy of RGC culture was initiated after addition of either vehicle or 3.0 μg/ml Shh. For some experiments, inhibitors to conventional PKC isoforms (Gö6976 or PKC_{β} inhibitor) were added to the cultures for 30 minutes prior to the time-lapse experiment. ***A,*** Bright field images of RGC axons at 0 and 5 min after the addition of vehicle control or Shh. Note that Gö6976 but not the PKC_{β} inhibitor abolished Shh-induced growth cone collapse. Arrows indicate collapsed growth cones. ***B,*** Percentages of RGC growth cones that collapsed within 5 minutes of addition of vehicle or Shh. Growth cone collapse was defined as loss of lamellipodia and reduction of filopodia number to three or less per growth cone. Data are represented as mean±SEM. **p*<0.0001, Student's *t* test. Numbers in parentheses indicate the total number of axons scored from three independent experiments.

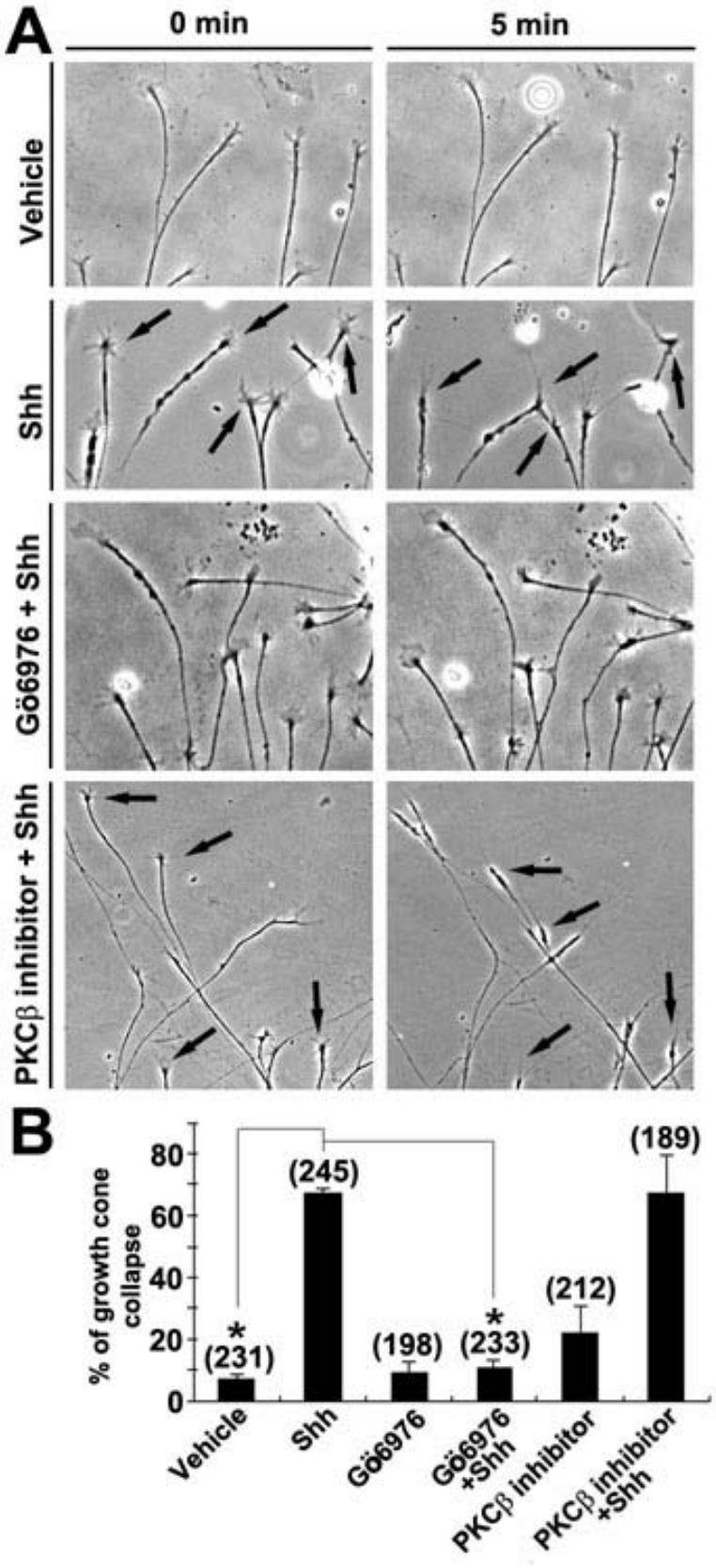
A
0 min
5 min
Vehicle
Shh
Gö6976 + Shh
PKCβ inhibitor + Shh
B
% of growth cone collapse
0
20
40
60
80
(231)
(245)
(198)
(233)
(212)
(189)
*
*
Vehicle
Shh
Gö6976
Gö6976 +Shh
PKCβ inhibitor
PKCβ inhibitor +Shh

One of the hallmarks of activation of various PKC isoforms is the translocation of PKC proteins from the cytosol to specialized cellular compartments (Dempsey et al., 2000, Shirai and Saito, 2002, Rosse et al., 2010). To examine the effect of Shh on PKC protein translocation, E6 chick retinas were dissected and incubated with Shh for 5 and 15 min. Retinal cells were then lysed and subjected to ultracentrifugation to separate the cytosolic proteins from the pellets. The pellets were subsequently extracted with TritonX-100 to further fractionate into TritonX-100 soluble membrane fraction and insoluble fraction, which includes the cytoskeletons and likely TritonX-100-insoluble lipid rafts. Equal amounts of total protein in these fractions were run on SDS-PAGE and blotted with antibodies recognizing PKC isoforms, including anti-PKCα, βI, δ, ζ or μ. Five minutes of Shh treatment lead to a significant increase in the amount of PKCα in the TritonX-100 soluble and TritonX-100 insoluble fractions (average 1.8 and 6.2 folds, respectively) (Fig. 2.2*A,B*). The translocation of other PKCs was not significant except for PKCμ which showed ~1.6 fold increase in the TritonX-100-insoluble fraction (Fig. 2.2*B*). The amount of PKCδ was detectable in cytosolic fraction but too low to be detected in the non-cytosolic fractions. A corresponding decrease of each isotype in cytosolic fraction was not observed, possibly due to the presence of large amount of PKC protein isoforms in the cytosol.

At E6, the newly differentiated RGCs and their elongating axons are exposed at the ganglion side of the retina whereas the undifferentiated cells are exposed at the ventricular side (Prada et al., 1991, Bao, 2008). We were not able to purify the RGCs, because we could not obtain the antibody recognizing the chicken Thy-1, which is

required for the panning procedure for purification of RGCs. To confirm that PKCα activation occurred in the RGC axons in response to Shh, we performed immunofluorescent staining with an antibody recognizing the phosphorylated Ser657 PKCα, or phospho-PKC (pan) antibody that recognizes PKCα, βI, βII, δ, ε, η and θ isoforms when phosphorylated on residues homologous to Ser657 of PKCα. PKCα Ser657 is phosphorylated in activated PKCα (Bornancin and Parker, 1997). Anti-phospho-PKCα Ser657 and anti-phospho-PKC (pan) staining appeared as relatively large puncta inside the axons. Many axons in the control samples appeared negative for the staining, and the most apparent effect of Shh treatment appeared to increase the number of axons containing the positive puncta. The number of puncta inside the axon was also increased. For quantification of the results, axons were randomly chosen throughout the coverslips and images were taken with a fixed exposure time set to minimize background signal and avoid saturation. A segmented line tracing tool was used to draw a line in the center of the axon in Image J to measure the fluorescence intensity from the tip of the growth cone to the end of the shaft in the image. Mean fluorescence intensity on the line was recorded to compare the results. Growth cone collapse did not significantly increase background fluorescence signal as shown in the experiments without the primary antibody (not shown). Compared to the vehicle control, 2 min treatment of Shh significantly increased the level of phospho-PKCα (Ser657), or phospho-PKC (pan) in the RGC axons (Fig. 2.2*C, D*). Because Ser657 or equivalent is the last site of the PKC autophosphorylation loop, phosphorylation of this site on PKCα can be inhibited by Gö6976 (Ginnan et al., 2004). Pretreatment of the RGC culture with Gö6976 at a low concentration of 5 nM, which reportedly inhibits PKCα

Figure 2.2. Shh preferentially activates the PKCα isoform. ***A,*** Chick retinal explants were treated with 3.0 ug/ml Shh for 5 and 15 min. Cell lysates were processed to result in cytosolic, Triton X-100 soluble and insoluble fractions. Western blots were carried out by using antibodies specific for various PKC isoforms and loading controls were shown blotted with GAPDH, Na^+/K^+-ATPase and α-tubulin antibodies. Representative gel image of three independent experiments is shown. ***B,*** Quantification of translocation of PKC isoforms to TritonX-100 soluble and TritonX-100 insoluble fractions. ***C, D,*** Chick RGC axon cultures were treated with vehicle control, Shh alone or Shh in the presence of Gö6976 or PKC_β inhibitor for 2 mins. Representative immunofluorescent images of antibody staining specific for phospho-PKCα (Ser657) and phospho-PKC (pan) were shown. The fluorescent signals were quantified by ImageJ (see Methods). Numbers in parentheses indicate the total number of axons measured from three independent experiments. Data are represented as mean±SEM. **p*<0.01, Student's *t* test.

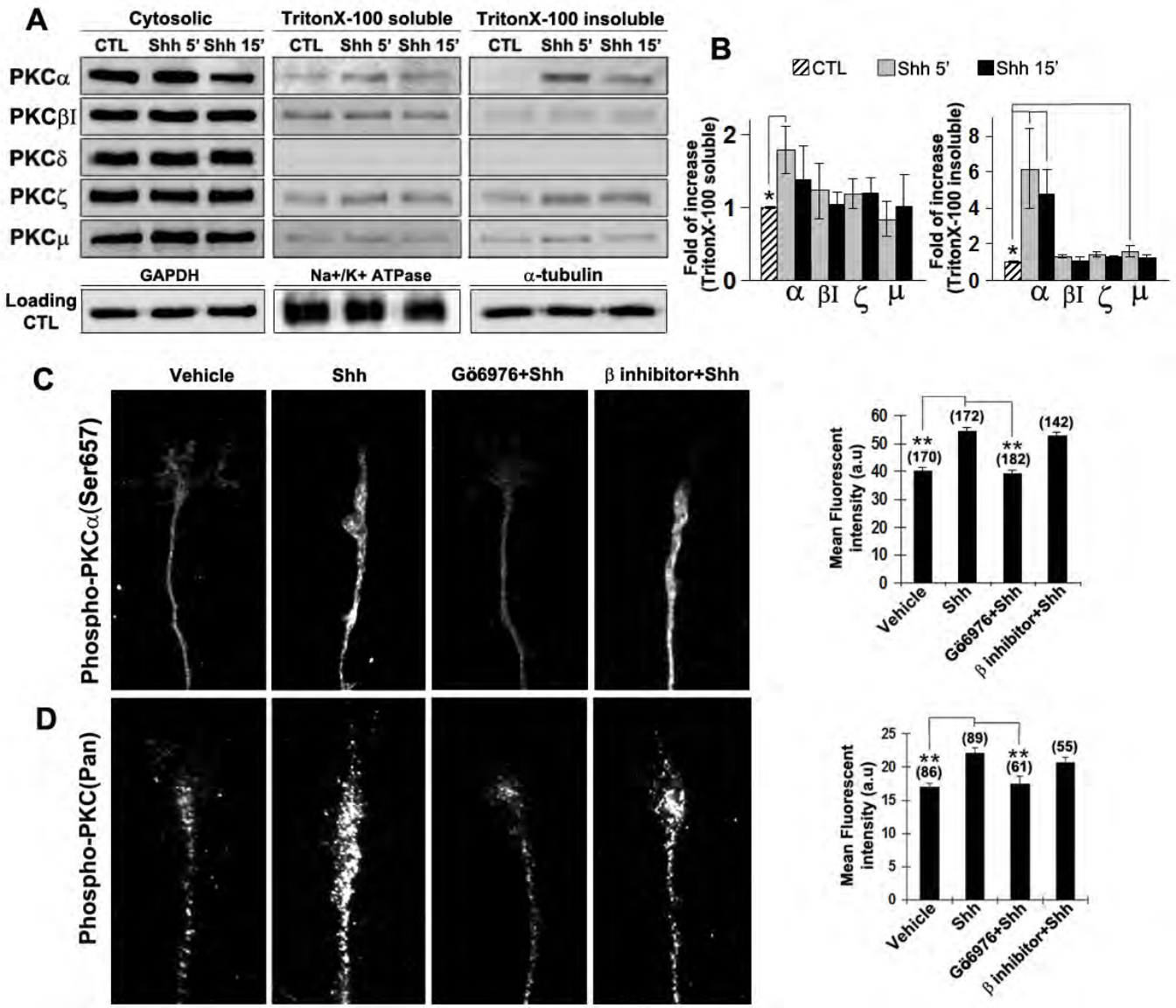
A
Cytosolic
TritonX-100 soluble
TritonX-100 insoluble
CTL Shh 5' Shh 15'
PKCα
PKCβI
PKCδ
PKCζ
PKCμ
GAPDH
Na+/K+ ATPase
α-tubulin
Loading CTL
B
CTL
Shh 5'
Shh 15'
Fold of increase (TritonX-100 soluble)
Fold of increase (TritonX-100 insoluble)
α βI ζ μ
C
Vehicle
Shh
Gö6976+Shh
β inhibitor+Shh
Phospho-PKCα(Ser657)
Mean Fluorescent intensity (a.u)
(170)
(172)
(182)
(142)
D
Phospho-PKC(Pan)
(86)
(89)
(61)
(55)

only (Martiny-Baron et al., 1993), abolished the increase of phospho-PKCα (Ser657) or phospho-PKC (pan) level in the RGC axons by Shh (Fig. 2.2*C,D*), while the PKC_{β} inhibitor did not have an effect. The fact that we observed a similar increase in the level of phospho-PKCα versus phospho-PKC (pan) in response to Shh, and the increase was abolished by pre-incubation with Gö6976 in both cases, suggests that PKCα is the main PKC isoform that is activated by Shh in the RGC axon.

To confirm the observation we obtained in chick RGC cells, we differentiated P19 cells, a pluripotent mouse embryonic carcinoma cell, into neuronal-like cells using retinoic acid and treated with 3.0ug/ml of Shh. As shown in Figure 2.3*A* and *B,* the neurites of the differentiated P19 cells showed rapid retraction within minutes of Shh application (65.8±2.9% Shh-treated vs 19.4±1.9% vehicle-treated), similar to what we saw on RGC cells, suggesting that the differentiated P19 cells were also responsive to Shh. Furthermore, Shh acutely translocated PKCα to TritonX-100 soluble and TritonX-100 insoluble factions of P19 cells, and phosphorylated PKCα at Ser657 site (Figure 2.3 *C* and *D*).

Growth-associated protein 43 (GAP-43), has been shown to be associated with the detergent-resistant lipid rafts in the growth cone through palmitoylation (Arni et al., 1998, Laux et al., 2000). To analyze if PKCα is translocated to detergent-resistant membrane fraction in response to Shh, possibly lipid rafts, RGC cultures were treated with Shh for two minutes and axons were co-stained with anti-GAP-43 and anti-phospho-PKCα (Ser657) antibodies. As shown in Figure 2.4*A*, the punctate staining patterns of GAP-43

Figure 2.3 Shh activates PKCα in differentiated P19 cells. ***A*** and ***B***, P19 cells were differentiated into neuronal-like cells using retinoic acid and cultured on PDL/Laminin coated coverlips 24 hrs before experiments. After vehicle control or Shh (3.0 ug/ml) was added to the culture, filming started. Shh induced rapid neurite retraction (arrow). Representative images of at least four independent experiments are shown. ***C,*** Differentiated P19 cells were treated with vehicle control or Shh (3.0 ug/ml), lysed, immunoprecipitated with anti-PKCα antibody and blotted with anti-phospho-pan antibody. Total PKCα was used as loading control. ***D,*** Translocation experiments were carried out similar to that in Figure 2.2***A***. PMA, a potent activator of PKC, was used as a positive control. For ***C*** and ***D,*** representative gel images of two independent experiments are shown.

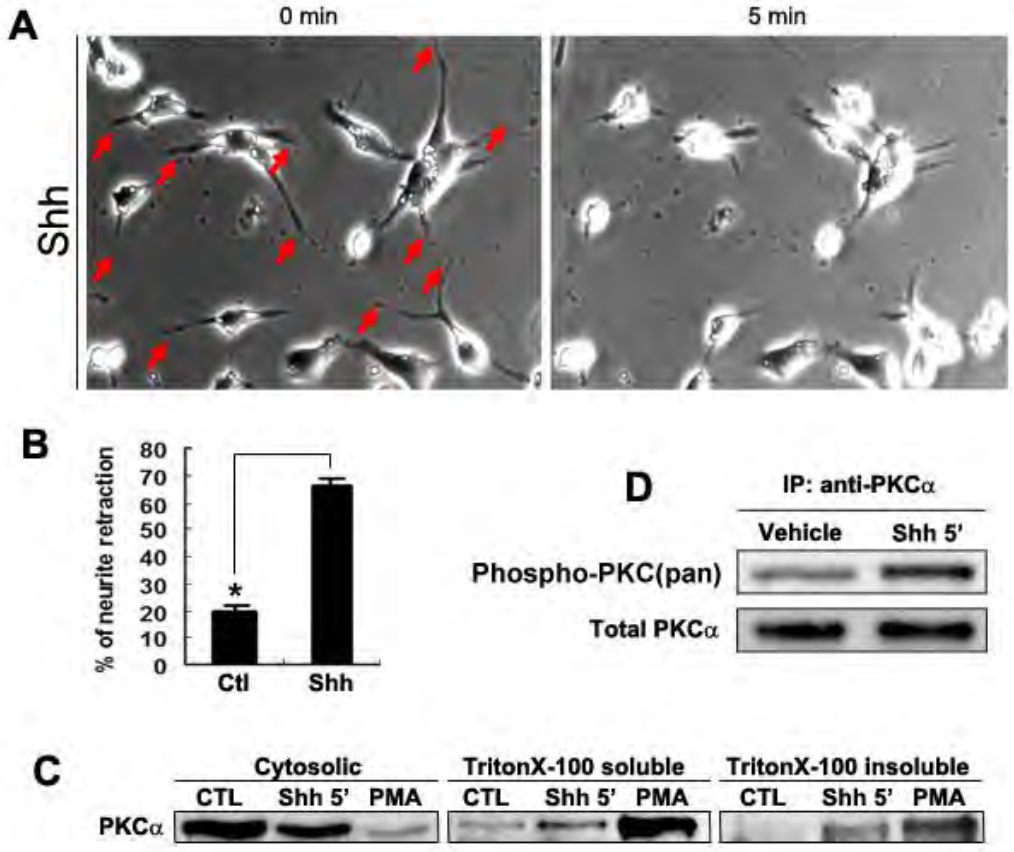
A
0 min
5 min
Shh
B
% of neurite retraction
80
70
60
50
40
30
20
10
0
*
Ctl
Shh
D
IP: anti-PKCα
Vehicle
Shh 5'
Phospho-PKC(pan)
Total PKCα
C
Cytosolic
TritonX-100 soluble
TritonX-100 insoluble
CTL
Shh 5'
PMA
PKCα

and phospho-PKCα (Ser657) were observed to have a marked increase in colocalization after 2 min treatment of Shh. The increase of colocalization was further confirmed by using a quantitative image analysis method designed for evaluation of colocalization of two fluorescent signals (Jaskolski et al., 2005). nMDP values (scaling between -1 to 1) indicate intensity correlation between the two channels with negative values representing non-correlated pixels and positive values representing correlated pixels. Shh significantly increased the number of pixels with positive nMDP values (data not shown), and consequently increased the mean index of correlation (I_{corr}) that measured the fraction of positive nMDP values over total nMDP values (Fig. 2.4*B*). These data suggest that Shh signaling activates PKCα, as shown by a significant increase in phosphorylation of PKCα and translocation from the cytosol to the plasma membrane, possibly concentrated in lipid rafts.

Binding of Ca^{2+} to the N-terminal C2 domain is required for the activation of conventional PKCs (Steinberg, 2008) . We therefore performed Ca^{2+} imaging using the cell-permeable Ca^{2+} indicator Fluo-3 AM. Shh was pulse-applied from a fine glass micropipette positioned at ~150 μm from the growth cone and at 45^{o} angle to the direction of axon extension. As shown in Figure 2.4*C, D*, Shh increased Ca^{2+} level in the growth cone seconds after the onset of Shh application. The magnitude of Ca^{2+} increase ($\Delta F/F$) ranged from ~25% to ~50% and the duration of the increase lasted from 50 seconds to a few minutes. 62.5% of Shh-treated growth cones showed Ca^{2+} increase (n=8) versus 10% in the vehicle treated samples (n=10). Pretreatment with cyclopamine, a specific inhibitor of Shh signaling pathway, reduced the number of growth cones

Figure 2.4. Shh increases colocalization of phospho-PKCα (Ser657) with GAP-43, and elevates Ca^{2+} in the growth cone. ***A-B,*** Shh treatment increased colocalization of phospho-PKCα (Ser657) with GAP-43 in the RGC growth cones. ***A,*** RGC axons were treated with vehicle or Shh for 2 min and stained with antibody specific for GAP-43 or phospho-PKCα (Ser657). Merged confocal images of antibody staining and nMDP quantitative colocalization maps are shown in the 3rd and 4th columns, respectively. In the nMDP colocalization maps, intensity correlation between the two channels, from less to stronger colocalization, is represented by cooler to hotter colors. ***B,*** Quantification of image correlation, I_{corr}, which represents the number of positive nMDP over total number of nMDP in a correlation image. The I_{corr} ranges from 0 to 1, where 0.5 represents randomly distributed signals. Numbers in parentheses indicate the total number of growth cones measured from three independent experiments. Data are represented as mean±SEM. *p<0.01, Student's t test. ***C,*** Shh induces Ca^{2+} elevation in chick RGC growth cone. Fluorescent images of Fluo-3 AM loaded growth cone before and after application of Shh. The fluorescent intensity is represented by pseudo-color in the linear scale (blue=0, red=377, arbitrary units). ***D,*** Average fluorescence change of Ca^{2+} in the growth cone after application of Shh (n=5), depicted as the percentage change normalized to the average fluorescent intensity before the onset of Shh application ($\Delta F/F$). Arrow indicates the onset of Shh pulse from the micropipette.

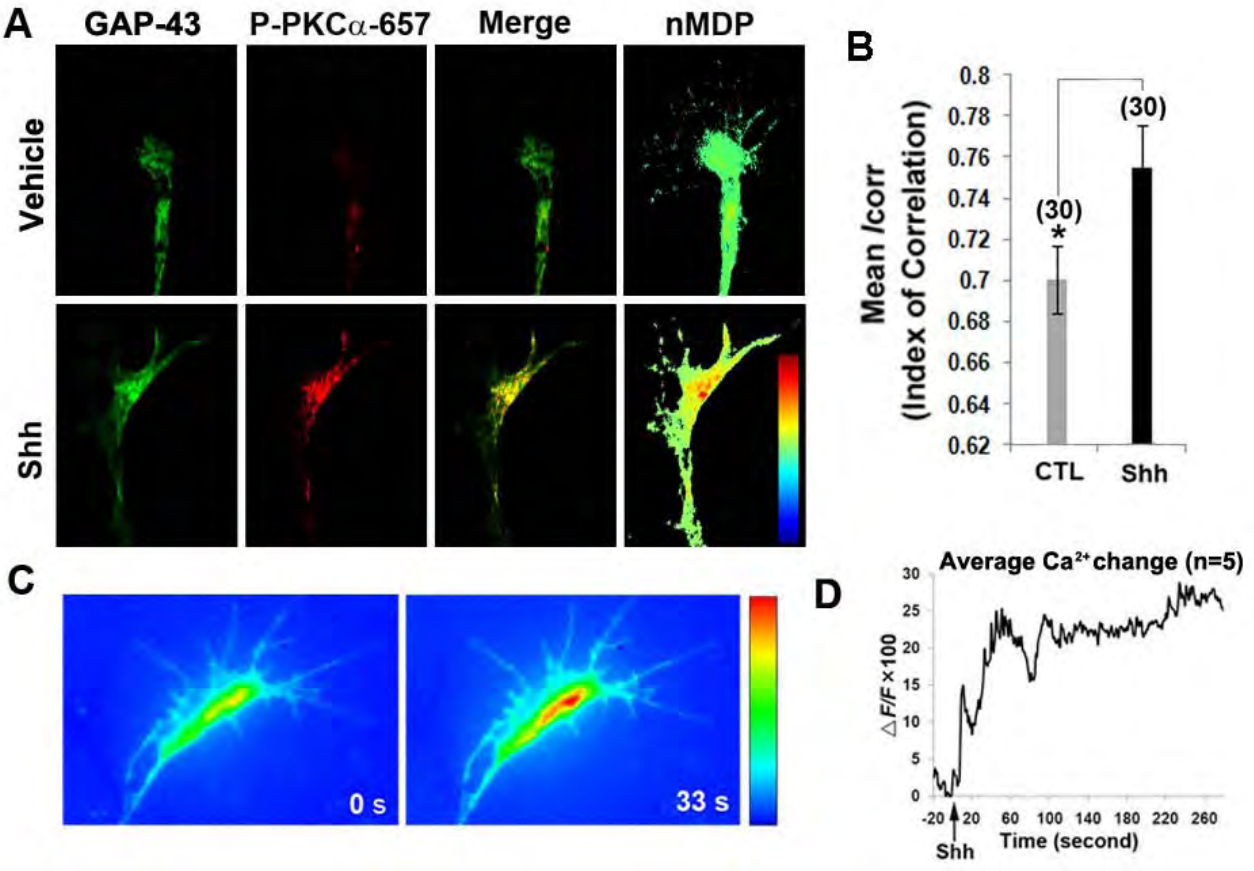
A
GAP-43
P-PKCα-657
Merge
nMDP
Vehicle
Shh
B
Mean /corr
(Index of Correlation)
0.8
0.78
0.76
0.74
0.72
0.7
0.68
0.66
0.64
0.62
(30)
(30)
*
CTL
Shh
C
0 s
33 s
D
Average Ca2+ change (n=5)
△F/F ×100
30
25
20
15
10
5
0
-20
20
60
100
140
180
220
260
Shh
Time (second)

responsive to Shh (2 out of 9 showing Ca^{2+} increase). These results demonstrate that Shh rapidly increases Ca^{2+} level in the RGC growth cones.

We next searched for proteins that act as downstream effectors of PKCα to mediate the effects of Shh in RGC axon guidance. The NetworKin algorithm predicts that PKCα may directly phosphorylate integrin-linked kinase (ILK) at threonine 173 (Linding et al., 2007). As ILK has been shown to be expressed in the neurites of hippocampal neurons, dorsal root ganglion and PC12 cells (Mills et al., 2003, Guo et al., 2007), we tested the possibility that ILK was downstream of Shh-PKCα by staining the RGC axons with an antibody specifically recognizing ILK that is phosphorylated at threonine 173 (ILK-T173). Compared to vehicle control, 2 min treatment of Shh significantly increased the level of phosphorylated ILK-T173 in the RGC axons; this effect was inhibited by pretreatment of RGC culture with Gö6976 prior to Shh (Fig.2.5*B*). Some of the phosphorylated ILK-T173-positive puncta also appeared to colocalize with the phosphorylated PKCα Ser657-positive puncta in RGC axons, although many did not, suggesting a rather transient association (data not shown). These data suggest that Shh increased phosphorylation of T173 on ILK through PKCα activation.

Recombinant wild type ILK protein (ILK-WT), as well as a mutant ILK protein with threonine 173 replaced by alanine (ILK-T173A) were produced. In vitro kinase assay was carried out by incubation of purified recombinant PKCα with the ILK proteins without addition of any cellular extracts. As shown in Figure 2.5*C*, high level of phosphorylation was observed in ILK-WT and the phosphorylation level was decreased

to ~50% in ILK-T173A mutant, suggesting that PKCα can directly phosphorylate ILK on T173 and on an additional unidentified site. A 3-D protein model of ILK was built by using Geno3D and AS2TS software and the potential ILK phosphorylation sites were mapped onto the 3-D model. Sites located on the surface of the protein and in close proximity to the T173 were selected for mutagenesis. Six additional sites (T172, T181, S186, S246, T310 and T332) were mutagenized to alanine in the ILK-T173A constructs to generate double mutants. As shown in Figure 2.5*D*, ILK double mutant T173A/T181A (ILK-DM) appeared not phosphorylated by PKCα in the in vitro phosphorylation assay, while other double mutants exhibited phosphorylation level similar to that of single mutant (ILK-T173A). Although mixed results were reported whether ILK can be auto-phosphorylated (Hannigan et al., 1996, Acconcia et al., 2007, Wickstrom et al., 2010), auto-phosphorylation of ILK was not detected in our assays (Fig. 2.5*C*).

ILK has been implicated in phosphorylating β1 integrin cytoplasmic domain at threonine 788 and 789 (Hannigan et al., 1996, Hannigan et al., 2005), although direct evidence is still lacking. Since β1 integrin has been shown to be important for chemorepulsion of growth cones by MAG (Hines et al., 2010), we examined whether Shh increased the phosphorylation of T788/T789 on β1 integrin. Both immunofluorescent staining on RGC axons and western blot analysis using whole retina showed that phosphorylation level of β1 integrin at T788/T789 appeared unaffected by Shh treatment (Fig 2.5*E, F*). However, this does not rule out that other sites (e.g. S785) may be phosphorylated by ILK.

Figure 2.5. Shh activates ILK through direct phosphorylation by PKCα. *A-B,* Chick RGC axon cultures were treated with vehicle control, Shh alone or Shh in the presence of Gö6976 for 2 mins. The immunofluorescent signals of phospho-ILK-T173 were quantified by ImageJ (see Methods). ***C,*** In vitro kinase reactions were carried out by mixing purified recombinant PKCα with wild type or a single mutant form of ILK (ILK-T173A). Phosphorylation of ILK was analyzed on SDS-PAGE followed by autoradiography. The upper band shows the autophosphorylation of PKCα (81 kDa) and the lower band shows the phosphorylation of ILK-GST fusion protein (≈76kDa). Without PKCα, auto-phosphorylation of ILK-WT was undetectable. ***D,*** Double mutations (ILK-T173A/T181A) but not the other double mutations further reduced ILK phosphorylation to the basal level. Equal loading of the gel was verified by western blot using an anti-GST antibody. ***E,*** Chick RGC axon cultures were treated with vehicle control or Shh for 2 mins. The immunofluorescent signals of phospho-β1-integrin-T788/T789 were quantified by ImageJ. ***F,*** E6 chick retinas were treated with vehicle or Shh for 5 mins, cell lysate were run on SDS-PAGE gel and probed with phospho-β1-integrin-T788/T789. Numbers in parentheses indicate the total number of axons measured from three independent experiments. Data are represented as mean±SEM. **p*<0.001, Student's *t* test.

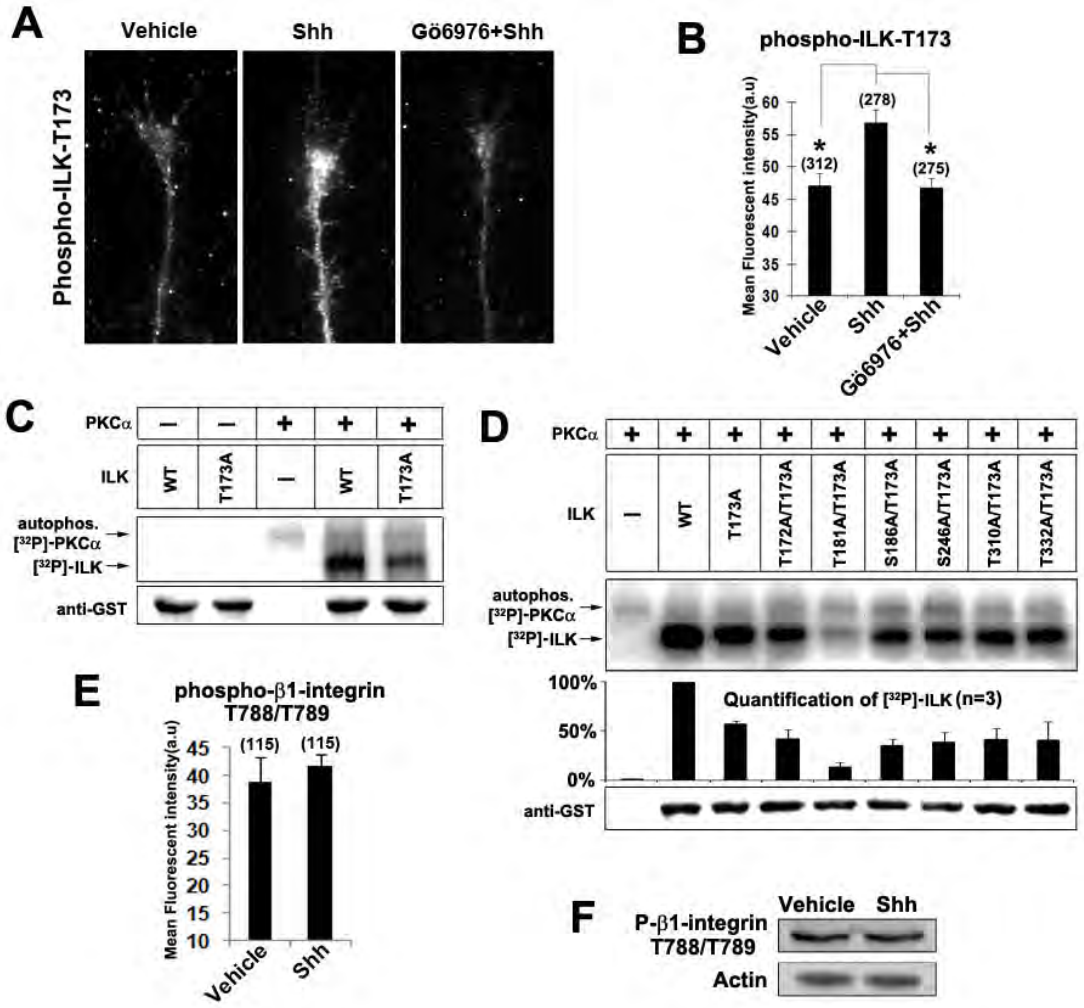
A
Vehicle
Shh
Gö6976+Shh
Phospho-ILK-T173
B
phospho-ILK-T173
Mean Fluorescent intensity(a.u)
(278)
(312)
(275)
Vehicle
Shh
Gö6976+Shh
C
PKCα
ILK
WT
T173A
autophos.
[32P]-PKCα
[32P]-ILK
anti-GST
D
PKCα
ILK
WT
T173A
T172A/T173A
T181A/T173A
S186A/T173A
S246A/T173A
T310A/T173A
T332A/T173A
autophos.
[32P]-PKCα
[32P]-ILK
Quantification of [32P]-ILK (n=3)
100%
50%
0%
anti-GST
E
phospho-β1-integrin
T788/T789
Mean Fluorescent intensity(a.u)
(115)
(115)
Vehicle
Shh
F
Vehicle
Shh
P-β1-integrin
T788/T789
Actin

We next set out to test whether PKCα and its downstream ILK play a role in Shh-induced axonal turning. As in our previous report (Kolpak et al., 2009), Shh (2.5-3.0μg/ml) pulsed from a micropipette positioned at a 45° angle with respect to the original direction of axon extension caused repulsive turning of the RGC axons. The majority of growth cones turned away from the Shh gradients, with an average turning angle of -32.89° compared to the control (< 5°) (Fig. 2.6*A-D*). Pre-treatment with Gö6976, but not the PKC_{β} inhibitor, abolished Shh-induced repulsive turning, yielding an average turning angle of 4.74° and - 26.43°, respectively (Fig. 2.6*B-D*). Random turning of RGC axons was observed in the Gö6976-treated cultures, suggesting that inhibition of PKCα does not affect the ability of the axon to turn but affects their turning response to Shh.

Dominant-negative PKCα (K368R) with a GFP fusion at C-terminus was also constructed into a replication-competent retroviral RCAS vector (RCAS-DN-PKCα). The K368R mutation at the ATP-binding site of the PKCα abolishes its kinase activity (Ohno et al., 1990). In addition, ILK-DM (T173A/T181A) fused with GFP at the C-terminus was also cloned into the RCAS vector (RCAS-ILK-DM). Retroviral stocks were produced and injected into optic vesicles in the chick embryos at E1.5. RGC cultures were prepared from E6 or E7 retina and wide spread infection was observed (Fig. 2.9 *A, C, E*). Axons infected with RCAS-DN-PKCα, RCAS-ILK-DM or control RCAS-GFP were identified by expression of GFP and selected for turning assays. Similar repulsive turning was observed in the RCAS-GFP-infected axons in response to Shh, compared to uninfected controls (- 23.04° vs - 32.89°, respectively) (Fig. 2.6*B-D*). A significant inhibition of Shh-induced turning was observed by expression of RCAS-DN-PKCα or

Figure 2.6. Activation of PKCα and ILK is required for the repulsive axon turning induced by Shh. ***A,*** Dark field images of RGC growth cones before (0 min) and after (10 min and 20 min) exposure to a vehicle or Shh gradient delivered by a micropipette positioned at 45^{o} angle to the direction of axon growth (arrow). ***B,*** Superimposed traces depict the trajectory of wild type RGC axon extension in the presence or absence of PKC signaling pathway inhibitors in the culture media (upper row). For some experiments, RGC axon cultures were derived from retinas infected with retroviruses, including RCAS-GFP, RCAS-DN-PKCα or RCAS-ILK-DM (lower row). Infected axons were selected based on GFP fusion protein signals. The origin is the centre of the growth cone at the beginning of the recording and the original direction of axon extension coincides with the *y*-axis. Arrows indicate the direction of the Shh protein gradient. Tick marks on the *x*- and *y*-axis represent 5μm. ***C,*** Average axonal turning angles and extension under various experimental conditions. Data are represented as mean±SEM. $*p<0.001$, $**p<0.05$, Student's *t* test. ***D,*** Cumulative distribution plots of axonal turning angles of each condition. Each point represents the turning angle of growth cone at the end of 20 min exposure to vehicle control or Shh. The percentage represents the percentage of growth cone bearing turning angle ≤ the value indicated on the *x* axis. Positive angles represent axon turning toward the pipette, whereas negative angles represent axon turning away from the pipette. Gö, Gö6976, β inhibitor, PKC_{β} inhibitor.

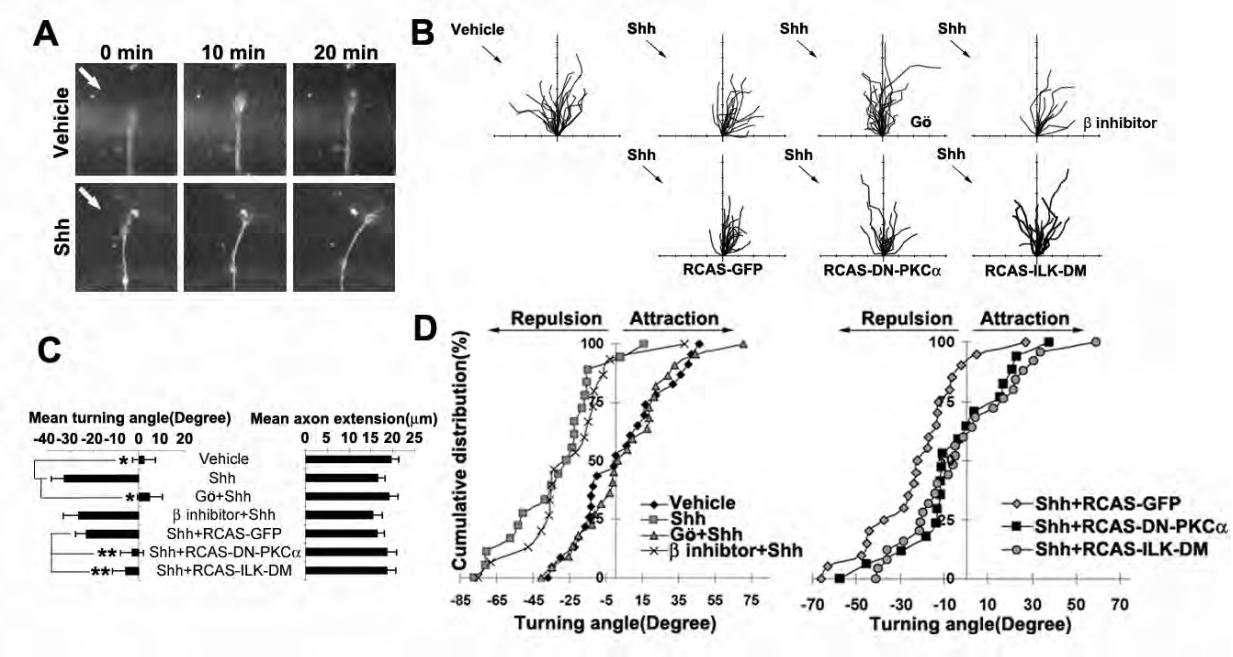
A
0 min
10 min
20 min
Vehicle
Shh
B
Vehicle
Shh
Shh
Shh
Gö
β inhibitor
Shh
Shh
Shh
RCAS-GFP
RCAS-DN-PKCα
RCAS-ILK-DM
C
Mean turning angle(Degree)
-40 -30 -20 -10 0 10 20
Mean axon extension(μm)
0 5 10 15 20 25
Vehicle
Shh
Gö+Shh
β inhibitor+Shh
Shh+RCAS-GFP
Shh+RCAS-DN-PKCα
Shh+RCAS-ILK-DM
D
Repulsion
Attraction
Cumulative distribution(%)
100
75
50
25
0
Vehicle
Shh
Gö+Shh
β inhibtor+Shh
-85 -65 -45 -25 -5 15 35 55 75
Turning angle(Degree)
Repulsion
Attraction
Shh+RCAS-GFP
Shh+RCAS-DN-PKCα
Shh+RCAS-ILK-DM
-70 -50 -30 -10 10 30 50 70
Turning angle(Degree)

RCAS-ILK-DM, with an average turning angle of -3.14° and -5.89°, respectively (Fig. 2.6*B-D*). In all cases, the rates of axon extension were not significantly affected by the viral infection (Fig. 2.6*C*). These results demonstrate that PKCα and ILK activities are required for Shh-induced repulsive axon turning.

We previously reported that negative factor-induced macropinocytosis plays a critical role in growth cone collapse and repulsive axon turning elicited by these factors (Kolpak et al., 2009). Shh-induced macropinocytosis preferentially occurred on the side of the growth cone facing the Shh protein gradient and inhibition of macropinocytosis appeared to block the growth cone collapse and repulsive axon turning induced by Shh (Kolpak et al., 2009). To assess the role of PKCα and ILK in Shh-induced macropinocytosis, RCAS virus-infected RGC axon cultures were labeled with fluorescently-conjugated dextran together with Shh for 2 min. As shown in Figure 2.7*A*, dextran-labelled macropinosomes were predominantly present in the growth cone. The control RCAS-GFP-infected axons showed similar percentages of axons containing dex+ vesicles as those in the uninfected samples, with or without the addition of Shh (data not shown). Samples infected with RCAS-DN-PKCα or RCAS-ILK-DM showed similar rates of dextran uptake in the basal condition without Shh, as those infected with RCAS-GFP (Fig. 2.7*A'*). However, the RCAS-DN-PKCα and RCAS-ILK-DM infected axons showed a significant reduction in Shh-induced macropinocytosis compared to RCAS- GFP-infected samples (Fig. 2.7*A'*). These results demonstrate that disruption of PKCα and ILK function diminished macropinocytosis in RGC axons in response to Shh.

Figure 2.7. Expression of DN-PKCα and ILK-DM inhibited Shh-induced dextran uptake. ***A, A',*** RGC axons infected with various RCAS viruses were treated with vehicle control or Shh for 2 mins with 10K rhodamine dextran. Representative fluorescent images of GFP-positive axons are shown. Arrowheads indicate dextran labeled macropinosomes. Percentages of dextran^{+} axons were quantified in the infected GFP-positive axons and the data were normalized to control. ***B, B',*** Growth cone collapse was also scored in the RCAS virus-infected RGC axons in response to 5 min treatment of vehicle control or Shh. Data are represented as mean±SEM. * p<0.05, ** p< 0.01, Student's t test. Numbers in parentheses indicate the total number of axons scored from three independent experiments. Scale bars, 5μm.

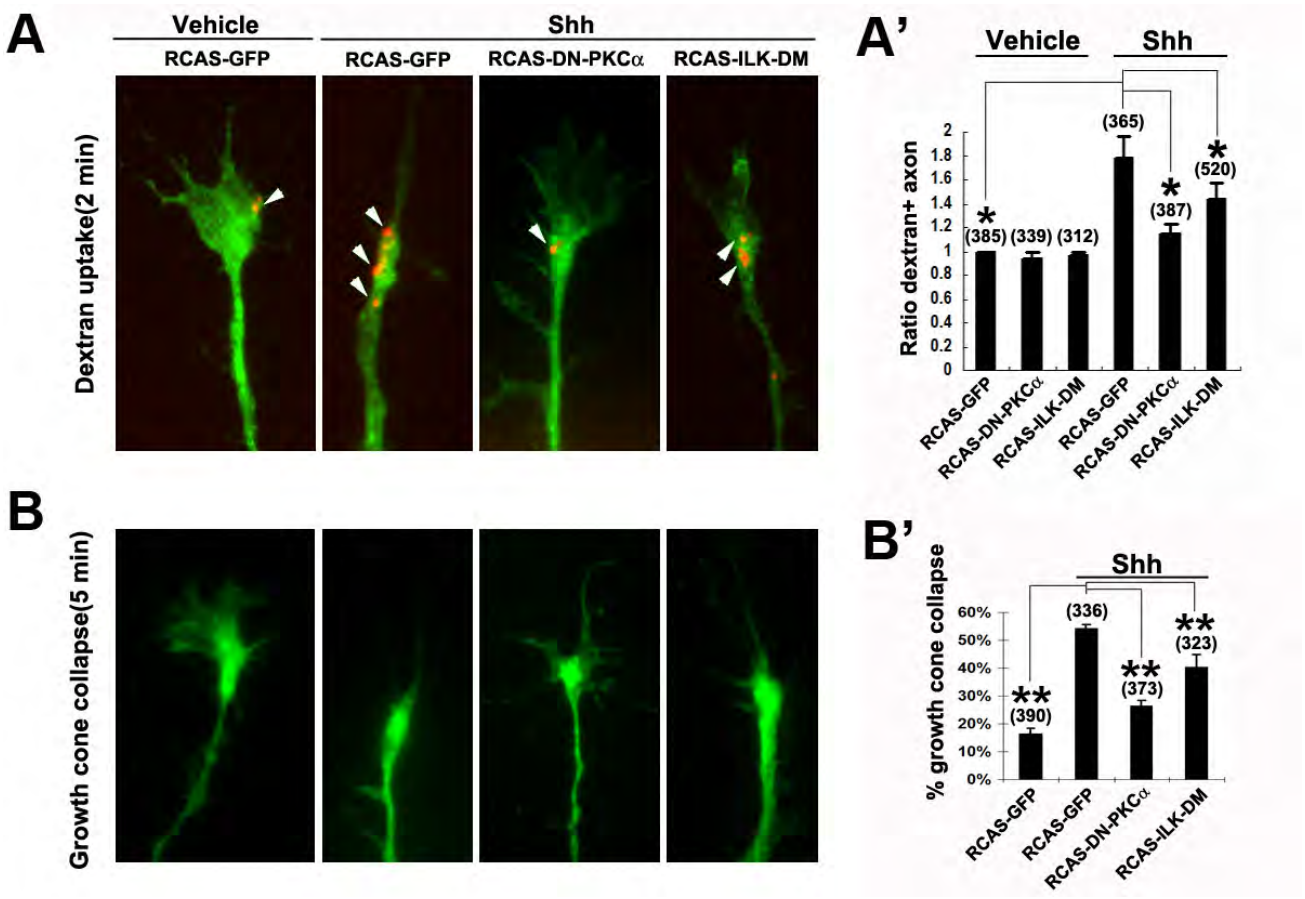
A
Vehicle
Shh
RCAS-GFP
RCAS-GFP
RCAS-DN-PKCα
RCAS-ILK-DM
Dextran uptake(2 min)
A'
Vehicle
Shh
Ratio dextran+ axon
(385)
(339)
(312)
(365)
(387)
(520)
RCAS-GFP
RCAS-DN-PKCα
RCAS-ILK-DM
RCAS-GFP
RCAS-DN-PKCα
RCAS-ILK-DM
B
Growth cone collapse(5 min)
B'
Shh
% growth cone collapse
(390)
(336)
(373)
(323)
RCAS-GFP
RCAS-GFP
RCAS-DN-PKCα
RCAS-ILK-DM

Consistently, expression of DN-PKCα and ILK-DM significantly inhibited the Shh-induced RGC growth cone collapse (Fig. 2.7*B, B'*). Expression of DN-PKCα appeared to completely abolish the Shh-induced growth cone collapse, whereas expression of ILK-DM resulted in a significant inhibition of axonal response to Shh but to a lesser extent than that of DN-PKCα (Fig. 2.7*B'*). These observations are consistent with the notion that negative factor-induced macropinocytosis is closely associated with repulsive axon turning and growth cone collapse elicited by these factors.

Finally, we analyzed the roles of PKCα and ILK in Shh-mediated RGC axonal guidance in vivo. It has been shown that a high levels of Shh are present at the anterior and posterior borders of the developing chick optic chiasm to confine the RGC axon projection within the borders at the chiasm (Trousse et al., 2001). In mouse, injection of an antibody-producing hybridoma to neutralize Shh protein at the chiasm region resulted in an increase of RGC axonal projections into the ipsilateral tract and contralateral optic nerve (Sanchez-Camacho and Bovolenta, 2008). However, the signaling pathway that mediates the effect of Shh on RGC pathfinding at the chiasm remains unclear. To determine whether the PKCα-ILK pathway may be involved in the effect of Shh on guiding the RGC axon at the chiasm, optic vesicles were injected with the replication-competent RCAS viruses expressing GFP, or the GFP fusion with the DN-PKCα or ILK-DM at E1.5. At E7, Dil was injected unilaterally into the right eye cups to label the RGC axons. In chicken, 100% of RGC axons cross at the optic chiasm to the contralateral side. In the control group expressing GFP, 1 out of 10 embryos showed minor projection abnormality.

Figure 2.8. Expression of DN-PKCα and ILK-DM resulted in misguidance of chick RGC axons at optic chiasm. The optic vesicles of the chick embryos were injected with RCAS viruses and DiI was injected into the optic disc of one eye at E7. DiI was allowed to diffuse for 2 to 3 weeks to label the RGC axon pathway. ***A,*** In RCAS-GFP infected retina, DiI-labeled RGC axon exhibit normal pathfinding at the chiasm projecting into the contralateral optic tract (asterisk). ***B-E',*** Misprojection of RGC axons was found at the chiasm in the samples infected with RCAS-DN-PKCα (***B-D***) or RCAS-ILK-DM (***E, E'***). Axons were misrouted into the ipsilateral optic tract (arrowheads) and contralateral optic nerve (arrows). ***A', B', E'*** are higher magnification views of the regions boxed in ***A, B, E,*** respectively. ***C, D,*** Confocal images of two consecutive sections of a RCAS-DN-PKCα infected sample. Vertical dash line indicates the midline. * represents the contralateral optic tract.

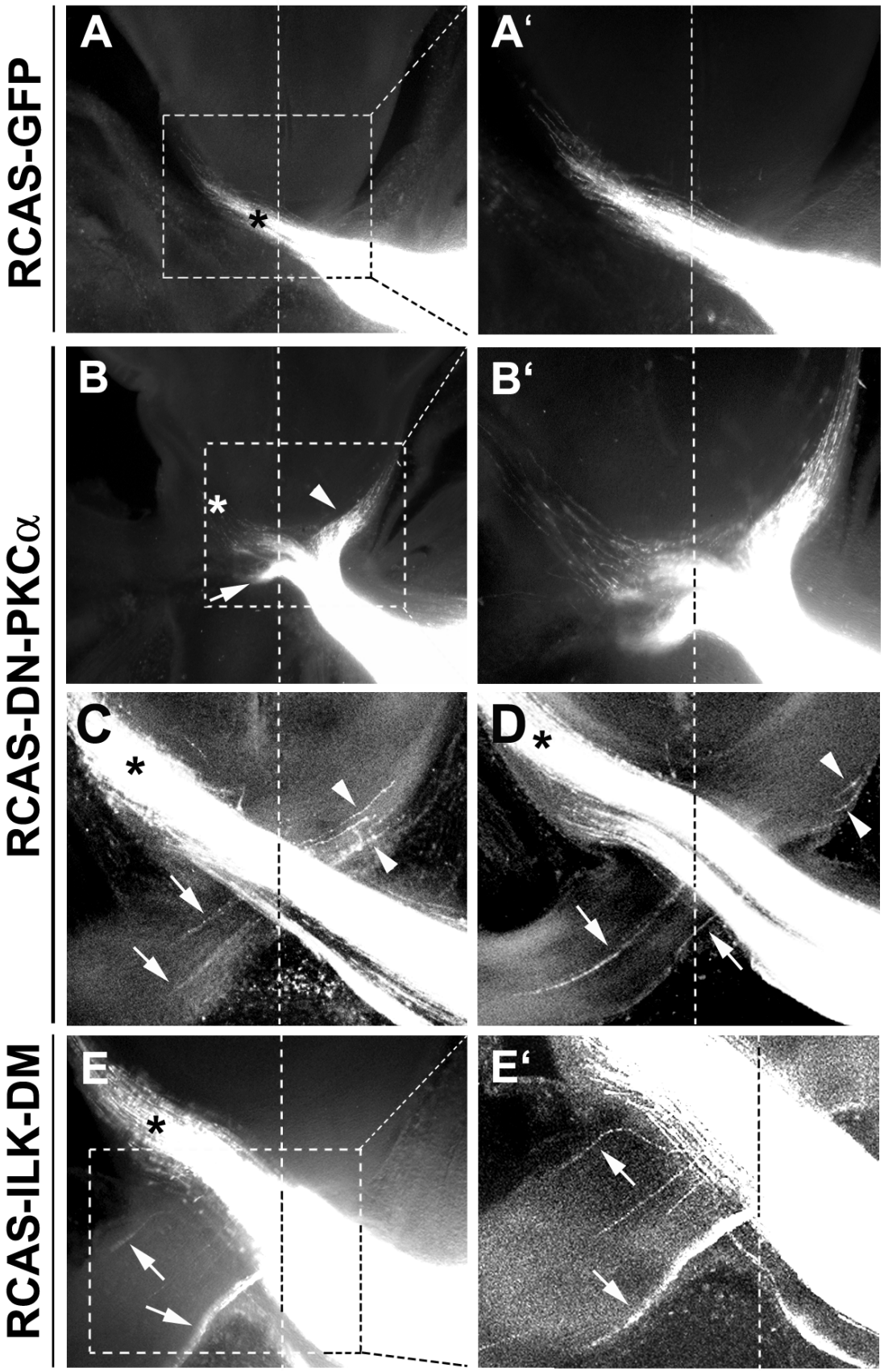
RCAS-GFP
RCAS-DN-PKCα
RCAS-ILK-DM
A
A'
B
B'
C
D
E
E'

A small number of errors of axon projection are known to occur during embryonic development which is corrected at later stages (O'Leary et al., 1983). In the embryos with expression of DN-PKCα, the optic nerve appeared loose at the chiasm, and RGC axon misprojection at the chiasm was observed in 100% of the injected embryos (n=10 embryos). In 2 out of 10 embryos injected with RCAS-DN-PKCα, severe misprojection of RGC axons was observed at the chiasm; a large fraction of axons failed to cross the diencephalon midline and projected ipsilaterally, or crossed the midline but deviated into the contralateral optic nerve of the un-labeled eye (Fig. 2.8*B*, *B'*). Axons that did project to the correct contralateral optic tract appeared disorganized at the midline and some splayed out from the bundle (Figure. 2.8*B'*). In the rest of the embryos (n=8), a less severe phenotype was observed; small bundles of axons were observed to erroneously traverse into the opposite optic nerve or ipsilateral optic tract (Fig. 2.8*C-D*). 100% of embryos injected with RCAS-ILK-DM (n=10) also showed axon misprojection at the chiasm, similar to the less severe phenotypes in the RCAS-DN-PKCα injected samples (Fig. 2.8*E-E'*). Axons appeared disorganized, splayed out from the bundle, and erroneously projected to the opposite optic nerve or ipsilateral optic tract. No obvious axonal growth effect was observed in the injected embryos. We previously reported that a low concentration of Shh acted as a positive factor in guiding the RGC axon toward the optic disc (Kolpak et al., 2005). We examined the RGC axon projection patterns inside the retina in the injected embryos. No obvious defect of intraretinal projection of RGC axons towards the optic disc was observed by expression of DN-PKCα or ILK-DM (Fig. 2.9). This is consistent with the in vitro experimental results that the positive effect of low concentrations of Shh on RGC axons was not inhibited by pre-treatment of PKCα

inhibitor Gö6976 (data not shown). Therefore, PKCα-ILK pathway along with other signaling events in the axons specifically mediates the negative guidance effect of high concentration of Shh on RGC axons.

Figure 2.9. Intraretinal projection of RGC axons was not affected by expression of DN-PKCα and ILK-DM. The optic vesicles of the chick embryos were injected with RCAS-GFP, RCAS-DN- PKCα or RCAS-ILK-DM at E1.5. Retinas were harvested at E7, flat-mounted with the ganglion side up, and wide-spread GFP expression was observed (***A, C, E***). Immunofluorescent staining with an anti-neurofilament antibody (***B, D, F)*** showed the trajectories of RGC axons. In all cases, the projection patterns of RGC axon toward the optic disc appeared normal (some minor aberrance is due to the curvature of the retinal surface). Arrows indicate the direction to the optic disc.

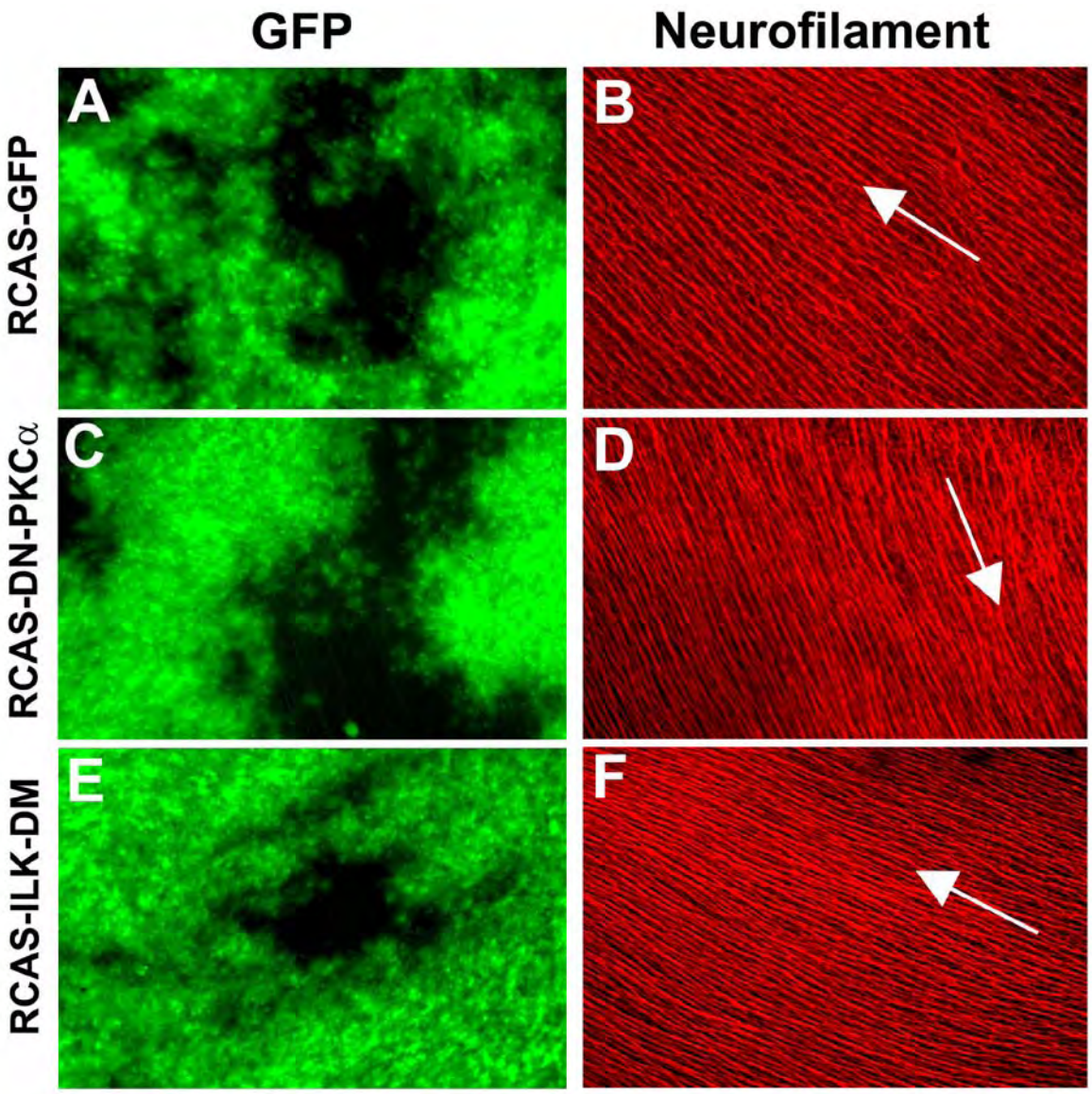
GFP
Neurofilament
RCAS-GFP
RCAS-DN-PKCα
RCAS-ILK-DM
A
B
C
D
E
F

DISCUSSION

In this paper, by both in vitro and in vivo experiments, we demonstrate that a novel signaling pathway consisting of PKCα and ILK specifically mediates the negative guidance effects of high concentrations of Shh on RGC axons. Despite the reports of direct actions of Shh on growth cones of various axons, noncanonical signaling pathways of Shh mediating its effects in axon guidance have just begun to be elucidated. Shh rapidly increased Ca^{2+} concentration, and activated PKCα and ILK in the growth cones of RGC axons. By in vitro kinase assay, we found that PKCα directly phosphorylated ILK, and identified two phosphorylation sites on ILK. Inhibition of PKCα or expression of a mutant form of ILK (T173A/T181A) that eliminates the phosphorylation by PKCα significantly inhibited the negative guidance effects of Shh, both in vitro and in vivo.

Expressed in the dorsal and posterior borders of the chiasm in chick and mouse embryos, Shh has been implicated to play an important role in promotion of axon fasciculation and defining a constrained pathway for RGC axon pathfinding at the chiasm (Trousse et al., 2001, Sanchez-Camacho and Bovolenta, 2008). Injection of E13.5 mouse embryos with a hybridoma producing a Shh-blocking antibody resulted in RGC axon guidance defects at the chiasm; the RGC axon bundles were disorganized and expanded at the chiasm region (Sanchez-Camacho and Bovolenta, 2008). Although Shh could act directly onto the RGC axons in vitro, patterning defects in the midbrain region around the chiasm during retinal axon development due to neutralizing of Shh activity for a few days, could not be completely ruled out as a contributing factor to the aberrant axon

Figure 2.10. Model of PKCα- ILK signaling in RGC axon guidance. ***A,*** In chick RGC axons, Shh decreases $[cAMP]_i$ (Trousse et al., 2001a) and increases $[Ca^{2+}]_i$ leading to phosphorylation and translocation of PKCα to the plasma membrane. Activated PKCα phosphorylates ILK. The PKCα-ILK and the Rho GTPase pathways (Kolpak et al., 2009) are critical for Shh-induced negative axon guidance effects. ***B,*** In wild-type chick embryos, RGC axons that originate from optic disc cross at the optic chiasm to the contralateral optic tract. ***B',*** Expression of DN-PKCα or ILK-DM results in a portion of axons that fail to respond to Shh, leading to aberrant axon pathfinding at the chiasm. PM, plasma membrane; V, Ventral; D, dorsal; N, nasal; T, temporal; on, optic nerve; ot, optic tract.

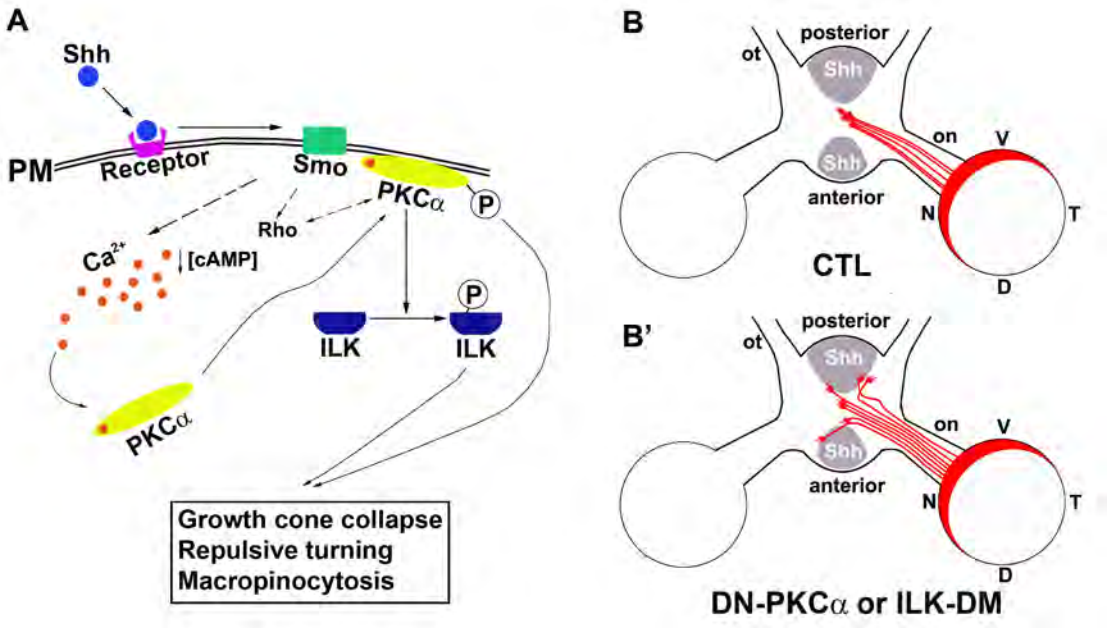
A
Shh
PM
Receptor
Smo
PKCα
P
Rho
Ca2+
[cAMP]
ILK
P
ILK
PKCα
Growth cone collapse
Repulsive turning
Macropinocytosis
B
posterior
ot
Shh
on
V
Shh
anterior
N
T
CTL
D
B'
posterior
ot
Shh
on
V
Shh
anterior
N
T
D
DN-PKCα or ILK-DM

pathfinding at the chiasm (Sanchez-Camacho and Bovolenta, 2008). In our experiment, expression of dominant negative PKCα and the double mutant of ILK (T173A/T181A) resulted in a defasciculation, disorganization and misprojection of RGC axons at the chiasm (Fig. 2.10), similar to the phenotypes reported by injection of anti-Shh antibody in chiasm region in mouse embryos (Sanchez-Camacho and Bovolenta, 2008). These results support the previous suggestion that Shh may act directly on the RGC axons as a guidance factor rather than patterning the neural tube indirectly (Trousse et al., 2001, Sanchez-Camacho and Bovolenta, 2008). The presence of other guidance factors such as Slit1 and Slit2 in the area may help confine the misprojected axons to existing axonal tracks including ipsilateral optic tract and the contralateral optic nerve rather than entering the preoptic or hypothalamic area, when the response to Shh was interfered at the chiasm (Marcus and Mason, 1995, Erskine et al., 2000).

A novel PKC isoform, PKCδ, was shown to be essential for GLI-dependent reporter transcription in the canonical signaling pathway in the mouse LIGHT2 cells (Riobo et al., 2006). However, the involvement of PKCα in Shh signaling has not been previously demonstrated. Translocation experiments and immunocytochemical staining with antibodies specific for anti-phospho-PKCα and anti-phospho-PKC (pan) confirmed that PKCα was rapidly and most predominantly activated by high-concentrations of Shh. Inhibition of PKCα abolished the negative guidance effects of high-concentrations of Shh on RGC axons both in vitro and in vivo, suggesting that PKCα is specifically required in Shh-induced negative guidance effects. Increasing evidence indicates that PKC signaling pathways play important roles in axon guidance. Thrombin and protein tyrosine

phosphatase μ (PTPμ)-induced growth cone collapse of rat dorsal root ganglion axons and chick RGC axons were shown to result from selective activation of novel PKCε and PKCδ, respectively (Ensslen and Brady-Kalnay, 2004); while Wnt-mediated attractive guidance of rat commissural axons requires atypical PKCζ (Wolf et al., 2008). The distinct roles of individual PKCs may be attributed to the differences in their molecular structures, mechanisms that regulate their activation, and isoform-selective interacting proteins targeting them to specific substrates (Steinberg, 2008).

Lipid rafts are implicated in signal transduction, endocytosis, membrane trafficking and cytoskeletal reorganization (Pike, 2009). Colocalization of activated PKCα with GAP-43 suggests that PKCα is translocated to lipid rafts upon Shh treatment. Shh signaling components, such as Patched and Smo, are reportedly enriched in lipid raft fractions (Karpen et al., 2001). Phospholipase D, a substrate of PKCα that is required for Src- and EGF-induced macropinocytosis, also localizes to lipid rafts fraction of plasma membrane (Kim et al., 1999, Xu et al., 2000). Therefore, lipid rafts possibly serve as platforms where activated PKCα lies in close proximity to its activators and substrates to induce the formation of macropinosomes.

Our results demonstrate that ILK can be directly phosphorylated by PKCα on T173 and T181 in vitro and expression of the ILK-DM significantly abolished the repulsive effects of Shh, suggesting a new role of ILK in axonal guidance. Based in molecular modeling, phosphorylation of T173/T181 likely alters the regional surface electrostatic potential of ILK influencing its interaction with other proteins. It may be interesting to note that ILK

is also directly phosphorylated by p21-activated kinase 1 (PAK1) (Acconcia et al., 2007), and PAK1 has been shown to be critical for macropinocytosis (Dharmawardhane et al., 2000). ILK-DM is less effective than DN-PKCα in inhibition of Shh-induced negative axon guidance effects, suggesting that other effector(s) downstream of PKCα could potentially mediate the negative effects of Shh. Although we did not observe increased phosphorylation of β1 integrin on threonine 788 and 789 by Shh treatment (Hannigan et al., 1996, Hannigan et al., 2005), we cannot rule out the possibility that other sites may be phosphorylated by ILK. The exact role of ILK in Shh-mediated negative axon guidance is currently unclear. The effects of ILK were thought to result from the putative kinase activity of ILK (Guo et al., 2007). However, whether ILK possesses kinase activity has been challenged, especially by the recently available crystal structure of ILK (Fukuda et al., 2009, Wickstrom et al., 2010). ILK may function as an adaptor coupling integrin and growth factor signaling through interactions with many proteins including, PINCH, parvin, paxillin, and ILKAP (Legate et al., 2006).

Chapter III Rho and cAMP regulate opposite guidance effects of Shh

Abstract

Rho-GTPases and cyclic nucleotides have been shown to play important roles in mediating axon guidance. Here, we show that high concentrations of Shh-induced growth cone collapse and repulsive axon turning can be blocked by C3 transferase and Y-27632, specific inhibitors of Rho and ROCK, respectively. Biochemical analysis showed that high concentrations of Shh rapidly activated Rho in the retina. Inhibition of Rho also blocked PMA-induced growth cone collapse, suggesting that Rho possibly functions downstream of PKC. On the other hand, we found that low concentrations of Shh can induce attractive axon turning, and antagonizing cAMP signaling inhibits the effect of low Shh. We suggest that the opposing effects of Shh on axon guidance are mediated through distinct signaling machineries.

Introduction

Guidance molecules activate a series of intracellular events that ultimately lead to cytoskeleton rearrangement for axon navigation. A large body of work shows that Rho-GTPases (Rac, Cdc42 and Rho) orchestrate actin filaments and microtubule dynamics by controlling their assembly, disassembly and reorganization (Raftopoulou and Hall, 2004). Perturbation of Rho-GTPases signaling causes marked changes in the motility and navigation of axons both *in vitro* and *in vivo* (Hall and Lalli, 2010). Several well-studied guidance factors, including semaphorins, ephrins, netrins and slits, have been shown to regulate Rho-GTPase activities (Bashaw and Klein, 2010). For instance, netrins increase Rac and Cdc42 activity, but inhibit Rho activity when they induce axon attraction (Li et al., 2002, Gitai et al., 2003). Slits, which normally induce growth collapse and axon repulsion, increase Rac and Rho but decrease Cdc42 activity (Wong et al., 2001, Fan et al., 2003). In general, Rho and Rac/Cdc42 function antagonistically, with the former associated with negative factors causing growth cone collapse and growth inhibition.

One previous study suggested that Rho is likely involved in Shh-mediated neurite outgrowth (Kasai et al., 2004). The authors showed that over-expression of Smo in Neuro2A cells inhibits neurite outgrowth, but co-transfection of dominant-negative Rho rescued the phenotype. They also showed that activation of Rho increased the activities of transcription factor Gli1, and inhibition of Rho substantially decreased the nuclear transport of Gli3, suggesting that Rho is an important regulator of the transcriptional factors in the Shh pathway (Kasai et al., 2004). However, it is unclear from these

experiments if the transcription regulation determines the inhibition of neurite outgrowth by Shh.

In addition, previous studies showed that high Shh rapidly decreases the concentration of cyclic AMP (cAMP) within the growth cones of chick RGC axons (Trousse et al., 2001), whereas Sema III-induced growth cone collapse of rat DRG can be inhibited by activation of the cGMP pathway (Song et al., 1998), suggesting a role of cyclic nucleotides in negative guidance factors induced growth cone collapse. Several studies also showed that axon attractive turning can be converted to repulsive turning, or vice versa, by manipulating the activity or the relative ratio of cAMP and cGMP in axon (Song et al., 1998, Nishiyama et al., 2003), suggesting the importance of cyclic nucleotides in the bi-directional axon guidance. It seems that an increase of cyclic nucleotide activity (or high cAMP/cGMP ratio) favors positive guidance effects while a decrease of cyclic nucleotide activity (or low cAMP/cGMP ratio) favors negative guidance effects (Bashaw and Klein, 2010) .

We previously showed that Shh acts as a positive factor to promote RGC axonal growth at low concentrations (~0.5ug/ml). This result prompted us to investigate if low Shh induces attractive turning and if cyclic nucleotides mediate the process. Since high Shh (~3.0ug/ml) rapidly induces growth cone collapse and axon retraction, we were also interested in whether Rho is involved in the negative effects of Shh.

Materials and Methods

RGC axon culture

Standard specific pathogen-free white Leghorn chick embryos were provided fertilized by Charles River Laboratories (North Franklin, Connecticut) and incubated in a moisturized 38^{o}C incubator. Chick retinas were harvested at embryonic day 6 (E6), mounted on nitrocellulose filters, cut into approximately 300 μm-wide strips and cultured on glass bottom dishes coated with 10 μg/ml poly-D-lysine (Sigma) and 5-10 μg/ml laminin (Invitrogen). The retinal explants were cultured for 16-20 hours in F-12 media (Invitrogen) containing 0.4% methyl cellulose (Sigma) and penicillin/streptomycin to allow for axon outgrowth.

Time-lapse video microscopy and turning assay

Time-lapse experiments were performed on a Carl Zeiss Axiovert 200 microscope equipped with a 37°C heated stage. Time-lapse images were recorded for 30 minutes at 1-minute intervals using the Zeiss Axiovision LE software. For some experiments, axon culture were pre-treated for 90 min with membrane permeable Rho inhibitor C3 transferase (1.0μg/ml), or 30 mins of ROCK inhibitor Y-27632(20μM) before adding vehicle, Shh (recombinant Shh-N, R&D system) or PMA. Growth cone collapse was scored by a loss of lamellipodia and decrease of filopodia number to three and less per growth cone.

Axon turning assay and data analyses were carried out similar to our previous study. A custom software was generated to control the picospritzer to apply positive pressure to the pipette at a frequency of 2 Hz and a pulse duration of 2 msec. A micromanipulator

was used to position the pipette at ~150 μm distance from the growth cone and at an angle of 45^o from the initial direction of axonal extension. Time-lapse movies were produced to record the movement of the growth cone for 30 minutes. Vehicle control, 0.3-0.5 μg/ml or 3.0 μg/ml of Shh protein was loaded in the capillary pipette. To study the effect of Rp-cAMPs (20 μM), Sp-cAMPs (20 μM) or Gö6976 (5 nM) on low concentration of Shh-induced axonal turning, RGC cultures were pre-incubated with each inhibitor for 30 minutes prior to the turning assays.

For data analysis, the positions of the growth cone centers were marked throughout the time course of the gradient application. Only axons that extended more than 5 μm in the period of 20 minutes were included in the analysis. The turning angle α^o was determined as the angle of the original direction of axon extension and a line connecting the positions of growth cones at the beginning and the end of gradient application. The lengths of axon extension were calculated by subtracting the axon lengths at the beginning time point (L_0) from the length at the end (L_t) and converted to μm based on the scale bar.

Rho activation assay

E6 chick retinas were harvested, starved for 15 to 30 minutes, and then treated with vehicle control, 0.5ug/ml or 3.0ug/ml Shh for 2 minutes. Retinas are washed in ice-cold PBS twice and lysed by repeated pipetting. Rho activity was assayed using Rho activation kit, according to the instructions of the manufacturer (Upstate). Briefly, the cell lysate was incubated with GST-tagged Rho binding domain of Rhotekin, a Rho effector protein that binds specifically to the GTP-bound form of Rho. Then agarose beads pellet

are washed, resuspended by 2X Laemmli reducing sample buffer and boil for 5 minutes. Equal amounts of protein were loaded onto the SDS-PAGE gel and blotted with anti-Rho. Total Rho was used as loading control.

Results

We and others previously showed that Shh acts as a negative factor to induce growth cone collapse of chick RGC axons at higher concentrations (2.5-3.0 µg/ml) (Kolpak et al., 2005, Kolpak et al., 2009). To analyze the signaling pathways mediating the effects of high concentration of Shh, we carried out a small scale screen using pharmacological inhibitors. RGC axon cultures were pre-incubated with inhibitors of the Rho signaling pathway before addition of vehicle control or high Shh (3.0µg/ml). C3 transferase, a specific Rho inhibitor, inhibits Rho activity by ADP-ribosylation in the effector binding domain of the GTPase (Sehr et al., 1998). Y-27632, a specific inhibitor of ROCK downstream of Rho, inhibits ROCK kinase activity by binding to its catalytic site (Ishizaki et al., 2000). C3 transferase or Y-27632 alone did not significantly affect the growth pattern of chick RGC axons (Fig. 3.1*A*). Pre-treatment of C3 transferase or Y-27632, however, abolished the effect of high Shh on RGC axons. Growth cones did not collapse after addition of Shh, rather remained dynamic with motile lamellipodia and filopodia, and no significant axon retraction was observed (11.4±1.3% (C3-pretreated); 13.9±2.4% (Y-27632 pre-treated) vs 60±4.8% (high Shh alone), $p<0.01$). These data suggest that high Shh-induced growth cone collapse requires Rho-ROCK signaling.

High Shh can induce growth cone collapse within minutes; thus, we wanted to determine whether Shh treatment activated Rho in a similar time frame. E6 retinas were harvested, treated with vehicle control, low Shh(0.5µg/ml) or high Shh (3.0µg/ml) for 2 minutes and the activated GTP-bound Rho were pulled down by Rhotekin, a Rho effector protein that

Figure 3.1. Rho signaling is required for high Shh-induced axon repulsive effects.

A, E6 RGC culture was treated with either vehicle control or Shh (3.0 μg/ml). For some experiments, cultures were pre-incubated with C3 transferase or Y-27632 for 90 minutes and 30 minutes, respectively. ***B,*** To analyze the Rho activity, cell extracts from the retinal tissues treated with vehicle control, low Shh (0.5 μg/ml) or high Shh (3.0 μg/ml) for 2 min were immunoprecipitated by using RBD domain of Rhotekin and blotted by an anti-Rho antibody. Representative gel image of three independent experiments is shown. ***C,*** E6 RGC culture was treated with either vehicle control or PMA. For some experiments, cultures were pre-incubated with C3 transferase for 90 minutes. ***D,*** Turning assay to determine whether Rho is required for high Shh-induced repulsive axon turning. Trajectories of RGC growth cone movement were traced in the presence or absence of C3 transferase in culture media. The origin is the center of the growth cone at the beginning of the recording and the original direction of axon extension coincides with the *y*-axis. Tick marks on the *x*- and *y*-axis represent 5μm. ***E,*** Average axonal turning angles under experimental conditions in ***D.*** Data are represented as mean±SEM. * $p<0.01$, Student's *t* test.

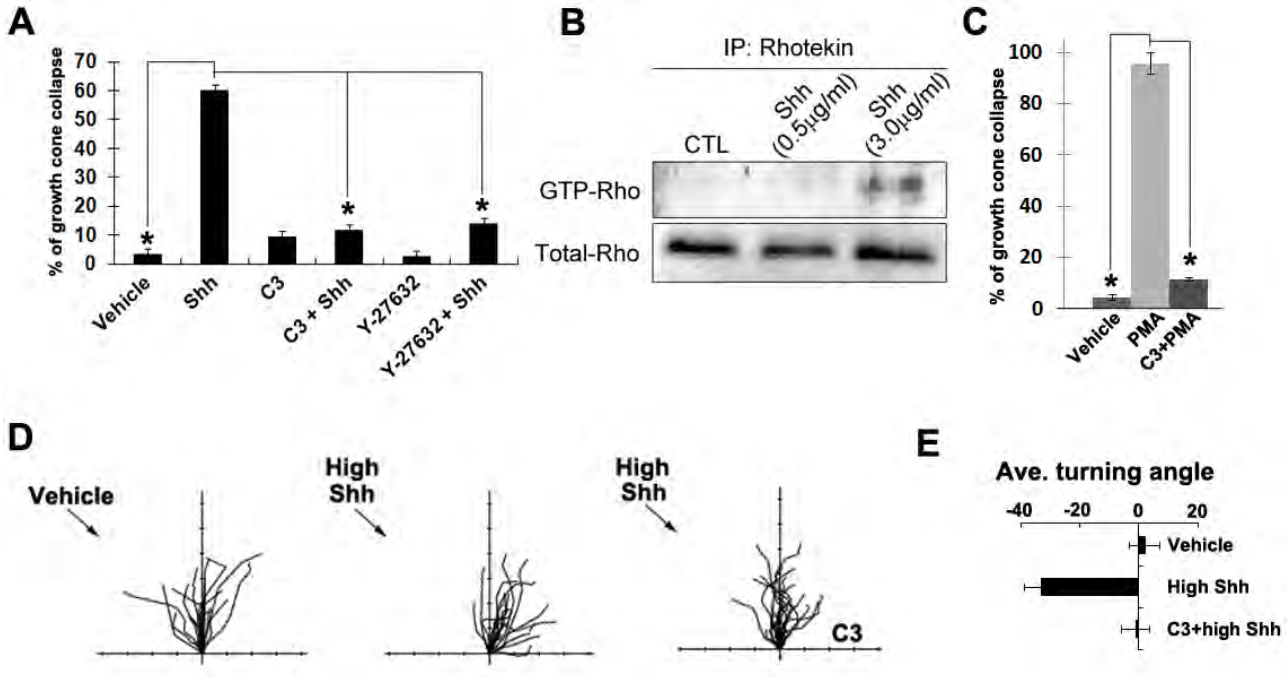
A
% of growth cone collapse
70
60
50
40
30
20
10
0
Vehicle
Shh
C3
C3 + Shh
Y-27632
Y-27632 + Shh
B
IP: Rhotekin
CTL
Shh (0.5μg/ml)
Shh (3.0μg/ml)
GTP-Rho
Total-Rho
C
% of growth cone collapse
100
80
60
40
20
0
Vehicle
PMA
C3+PMA
D
Vehicle
High Shh
High Shh
C3
E
Ave. turning angle
-40
-20
0
20
Vehicle
High Shh
C3+high Shh

binds specifically to the GTP-bound form of Rho. Two minute treatment of 3.0ug/ml Shh significantly increased the GTP-bound Rho (Fig.3.1*B*). The response is consistent with a previous report where 5 min treatment of Shh on Hek 293 cells also markedly increased the Rho activity (Kasai et al., 2004). We previously reported that high Shh could not activate Rac (Kolpak et al., 2009), suggesting that Shh-induced growth cone collapse is mediated by Rho activation but not Rac. Interestingly, 0.5ug/ml Shh did not increase the GTP-bound Rho (Fig.3.1*B*), indicating that Rho activation is probably specific to high Shh.

We next examined whether Rho is involved in high Shh-induced axon repulsive turning. Shh (3.0-3.5 ug/ml) was loaded into a fine capillary glass pipette, and positioned ~150 μm away from the growth cone and 45^{o} angle to the original direction of axon extension to generate a gradient. As shown in Figure 3.1 *D-E*, the majority of growth cones turned away from the micropipette within 20 min of initiation of Shh delivery through the micropipette. The average turning angle for the axons was -32.9^{o} (n=19 axons) in the high Shh experiments, compared with 2.2° (n=24 axons) in vehicle control. However, pre-incubation with C3 transferase abolished the Shh-induced repulsive axon turning, eliciting an average turning angle of -0.9° (n=22 axons). Collectively, these data indicated that Rho signaling is responsible for both high Shh-induced growth cone collapse and repulsive turning of chick RGC axons.

In chapter II, we showed that pre-incubation of PKCα inhibitor or over-expression of DN-PKCα in chick RGCs effectively abolished the high Shh-induced growth cone

collapse. We next investigated how PKC and Rho signaling interact with each other to mediate the negative effect of Shh. Since there is no good method to activate the PKCα isoform alone, PMA was used to activate both conventional and novel PKCs. Consistent with previous reports that PMA induced growth cone collapse/retraction in several neuronal cell types (Bonsall and Rehder, 1999, Zhou and Cohan, 2001), rapid growth cone collapse of chick RGC axons were observed minutes after addition of PMA (Fig.3.1*C*) (4.5±1.2% of vehicle controls vs 95.8±4.2% of PMA-treated, $p<0.001$). However, the effect is blocked by pre-incubation of C3 transferase in the culture (11.6±0.6% of growth cone collapse, $p<0.001$) (Fig.3.1*C*), suggesting that Rho may function downstream of PKC to mediate the negative guidance effects.

By a stripe assay, we previously showed that chick RGC axons preferentially grow onto low Shh coated stripes compared to BSA-coated stripes, but avoid high Shh coated stripes (Kolpak et al., 2005). However, direct evidence of low Shh inducing attractive turning of chick RGC axons was not available. Turning assays were thus carried out by pulsing 0.3~0.5 µg/ml of Shh from the micropipette. As shown in Fig.3.2*A-D*, the majority of growth cones turned toward the micropipette within 20 min of initiation of Shh delivery. The average turning angle for the axons was 18.81^{o} (n=28 axons) in the low Shh experiments, compared with -0.39° (n=23 axons) in vehicle controls, suggesting that low Shh induces attractive axon turning.

Since inhibition of PKCα activity effectively abolished high Shh-induced repulsive turning, we next investigated if PKCα is required for low Shh-induced attractive turning.

Interestingly, pre-incubation of Gö6976 at 5nM concentration, which specifically inhibits PKCα isoform, was ineffective to block low Shh-induced attractive turning (Fig. 3.3*A*-*B*), suggesting that PKCα activity is required for high Shh, but not low Shh effects on chick RGC axons.

To investigate the signaling mechanism for low Shh-induced attractive turning, we focused on cAMP as one previous study showed that high Shh (2.5μg/ml) reduced the cAMP level in the growth cone of chick RGC (Trousse et al., 2001b), suggesting that cAMP could be a mediator for Shh signaling. Since cyclic nucleotides are important second messengers in regulating axon turning, we next investigated whether cAMP signaling is involved in low Shh-induced attractive turning, RGC axons were pretreated with cAMP antagonist Rp-cAMPS or agonist Sp-cAMPS in bath, before a low concentration of Shh or vehicle control was delivered from the micropipette. While Rp-cAMPS and Sp-cAMPS did not significantly affect the growth rates of RGC axons, pre-treatment of cAMP antagonist Rp-cAMPS abolished Shh-induced attractive turning, yielding an average turning angle of -1.68^{o} (n=31 axons) (Fig. 3.2*B*–*D*). On the other hand, cAMP agonist Sp-cAMPS did not affect Shh-induced attractive axon turning. These data indicate that antagonizing cAMP signaling inhibits the effect of low Shh on attractive axon turning.

Figure 3.2. cAMP activity is required for low Shh-induced attractive axon turning. ***A.*** Dark field images of RGC axons immediately before (0 min) and 10 and 20 min after exposure to vehicle or low concentrations of Shh delivered by a micropipette positioned at a 45^{o} angle to the direction of axon growth (arrows). ***B.*** Trajectories of RGC growth cone movement in the presence or absence of Rp-cAMPS or Sp-cAMPS in culture media. The origin is the centre of the growth cone at the beginning of the recording and the original direction of axon extension coincides with the *y*-axis. Arrows indicate the direction of the protein gradient. Tick marks on the *x*- and *y*-axis represent 5μm. ***C.*** Average axonal turning angles and extension under experimental conditions in ***B***. ***D.*** Cumulative distribution plots of axonal turning angles of each condition. Each point represents the turning angle of a growth cone at the end of 20 min. Positive angles represent axon turning toward the pipette, whereas negative angles represent axon turning away from the pipette.

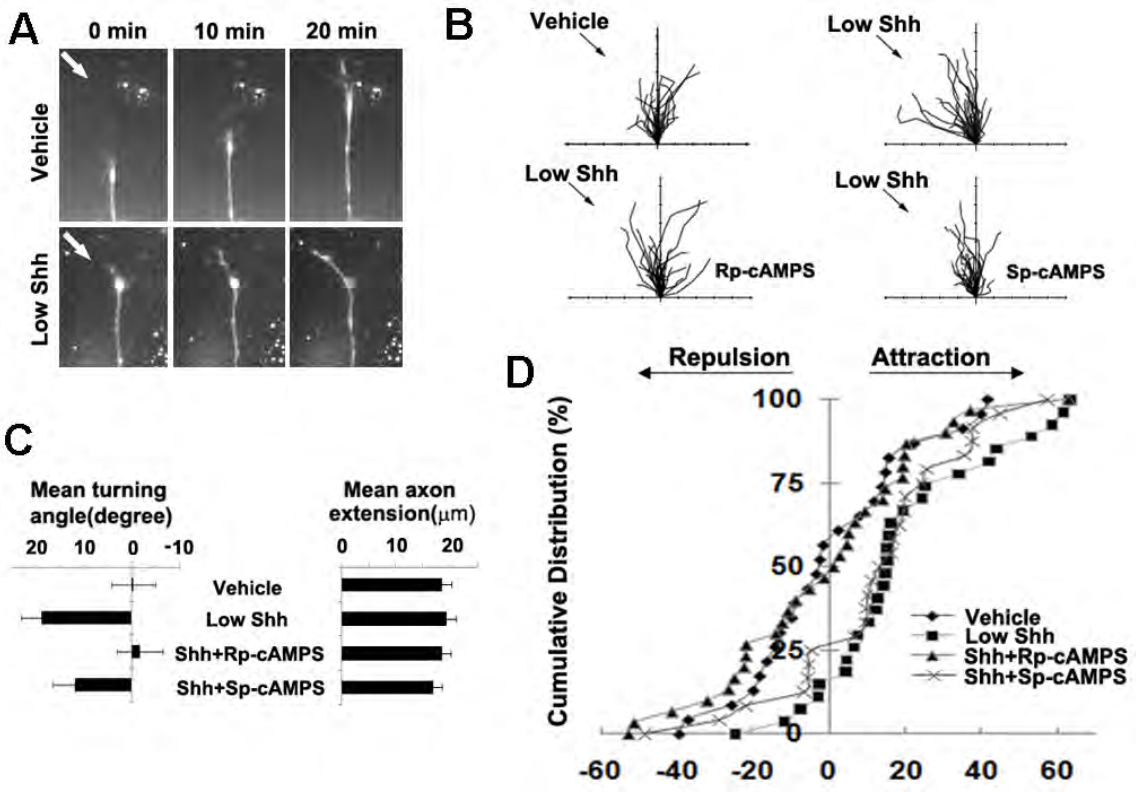
A
0 min
10 min
20 min
Vehicle
Low Shh
B
Vehicle
Low Shh
Low Shh
Rp-cAMPS
Low Shh
Sp-cAMPS
C
Mean turning angle(degree)
20 10 0 -10
Mean axon extension(μm)
0 10 20
Vehicle
Low Shh
Shh+Rp-cAMPS
Shh+Sp-cAMPS
D
Repulsion
Attraction
Cumulative Distribution (%)
100
75
50
25
0
-60 -40 -20 0 20 40 60
Vehicle
Low Shh
Shh+Rp-cAMPS
Shh+Sp-cAMPS

Figure 3.3. PKCα doesn't mediate low Shh-induced attractive turning. ***A,*** Superimposed traces depict the trajectory of wild type RGC axon extension in the presence or absence of Gö6976 in the culture media. Arrows indicate the direction of low concentration of Shh gradient. ***B,*** Average axonal turning angles and extension of each condition. ***C,*** Cumulative distribution plots of axonal turning angles of each condition. Each point represents the turning angle of growth cone at the end of 20 min exposure to low concentration of Shh alone, or in the presence of Gö6976. The percentage represents the percentage of growth cone bearing turning angle $\leq$ the value indicated on the *x* axis. Positive angles represent axon turning toward the pipette, whereas negative angles represent axon turning away from the pipette. Gö, Gö6976.

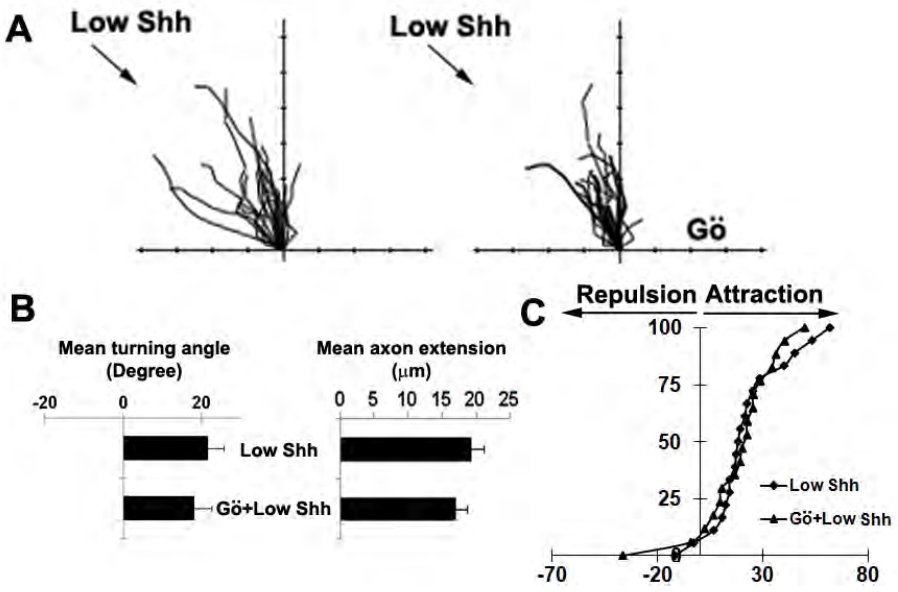
A
Low Shh
Low Shh
Gö
B
Mean turning angle
(Degree)
-20
0
20
Low Shh
Gö+Low Shh
Mean axon extension
(μm)
0
5
10
15
20
25
C
Repulsion Attraction
100
75
50
25
0
Low Shh
Gö+Low Shh
-70
-20
30
80

Discussion

In chaptor II, we reported that PKCα is required for high Shh-mediated negative effects on axon guidance. Here, we report that Rho signaling is also required for such events and Rho likely functions downstream of PKC in mediating chemorepulsion.

As growth cone navigation involves a complex coordinated reorganization of the cytoskeleton, regulated membrane retrieval and addition, and local protein translation and degradation (Dent and Gertler, 2003, Lowery and Van Vactor, 2009), it is not surprising that more than one signaling component is activated by guidance molecules. In other systems, it has been shown that PKCα and Rho can either directly or indirectly influence the activity of each other. In vitro, Rho can directly activate purified PKCα to a greater degree than other PKC isoforms, and the activity of PKCα is dependent on the GTP/GDP-bound state of the Rho GTPases (Slater et al., 2001, Pang and Bitar, 2005). In vivo, PKCα can activate Rho through phosphorylation of Rho-GDP guanine nucleotide dissociation inhibitor (GDI) to regulate endothelial barrier function, or decrease Rho activity through phosphorylation of another small GTPase Rnd3 to regulate cytoskeleton dynamics (Mehta et al., 2001, Madigan et al., 2009). Therefore, it is possible that crosstalk between PKCα and Rho GTPase enables them to coordinate their activities in regulating the guidance effects of Shh.

However, the attractive turning effect of low Shh is abolished by inhibition of cAMP but not PKCα, suggesting that low and high Shh utilize different signaling cascades to mediate attractive or repulsive effects. Indeed, Shh was shown to attract commissural

axons by binding to receptor Boc (Okada et al., 2006, Yam et al., 2009), but repel post-commissural axons through receptor Hip (Bourikas et al., 2005), indicating Shh binds to different receptors to initiate divergent intracellular signaling. However, Boc can also mediate axon repulsion as it has been shown recently that Shh repels mouse ipsilateral RGC axons at the optic chiasm via receptor Boc (Fabre et al., 2010). Right now it is unclear how Boc mediates the opposing effects of Shh. In the case of Netrin-induced axon guidance, Netrin attracts axons by binding to DCC receptors, but repels axons when receptor UNC5 is co-expressed (Hong et al., 1999). It is possible that the opposing guidance effects of Shh are mediated by different Boc receptors forming complexes with different proteins, resulting in activation of distinct downstream signaling cascades.

cAMP signaling is known to be involved in the canonical signaling pathway of Shh (Epstein et al., 1996, Hammerschmidt et al., 1996, Trousse et al., 2001). In chick RGC axons, high Shh was shown to rapidly decrease the concentration of cAMP in the growth cone (Trousse et al., 2001). In this study, we found that the effect of low Shh on attractive axon turning requires cAMP signaling. Pre-treatment with a cAMP antagonist abolished low Shh-elicited attractive axon turning. Cyclic nucleotides have been shown to play important roles in modulation of the response of axons to guidance factors, although the underlying mechanisms are not completely understood. A decrease of cyclic nucleotide signaling has been associated with converting positive guidance factor-induced attraction to repulsion, whereas an increase of cyclic nucleotide signaling converts negative factor-induced repulsion to attraction. However, in our case, when

cAMP was inhibited by an antagonist, we didn't observe the conversion from attraction to repulsion by low Shh, rather axons appeared to turn randomly. It has been shown that axons cultured on different extracellular matrix protein-coated surfaces can respond differently to the same guidance cue. *Xenopus* retinal axons turn towards Netrin-1 when cultured on fibronectin but turn away from Netrin-1 when cultured on laminin, and laminin decreases cAMP level within the growth cone (Hopker et al., 1999). Our chick RGC axons need to be cultured on laminin-coated coverslip. Right now it is unclear why no such turning conversion occurs. It is possible that additional extrinsic or intrinsic factors may modulate the responsiveness of axons to the decreased cAMP in combination of low Shh. Further experiments such as gradually decreasing the concentration of laminin on the coverslip, or examining whether activation of cAMP converts high-Shh induced repulsion to attraction may help explain the results.

Inhibition of PKCα abolished high Shh-induced repulsive turning but not low Shh-induced attractive turning. This means that PKCα activity is specific to high Shh signaling. As previously suggested, a guidance cue executes opposing guidance effects via regulation at multiple levels, including receptors at the cell surface (single receptor vs multiple receptors), the magnitude of calcium elevation (local verse global), the ratio of cyclic nucleotide (cAMP vs cGMP) and the differential activation of Rho-GTPase members (Cdc42, Rac and Rho). Much work needs to be done to dissect the divergence of Shh signaling. One immediate question to be addressed is the identity of the receptors that are responsible for the opposing guidance effects of Shh, which would shed light on the downstream signaling events.

Chapter IV: Discussion and Perspectives

In summary, we present evidence in this dissertation that Shh acts through novel noncanonical signaling pathways to direct RGC axon guidance. The negative guidance effects of Shh are mainly mediated by PKCα, Rho and ILK, whereas the positive guidance effect of Shh involves cAMP. Though a member of PKC (PKCδ) and Rho have been shown to play roles in Shh canonical signaling pathway (Kasai et al., 2004, Riobo et al., 2006), we show PKCα and Rho are important components of a novel Shh non-canonical pathway mediating axon guidance. In vitro, high concentrations of Shh elevates growth cone Ca^{2+} concentration within seconds, and activates PKCα and Rho within minutes, as assessed by acute increase of GTP-bound Rho and translocation/phosphorylation of PKCα. Consistently, pharmacological inhibition and/or dominant-negative suppression of either protein abolished the negative effects of high Shh. We further found ILK is an immediate downstream effecter of PKCα and identified two new PKCα phosphorylation sites on ILK. ILK mutant also lessened the negative effects of Shh, but not as effectively as PKCα inhibition. These results indicate that Shh acts directly on the RGC axons in a rapid manner, independent of transcriptional regulation of Shh. The view is supported by previous observations that Shh-induced turning of commissural axons is independent of both transcriptional and translational repression (Yam et al., 2009). In vivo, expression of dominant negative PKCα or ILK mutant caused misprojection of RGC axons at the chiasm. Our data support the notion that spatial-temporal regulation of Shh at the chiasm restricts RGC axon within the optic

bundles, and we provide the first insight into the signaling mechanism mediating this process.

Many previous studies focused on the roles of actin and microtubules in axon guidance. Indeed, the two major cytoskeleton elements within the growth cone undergo dynamic reorganization in response to guidance cues and can easily be envisioned as the major driving force for axon steering. The fundamental roles of Rho-GTPases in regulating cytoskeletal reorganization have begun to be established, but a general role of PKC in such events is still missing. This could be due to the fact that the numbers of PKC isoforms are large. Though each member shares a high degree of homology with the others, it seems that the non-homologous region renders a unique specificity to each isoform. For example, despite a 94% protein sequence similarity (highest in PKC family), PKCβ1 and PKCβ2 differ in their expression profiles (Chalfant et al., 1995), subcellular localizations at the resting state (Disatnik et al., 1994, Ron et al., 1995), translocations at the activated state (Goodnight et al., 1995, Blobe et al., 1996), and binding partners (Steinberg, 2008). Therefore, members of PKCs may function in highly specialized manners with only minor sequence differences. We show that within the PKC family, PKCα activity is specifically required for the negative effects of high Shh. Other studies also indicate a PKC isoform-specific mechanism underlying the guidance effects of different factors. For example, thrombin-induced growth cone collapse of DRG was shown to result from selective activation of PKCε (Mikule et al., 2003); PTPμ-induced growth cone collapse of chick RGC axon requires PKCδ (Ensslen and Brady-Kalnay, 2004). Wnt-mediated attractive guidance of commissural axons requires an atypical

PKCζ (Wolf et al., 2008). Taken together, present data suggest that PKC isotypes exhibit specificity in response to different stimuli.

Rho-GTPases (primarily Cdc42, Rac and Rho) are well-studied regulators of actin dynamics in non-neuronal cells (Burridge and Wennerberg, 2004). Increasing evidence shows that they regulate actin reorganization in the growth cones (Hall and Lalli, 2010). Activated Cdc42 binds to members of WASP (Wiskott-Aldrich Syndrome Protein) family proteins which in turn activate Arp2/3(actin-related protein 2/3), proteins that serve as nucleation sites for new actin filaments, to stimulate actin assembly (Rohatgi et al., 1999). Pak kinase, serving as a common effecter of both Rac and Cdc42, activates LIM kinase but inhibits MLCK (myosin light chain kinase) (Manser et al., 1994, Edwards et al., 1999, Sanders et al., 1999). This pathway is believed to control actin filament turnover and retrograde flow to steer the growth cone (Lin et al., 1996). Rho can directly bind to downstream ROCK which subsequently phosphorylates MLC and myosin light chain phosphatase, both of which lead to contraction of actomyosin network (Amano et al., 1996, Kimura et al., 1996, Hirose et al., 1998, Wahl et al., 2000). Though much progress has been made to elucidate the roles of Rho-GTPases in growth cone motility, many questions remain unanswered. For instance, inhibition of Rho signaling blocks the negative effect of a list of guidance cues including Ephrin-A5 (Wahl et al., 2000), Semaphorin (Liu and Strittmatter, 2001), Neogenin (Conrad et al., 2007), LPA (Jalink et al., 1994) and Shh; it remains to be determined how a single protein Rho interprets different signaling inputs in a similar manner. Furthermore, the mechanism of signaling crosstalk between PKC and Rho-GTPases in regulating axon guidance is also unclear.

One study showed that inhibition of conventional PKCs by specific inhibitors reduced ryanodine-induced activation of Cdc42 and inhibition of Rho. Accordingly, the inhibitors also abolished ryanodine-induced attractive growth cone turning (Jin et al., 2005), suggesting that PKCs may function upstream of Rho-GTPases in such process. Studies carried out in other systems also indicated that PKC and Rho-GTPases can interact directly or through mediators between them (Mehta et al., 2001, Slater et al., 2001, Pang and Bitar, 2005, Madigan et al., 2009). For our study, one question to be addressed is whether PKCα interacts with Rho directly or indirectly to mediate the negative guidance effects of Shh.

In addition to Rho, we also identified ILK as an immediate downstream effecter of PKCα in the Shh signaling cascade. There is a general consensus that ILK functions as an adaptor protein linking extracellular signaling to the regulation of actin cytoskeleton. ILK contains three major domains featuring multiple protein binding sites. In addition to integrin β1 and β3, the C-terminus of putative kinase domain of ILK binds paxillin, Mig-2 and parvins (α/β/γ) directly, and interacts with a number of actin-binding proteins such as α-actinin and TESK1 through parvins (Hannigan et al., 2005). These binding partners play important roles in anchoring the actin cytoskeleton to cell adhesion sites where ILK accumulates with integrin cytoplamic tails. Additionally, increasing evidence shows crosstalk between ILK and Rho-GTPases signaling. ILK can activate Rac1/Cdc42 or Rho in cell-type specific manner. Over-expression of ILK, β-parvin or αPIX leads to activation of Rac/Cdc42 and significant actin reorganization in several cell lines (Mishima et al., 2004, Filipenko et al., 2005), whereas elevated Rho signaling and

corresponding cell morphology change were observed in some other cells in which ILK or α-parvin is depleted (Montanez et al., 2009). These studies collectively show that ILK, acting as an adaptor protein, regulates actin cytoskeleton through its binding partners and/or interaction with Rho-GTPases.

Ca^{2+} signaling also has varied effects on growth cone turning. Previous studies carried out on *Xenopus* spinal neurons showed that guidance cues applied from a point source can elevate growth cone Ca^{2+} concentration facing the cues and the preferentially elevated Ca^{2+} seems to be maintained during the entire turning process (Hong et al., 2000, Henley et al., 2004). Here, we showed that high Shh applied from a point source induces both repulsive turning and Ca^{2+} elevation in the chick RGC growth cone. However, in most cases, the Ca^{2+} elevation in response to high Shh was not observed in the growth cones facing the Shh source, rather the elevation spans the entire growth cone. In a few cases, we observed that the Ca^{2+} elevation first occurred in the growth cone proximal to the Shh source, and then quickly spread to the distal growth cone within 10 to 20 seconds. Furthermore, the Ca^{2+} elevation in response to Shh lasts from 50 seconds to a few minutes, and seemingly does not accompany the entire turning process observed in the turning assay. In contrast to *Xenopus* spinal neurons, chick RGC axons are more sensitive to the fluctuations in the environment (dish movement, transient change of temperature and CO_2, exchange of the medium, etc). Before Ca^{2+} imaging, a required additional step to wash out the extracellular Ca^{2+} indicator Fluo-3 rendered chick RGC axons stationary. Therefore, it is possible that the preferential elevation of Ca^{2+} and its maintenance in response of Shh can only be observed in the growing axons which can subsequently turn.

Technical improvements may help resolve the issue. It is also possible that the transient elevation of Ca^{2+} beginning from one side of the growth cone is sufficient to initiate local downstream signaling machinery. It has been shown that stimuli-triggered repetitive Ca^{2+} spikes (with each spike only spanning a few seconds) can induce synchronous translocation of PKCs between the plasma membrane and cytosol , suggesting that transient Ca^{2+} elevation can activate PKC in a rapid manner (Oancea and Meyer, 1998, Mogami et al., 2003). It will be interesting to see whether high Shh induces translocation of PKCα to the side of the growth cone facing the Shh source.

Moreover, it has been suggested that modest elevation of Ca^{2+} induces growth cone attraction, whereas small and large elevation results in growth cone repulsion/collapse (Gomez and Zheng, 2006). In our experiments, the magnitude of Ca^{2+} elevation in response to high Shh ranges from 25% to 50% compared to the baseline. As different groups use different Ca^{2+} indicators (BAPTA-1-dextran, fura-2, Fluo-3 and Fluo-4) and the binding affinity of these indicators with Ca^{2+} varies, it is impractical to compare high Shh-induced Ca^{2+} elevation with those in other studies. Since low Shh induces attractive turning of chick RGC axons, examining the magnitude of Ca^{2+} elevation by low Shh would provide a comparable reference for our system.

Though much previous research focused on the roles of cytoskeleton in axon guidance, recent studies carried out in our lab and others have suggested an alternative, membrane trafficking-based mechanism underlying growth cone navigation. Asymmetric clathrin-mediated endocytosis contributes to the repulsive growth cone turning caused by

Sema3A and MAG, with more endocytosis events observed in growth cone facing the guidance factors (Tojima et al., 2010). Similarly, high Shh preferentially induced more macropinosome formation at the side of growth cone facing the Shh gradients (Kolpak et al., 2009). Inhibition of both types of endocytosis by specific inhibitors or dominant negative approaches abolishes the repulsive turning in response to these guidance factors. Therefore, asymmetric removal of the growth cone surface area may contribute to the repulsive turning. On the other hand, inhibition of VAMP2-mediated exocytosis prevents growth cone attraction but not repulsion (Tojima et al., 2007), and stimulation of asymmetric exocytosis by directional application of α-latrotoxin induces attractive growth cone turning toward the side with more exocytosis (Tojima et al., 2010), suggesting that exocytosis may be responsible for growth cone attraction. Taken together, growth cone navigation may require cooperative regulation at both cytoskeleton level and membrane level. Indeed, the formation of macropinosomes has been shown to be initiated by transient actin redistribution around the membrane ruffles which subsequently fold and fuse to form macropinosomes (Jones, 2007). Disassembly of actin filaments by cytochalasin D or latrunculin, or inhibition of F-actin dynamics by jasplakinolide, significantly reduced Shh-induced macropinocytosis in RGC axons and adenovirus-triggered macropinocytosis in epithelial cells (Meier et al., 2002, Kolpak et al., 2009)

We found that inhibition of PKCα and ILK significantly reduced high Shh-induced macropinocytosis. Accordingly, inhibition of these proteins effectively antagonizes the growth cone collapse and repulsive turning caused by high Shh, suggesting that

macropinosome-mediated membrane removal is associated with the negative effects of Shh. Because of their relatively large sizes, macropinocytosis can be considered as an efficient measure to decrease the surface area of the growth cone. Previous studies have shown the importance of PKC isoforms in regulating macropinocytosis but the exact mechanism and consequence are not completely understood. PMA, an activator of conventional and novel PKCs, can induce membrane ruffling and macropinocytosis in A431 cells (Grimmer et al., 2002). Receptor-independent macropinocytosis of cholesterol LDL in macrophages seems to require PKCβ and PKCδ (Ma et al., 2006). Furthermore, adenovirus-triggered macropinocytosis in epithelial cells (Meier et al., 2002) and constitutive macropinocytosis in dendritic cells (Sarkar et al., 2005) have been found to be mediated by conventional PKC and novel PKC, respectively. These studies indicate that different members of PKC family proteins may regulate macropinocytosis in different cellular contexts and possibly through distinct downstream events. Stimulation of macropinocytosis also depends on other signaling components, including Rho-GTPases, p21-activated kinase, Src tyrosine kinase and PI3-kinase (Swanson, 2008). In general, the activation of these components triggers signaling cascades that ultimately lead to the actin-driven ruffles that are required for formation of macropinocytosis, and cause local membrane curvature required for the closure of the ruffles (Swanson, 2008). The finding that the ILK-mutant can reduce high Shh-induced macropinocytosis is not unexpected. Given the fact that ILK regulates actin dynamics through a group of actin-associated binding partners, it is possible ILK play roles in the ruffle formation process, but the exact mechanism is open to future research.

During development, RGC axons pathfinding from eye to brain provide an easily-accessible system to study growth cone behavior in response to guidance cues presented in the environment. Previous studies have identified that several well-conserved families of guidance cues such as Slits, Ephrins and Semaphorins are expressed at the chiasm region and play important roles in determining RGC axon navigations at that place. Though not conclusive, these chiasmatic guidance factors seem to exhibit minimal functional redundancy at this region. EphrinB2 is mainly required to repel ipsilateral turning axons originated from ventral-temporal (VT) RGC and has no effect on contralaterally projecting axons from non-VT RGC (Nakagawa et al., 2000, Williams et al., 2003). The repulsive effect of Slits1/2 were found to limit the escape of axons from their normal path and seemingly does not affect RGC axon divergence at the chiasm (Erskine et al., 2000, Plump et al., 2002). Semaphorin3D also functions negatively on RGC axons, likely to "push" away the axons after they cross the midline (Sakai and Halloran, 2006). It should be noted that, due to the fact that RGC axons of fish and chick only project contralaterally, the mechanism by which chiasmatic guidance cues mediate ipsilateral axon turning in higher vertebrate species does not take place in lower vertebrate species. Consistently, EphrinB2 is not detected at the chiasm of fish and chick (Nakagawa et al., 2000). Therefore, it is possible that guidance factors in the chiasm of lower vertebrate species may function in a simpler manner, providing a "corridor" for all contralateral projecting axons. Interestingly, the development and architecture of the chiasm of different species shows marked variation, thus potentially influencing the function of the chiasm as an axon guidance source (Jeffery and Erskine, 2005).

The spatial-temporal regulation of Shh expression at the chiasm indeed points to the "corridor" mechanism and provides a system to test the hypothesis. The reaching of RGC axons to the midline is accompanied by a loss of expression of Shh at the chiasm, but retaining expression of Shh bordering the anterior and posterior edges of the chiasm (Trousse et al., 2001). Over-expression of Shh at the chiasm reduced RGC axons reaching the region (Trousse et al., 2001), while blocking Shh by a neutralizing antibody broadened the axon bundle at the chiasm and increased axon misprojection (Sanchez-Camacho and Bovolenta, 2008). In this thesis, we provide the first evidence that PKCα and ILK play important roles in axon pathfinding at the chiasm. Inhibition of the signaling renders chick RGC axons insensitive to the chiasmatic Shh such that axons splay out from the bundle and project erroneously.

Though our works uncover a new signaling cascade for the Shh-induced axon guidance, many questions remain unanswered. Different receptor complexes presented at the cell surface have been shown to regulate the opposing effects of the same guidance cue. It is unclear at present what receptors are responsible for the concentration-dependent effects of Shh. Since Shh's receptor Boc has been shown to be responsible for both attractive and repulsive effects of Shh (but in different cell types), knocking-down Boc expression in RGC cells, and examining how RGC axons respond to low or high concentrations of Shh would provide information of the function of Boc receptor: is Boc only required for low Shh effect or is it only required for high Shh effect? It is also feasible to treat RGC axons culture with low or high concentrations of Shh, pull-down Boc with anti-Boc antibody, and examine whether Boc form different protein complexes in response to different

concentration of Shh by Mass Spectrometry. This method can be particularly useful to investigate the binding partners of another Shh receptor, Hip, as Hip has been shown to regulate the negative effect of Shh in postcommissural axons but Hip itself lacks intracellular domains. Potentially, knocking-down a single receptor of Shh in RGC may not enough to clarify the function of this receptor. Simultaneous down-regulating several receptor candidates of Shh are probably required to examine the concentration-dependent effects of Shh.

Endocytosis/exocytosis-mediated membrane removal/addition has begun to be uncovered as important measures for growth cone steering. However, it is unclear where the Shh-induced macropinosomes form, on the apical surface of the growth cone to remove bulk membrane, or on the substrate-facing surface to "lift" cell adhesion sites? TIRF microscopy can be used in future to answer this question. Furthermore, the fate of these vesicles remains elusive. It is possible that the roles of these vesicles are to remove bulk membrane from one side of the growth cone to the other side to implement turning. Long-term tracing of these vesicles using bleaching-resistant fluorescent dye would help answer the question.

Though inhibition of PKCα and ILK markedly abolished Shh-induced macropinocytosis, the colocalization of PKCα and ILK with macropinosomes isn't significant, suggesting that either the association is transient, or that PKCα and ILK regulate macropinocytosis indirectly. Another future aim is to study the mechanism by which PKCα and ILK facilitate the formation of macropinosomes. As PKC family proteins and ILK have been

shown to regulate actin dynamics indirectly (Brandt et al., 2002), and the formation of macropinosomes requires actin rearrangement around the endocytic cup, characterizing the mediator between PKC-ILK signaling and actin would provide insight into the mechanism of macropinosome formation. Several PKC substrates, such as MARCKS, GAP43, adductin, fascin and etc, can be served for future study as they directly associated with the actin (Larsson, 2005).

Multiple intracellular signaling components are required for Shh-induced axon steering. In terms of Shh-induced attractive axon turning, Src-family kinases have been shown to mediate attractive turning of commissural axons, whereas we show that cAMP is required for the attractive turning of RGC axons. Do the two signaling systems interact with each other, or do they act cell-type specifically? Addressing these unsolved issues would ultimately aid in our understanding of the mechanism governing Shh-induced axon guidance.

References

Acconcia F, Barnes CJ, Singh RR, Talukder AH, Kumar R (Phosphorylation-dependent regulation of nuclear localization and functions of integrin-linked kinase. Proc Natl Acad Sci U S A 104:6782-6787.2007).

Allen BL, Tenzen T, McMahon AP (The Hedgehog-binding proteins Gas1 and Cdo cooperate to positively regulate Shh signaling during mouse development. Genes Dev 21:1244-1257.2007).

Amano M, Ito M, Kimura K, Fukata Y, Chihara K, Nakano T, Matsuura Y, Kaibuchi K (Phosphorylation and activation of myosin by Rho-associated kinase (Rho-kinase). J Biol Chem 271:20246-20249.1996).

Arni S, Keilbaugh SA, Ostermeyer AG, Brown DA (Association of GAP-43 with detergent-resistant membranes requires two palmitoylated cysteine residues. J Biol Chem 273:28478-28485.1998).

Bao ZZ (Intraretinal projection of retinal ganglion cell axons as a model system for studying axon navigation. Brain Research 1192:165-177.2008).

Bashaw GJ, Klein R (Signaling from axon guidance receptors. Cold Spring Harb Perspect Biol 2:a001941.2010).

Birgbauer E, Cowan CA, Sretavan DW, Henkemeyer M (Kinase independent function of EphB receptors in retinal axon pathfinding to the optic disc from dorsal but not ventral retina. Development 127:1231-1241.2000).

Blobe GC, Stribling DS, Fabbro D, Stabel S, Hannun YA (Protein kinase C beta II specifically binds to and is activated by F-actin. J Biol Chem 271:15823-15830.1996).

Bolsover SR (Calcium signalling in growth cone migration. Cell Calcium 37:395-402.2005).

Bonsall J, Rehder V (Regulation of chick dorsal root ganglion growth cone filopodia by protein kinase C. Brain Res 839:120-132.1999).

Bornancin F, Parker PJ (Phosphorylation of protein kinase C-alpha on serine 657 controls the accumulation of active enzyme and contributes to its phosphatase-resistant state. J Biol Chem 272:3544-3549.1997).

Bosanac I, Maun HR, Scales SJ, Wen X, Lingel A, Bazan JF, de Sauvage FJ, Hymowitz SG, Lazarus RA (The structure of SHH in complex with HHIP reveals a recognition role for the Shh pseudo active site in signaling. Nat Struct Mol Biol 16:691-697.2009).

Bourikas D, Pekarik V, Baeriswyl T, Grunditz A, Sadhu R, Nardo M, Stoeckli ET (Sonic hedgehog guides commissural axons along the longitudinal axis of the spinal cord. Nat Neurosci 8:297-304.2005).

Briancon-Marjollet A, Ghogha A, Nawabi H, Triki I, Auziol C, Fromont S, Piche C, Enslen H, Chebli K, Cloutier JF, Castellani V, Debant A, Lamarche-Vane N (Trio mediates netrin-1-induced Rac1 activation in axon outgrowth and guidance. Mol Cell Biol 28:2314-2323.2008).

Brandt D, Mario G, Hillmann M, Haller H, Mischak H (Protein kinase C induces actin reorganization via a Src- and Rho-dependent pathway. J Bio Chem 277: 20903-20910. 2002)

Brittis PA, Canning DR, Silver J (Chondroitin sulfate as a regulator of neuronal patterning in the retina. Science 255:733-736.1992).

Burridge K, Wennerberg K (Rho and Rac take center stage. Cell 116:167-179.2004).

Butler SJ, Dodd J (A role for BMP heterodimers in roof plate-mediated repulsion of commissural axons. Neuron 38:389-401.2003).

Campeau E, Ruhl VE, Rodier F, Smith CL, Rahmberg BL, Fuss JO, Campisi J, Yaswen P, Cooper PK, Kaufman PD (A versatile viral system for expression and depletion of proteins in mammalian cells. PLoS One 4:e6529.2009).

Chalfant CE, Mischak H, Watson JE, Winkler BC, Goodnight J, Farese RV, Cooper DR (Regulation of alternative splicing of protein kinase C beta by insulin. J Biol Chem 270:13326-13332.1995).

Charron F, Stein E, Jeong J, McMahon AP, Tessier-Lavigne M (The morphogen Sonic Hedgehog is an axonal chemoattractant that collaborates with Netrin-1 in midline axon guidance. Cell 113:11-23.2003).

Chau MD, Tuft R, Fogarty K, Bao ZZ (Notch signaling plays a key role in cardiac cell differentiation. Mech Dev 123:626-640.2006).

Chilton JK (Molecular mechanisms of axon guidance. Dev Biol 292:13-24.2006).

Chizhikov VV, Millen KJ (Roof plate-dependent patterning of the vertebrate dorsal central nervous system. Dev Biol 277:287-295.2005).

Choi EJ, Wong ST, Hinds TR, Storm DR (Calcium and muscarinic agonist stimulation of type I adenylylcyclase in whole cells. J Biol Chem 267:12440-12442.1992).

Chuang PT, McMahon AP (Vertebrate Hedgehog signalling modulated by induction of a Hedgehog-binding protein. Nature 397:617-621.1999).

Connor RM, Allen CL, Devine CA, Claxton C, Key B (BOC, brother of CDO, is a dorsoventral axon-guidance molecule in the embryonic vertebrate brain. J Comp Neurol 485:32-42.2005).

Conrad S, Genth H, Hofmann F, Just I, Skutella T (Neogenin-RGMa signaling at the growth cone is bone morphogenetic protein-independent and involves RhoA, ROCK, and PKC. J Biol Chem 282:16423-16433.2007).

Dedhar S, Williams B, Hannigan G (Integrin-linked kinase (ILK): a regulator of integrin and growth-factor signalling. Trends Cell Biol 9:319-323.1999).

Delcommenne M, Tan C, Gray V, Rue L, Woodgett J, Dedhar S (Phosphoinositide-3-OH kinase-dependent regulation of glycogen synthase kinase 3 and protein kinase B/AKT by the integrin-linked kinase. Proc Natl Acad Sci U S A 95:11211-11216.1998).

Dempsey EC, Newton AC, Mochly-Rosen D, Fields AP, Reyland ME, Insel PA, Messing RO (Protein kinase C isozymes and the regulation of diverse cell responses. Am J Physiol Lung Cell Mol Physiol 279:L429-438.2000).

Dent EW, Gertler FB (Cytoskeletal dynamics and transport in growth cone motility and axon guidance. Neuron 40:209-227.2003).

Dharmawardhane S, Schurmann A, Sells MA, Chernoff J, Schmid SL, Bokoch GM (Regulation of macropinocytosis by p21-activated kinase-1. Mol Biol Cell 11:3341-3352.2000).

Disatnik MH, Buraggi G, Mochly-Rosen D (Localization of protein kinase C isozymes in cardiac myocytes. Exp Cell Res 210:287-297.1994).

Driessens MH, Olivo C, Nagata K, Inagaki M, Collard JG (B plexins activate Rho through PDZ-RhoGEF. FEBS Lett 529:168-172.2002).

Edwards DC, Sanders LC, Bokoch GM, Gill GN (Activation of LIM-kinase by Pak1 couples Rac/Cdc42 GTPase signalling to actin cytoskeletal dynamics. Nat Cell Biol 1:253-259.1999).

Elia D, Madhala D, Ardon E, Reshef R, Halevy O (Sonic hedgehog promotes proliferation and differentiation of adult muscle cells: Involvement of MAPK/ERK and PI3K/Akt pathways. Biochim Biophys Acta 1773:1438-1446.2007).

Engle EC (Human genetic disorders of axon guidance. Cold Spring Harb Perspect Biol 2:a001784.2010).

Ensslen SE, Brady-Kalnay SM (PTPmu signaling via PKCdelta is instructive for retinal ganglion cell guidance. Mol Cell Neurosci 25:558-571.2004).

Epstein DJ, Marti E, Scott MP, McMahon AP (Antagonizing cAMP-dependent protein kinase A in the dorsal CNS activates a conserved Sonic hedgehog signaling pathway. Development 122:2885-2894.1996).

Erskine L, Williams SE, Brose K, Kidd T, Rachel RA, Goodman CS, Tessier-Lavigne M, Mason CA (Retinal ganglion cell axon guidance in the mouse optic chiasm: expression and function of robos and slits. J Neurosci 20:4975-4982.2000).

Fabre PJ, Shimogori T, Charron F (Segregation of ipsilateral retinal ganglion cell axons at the optic chiasm requires the Shh receptor Boc. J Neurosci 30:266-275.2010).

Fan X, Labrador JP, Hing H, Bashaw GJ (Slit stimulation recruits Dock and Pak to the roundabout receptor and increases Rac activity to regulate axon repulsion at the CNS midline. Neuron 40:113-127.2003).

Fan Y, Gong Y, Ghosh PK, Graham LM, Fox PL (Spatial coordination of actin polymerization and ILK-Akt2 activity during endothelial cell migration. Dev Cell 16:661-674.2009).

Fielding AB, Dobreva I, McDonald PC, Foster LJ, Dedhar S (Integrin-linked kinase localizes to the centrosome and regulates mitotic spindle organization. J Cell Biol 180:681-689.2008).

Fielding AB, Lim S, Montgomery K, Dobreva I, Dedhar S (A critical role of integrin-linked kinase, ch-TOG and TACC3 in centrosome clustering in cancer cells. Oncogene 30:521-534.2011).

Filipenko NR, Attwell S, Roskelley C, Dedhar S (Integrin-linked kinase activity regulates Rac- and Cdc42-mediated actin cytoskeleton reorganization via alpha-PIX. Oncogene 24:5837-5849.2005).

Flanagan JG (Neural map specification by gradients. Curr Opin Neurobiol 16:59-66.2006).

Fukuda K, Gupta S, Chen K, Wu C, Qin J (The pseudoactive site of ILK is essential for its binding to alpha-Parvin and localization to focal adhesions. Mol Cell 36:819-830.2009).

Fukuda T, Chen K, Shi X, Wu C (PINCH-1 is an obligate partner of integrin-linked kinase (ILK) functioning in cell shape modulation, motility, and survival. J Biol Chem 278:51324-51333.2003).

Giger RJ, Hollis ER, 2nd, Tuszynski MH (Guidance molecules in axon regeneration. Cold Spring Harb Perspect Biol 2:a001867.2010).

Ginnan R, Pfleiderer PJ, Pumiglia K, Singer HA (PKC-delta and CaMKII-delta 2 mediate ATP-dependent activation of ERK1/2 in vascular smooth muscle. Am J Physiol Cell Physiol 286:C1281-1289.2004).

Gitai Z, Yu TW, Lundquist EA, Tessier-Lavigne M, Bargmann CI (The netrin receptor UNC-40/DCC stimulates axon attraction and outgrowth through enabled and, in parallel, Rac and UNC-115/AbLIM. Neuron 37:53-65.2003).

Goldberg S, Coulombre AJ (Topographical development of the ganglion cell fiber layer in the chick retina. A whole mount study. J Comp Neurol 146:507-518.1972).

Gomez TM, Zheng JQ (The molecular basis for calcium-dependent axon pathfinding. Nat Rev Neurosci 7:115-125.2006).

Goodnight JA, Mischak H, Kolch W, Mushinski JF (Immunocytochemical localization of eight protein kinase C isozymes overexpressed in NIH 3T3 fibroblasts. Isoform-specific association with microfilaments, Golgi, endoplasmic reticulum, and nuclear and cell membranes. J Biol Chem 270:9991-10001.1995).

Grashoff C, Aszodi A, Sakai T, Hunziker EB, Fassler R (Integrin-linked kinase regulates chondrocyte shape and proliferation. EMBO Rep 4:432-438.2003).

Grimmer S, van Deurs B, Sandvig K (Membrane ruffling and macropinocytosis in A431 cells require cholesterol. J Cell Sci 115:2953-2962.2002).

Guirland C, Buck KB, Gibney JA, DiCicco-Bloom E, Zheng JQ (Direct cAMP signaling through G-protein-coupled receptors mediates growth cone attraction induced by pituitary adenylate cyclase-activating polypeptide. J Neurosci 23:2274-2283.2003).

Guo W, Jiang H, Gray V, Dedhar S, Rao Y (Role of the integrin-linked kinase (ILK) in determining neuronal polarity. Developmental Biology 306:457-468.2007a).

Guo W, Jiang H, Gray V, Dedhar S, Rao Y (Role of the integrin-linked kinase (ILK) in determining neuronal polarity. Dev Biol 306:457-468.2007b).

Hall A, Lalli G (Rho and Ras GTPases in axon growth, guidance, and branching. Cold Spring Harb Perspect Biol 2:a001818.2010).

Hammerschmidt M, Bitgood MJ, McMahon AP (Protein kinase A is a common negative regulator of Hedgehog signaling in the vertebrate embryo. Genes Dev 10:647-658.1996).

Hanks SK, Quinn AM, Hunter T (The protein kinase family: conserved features and deduced phylogeny of the catalytic domains. Science 241:42-52.1988).

Hannigan G, Troussard AA, Dedhar S (Integrin-linked kinase: a cancer therapeutic target unique among its ILK. Nat Rev Cancer 5:51-63.2005).

Hannigan GE, Leung-Hagesteijn C, Fitz-Gibbon L, Coppolino MG, Radeva G, Filmus J, Bell JC, Dedhar S (Regulation of cell adhesion and anchorage-dependent growth by a new beta 1-integrin-linked protein kinase. Nature 379:91-96.1996).

Henley JR, Huang KH, Wang D, Poo MM (Calcium mediates bidirectional growth cone turning induced by myelin-associated glycoprotein. Neuron 44:909-916.2004).

Hines JH, Abu-Rub M, Henley JR (Asymmetric endocytosis and remodeling of beta1-integrin adhesions during growth cone chemorepulsion by MAG. Nat Neurosci 13:829-837.2010).

Hirose M, Ishizaki T, Watanabe N, Uehata M, Kranenburg O, Moolenaar WH, Matsumura F, Maekawa M, Bito H, Narumiya S (Molecular dissection of the

Rho-associated protein kinase (p160ROCK)-regulated neurite remodeling in neuroblastoma N1E-115 cells. J Cell Biol 141:1625-1636.1998).

Hong K, Hinck L, Nishiyama M, Poo MM, Tessier-Lavigne M, Stein E (A ligand-gated association between cytoplasmic domains of UNC5 and DCC family receptors converts netrin-induced growth cone attraction to repulsion. Cell 97:927-941.1999).

Hong K, Nishiyama M, Henley J, Tessier-Lavigne M, Poo M (Calcium signalling in the guidance of nerve growth by netrin-1. Nature 403:93-98.2000).

Hopker VH, Shewan D, Tessier-Lavigne M, Poo M, Holt C (Growth-cone attraction to netrin-1 is converted to repulsion by laminin-1. Nature 401:69-73.1999).

Ishii T, Satoh E, Nishimura M (Integrin-linked kinase controls neurite outgrowth in N1E-115 neuroblastoma cells. Journal of Biological Chemistry 276:42994-43003.2001).

Ishizaki T, Uehata M, Tamechika I, Keel J, Nonomura K, Maekawa M, Narumiya S (Pharmacological properties of Y-27632, a specific inhibitor of rho-associated kinases. Mol Pharmacol 57:976-983.2000).

Jalink K, van Corven EJ, Hengeveld T, Morii N, Narumiya S, Moolenaar WH (Inhibition of lysophosphatidate- and thrombin-induced neurite retraction and neuronal cell rounding by ADP ribosylation of the small GTP-binding protein Rho. J Cell Biol 126:801-810.1994).

Jaskolski F, Mulle C, Manzoni OJ (An automated method to quantify and visualize colocalized fluorescent signals. J Neurosci Methods 146:42-49.2005).

Jeffery G, Erskine L (Variations in the architecture and development of the vertebrate optic chiasm. Prog Retin Eye Res 24:721-753.2005).

Jenkins D (Hedgehog signalling: emerging evidence for non-canonical pathways. Cell Signal 21:1023-1034.2009).

Jin M, Guan CB, Jiang YA, Chen G, Zhao CT, Cui K, Song YQ, Wu CP, Poo MM, Yuan XB (Ca2+-dependent regulation of rho GTPases triggers turning of nerve growth cones. J Neurosci 25:2338-2347.2005).

Jin Z, Zhang J, Klar A, Chedotal A, Rao Y, Cepko CL, Bao ZZ (Irx4-mediated regulation of Slit1 expression contributes to the definition of early axonal paths inside the retina. Development 130:1037-1048.2003).

Jones-Villeneuve EM, McBurney MW, Rogers KA, Kalnins VI (Retinoic acid induces embryonal carcinoma cells to differentiate into neurons and glial cells. J Cell Biol 94:253-262.1982).

Jones AT (Macropinocytosis: searching for an endocytic identity and role in the uptake of cell penetrating peptides. J Cell Mol Med 11:670-684.2007).

Karpen HE, Bukowski JT, Hughes T, Gratton JP, Sessa WC, Gailani MR (The sonic hedgehog receptor patched associates with caveolin-1 in cholesterol-rich microdomains of the plasma membrane. J Biol Chem 276:19503-19511.2001).

Kasai K, Takahashi M, Osumi N, Sinnarajah S, Takeo T, Ikeda H, Kehrl JH, Itoh G, Arnheiter H (The G12 family of heterotrimeric G proteins and Rho GTPase mediate Sonic hedgehog signalling. Genes Cells 9:49-58.2004).

Kennedy TE, Wang H, Marshall W, Tessier-Lavigne M (Axon guidance by diffusible chemoattractants: a gradient of netrin protein in the developing spinal cord. J Neurosci 26:8866-8874.2006).

Kim JH, Han JM, Lee S, Kim Y, Lee TG, Park JB, Lee SD, Suh PG, Ryu SH (Phospholipase D1 in caveolae: regulation by protein kinase Calpha and caveolin-1. Biochemistry 38:3763-3769.1999).

Kim JY, Lee MJ, Cho KW, Lee JM, Kim YJ, Jung HI, Cho JY, Cho SW, Jung HS (Shh and ROCK1 modulate the dynamic epithelial morphogenesis in circumvallate papilla development. Dev Biol 325:273-280.2009).

Kimura K, Ito M, Amano M, Chihara K, Fukata Y, Nakafuku M, Yamamori B, Feng J, Nakano T, Okawa K, Iwamatsu A, Kaibuchi K (Regulation of myosin phosphatase by Rho and Rho-associated kinase (Rho-kinase). Science 273:245-248.1996).

Klein R (Axon guidance: opposing EPHects in the growth cone. Cell 121:4-6.2005).

Kolpak A, Zhang J, Bao ZZ (Sonic hedgehog has a dual effect on the growth of retinal ganglion axons depending on its concentration. J Neurosci 25:3432-3441.2005).

Kolpak AL, Jiang J, Guo D, Standley C, Bellve K, Fogarty K, Bao ZZ (Negative guidance factor-induced macropinocytosis in the growth cone plays a critical role in repulsive axon turning. J Neurosci 29:10488-10498.2009).

Kumar AS, Naruszewicz I, Wang P, Leung-Hagesteijn C, Hannigan GE (ILKAP regulates ILK signaling and inhibits anchorage-independent growth. Oncogene 23:3454-3461.2004).

Lange A, Wickstrom SA, Jakobson M, Zent R, Sainio K, Fassler R (Integrin-linked kinase is an adaptor with essential functions during mouse development. Nature 461:1002-1006.2009).

Larsson C (Protein Kinase C and the refulation of the actin cytoskeleton. Cellular Signaling 18: 276-284. 2006)

Laux T, Fukami K, Thelen M, Golub T, Frey D, Caroni P (GAP43, MARCKS, and CAP23 modulate PI(4,5)P(2) at plasmalemmal rafts, and regulate cell cortex actin dynamics through a common mechanism. J Cell Biol 149:1455-1472.2000).

Lee CS, Buttitta L, Fan CM (Evidence that the WNT-inducible growth arrest-specific gene 1 encodes an antagonist of sonic hedgehog signaling in the somite. Proc Natl Acad Sci U S A 98:11347-11352.2001).

Legate KR, Montanez E, Kudlacek O, Fassler R (ILK, PINCH and parvin: the tIPP of integrin signalling. Nat Rev Mol Cell Biol 7:20-31.2006).

Li X, Saint-Cyr-Proulx E, Aktories K, Lamarche-Vane N (Rac1 and Cdc42 but not RhoA or Rho kinase activities are required for neurite outgrowth induced by the Netrin-1 receptor DCC (deleted in colorectal cancer) in N1E-115 neuroblastoma cells. J Biol Chem 277:15207-15214.2002).

Lin CH, Espreafico EM, Mooseker MS, Forscher P (Myosin drives retrograde F-actin flow in neuronal growth cones. Neuron 16:769-782.1996).

Linding R, Jensen LJ, Ostheimer GJ, van Vugt MA, Jorgensen C, Miron IM, Diella F, Colwill K, Taylor L, Elder K, Metalnikov P, Nguyen V, Pasculescu A, Jin J, Park JG, Samson LD, Woodgett JR, Russell RB, Bork P, Yaffe MB, Pawson T (Systematic discovery of in vivo phosphorylation networks. Cell 129:1415-1426.2007).

Liu BP, Strittmatter SM (Semaphorin-mediated axonal guidance via Rho-related G proteins. Curr Opin Cell Biol 13:619-626.2001).

Liu Y, Shi J, Lu CC, Wang ZB, Lyuksyutova AI, Song XJ, Zou Y (Ryk-mediated Wnt repulsion regulates posterior-directed growth of corticospinal tract. Nat Neurosci 8:1151-1159.2005).

Lowery LA, Van Vactor D (The trip of the tip: understanding the growth cone machinery. Nat Rev Mol Cell Biol 10:332-343.2009).

Lundstrom A, Gallio M, Englund C, Steneberg P, Hemphala J, Aspenstrom P, Keleman K, Falileeva L, Dickson BJ, Samakovlis C (Vilse, a conserved Rac/Cdc42 GAP mediating Robo repulsion in tracheal cells and axons. Genes Dev 18:2161-2171.2004).

Lyuksyutova AI, Lu CC, Milanesio N, King LA, Guo N, Wang Y, Nathans J, Tessier-Lavigne M, Zou Y (Anterior-posterior guidance of commissural axons by Wnt-frizzled signaling. Science 302:1984-1988.2003).

Ma HT, Lin WW, Zhao B, Wu WT, Huang W, Li Y, Jones NL, Kruth HS (Protein kinase C beta and delta isoenzymes mediate cholesterol accumulation in PMA-activated macrophages. Biochem Biophys Res Commun 349:214-220.2006).

Mackinnon AC, Qadota H, Norman KR, Moerman DG, Williams BD (C. elegans PAT-4/ILK functions as an adaptor protein within integrin adhesion complexes. Curr Biol 12:787-797.2002).

Madigan JP, Bodemann BO, Brady DC, Dewar BJ, Keller PJ, Leitges M, Philips MR, Ridley AJ, Der CJ, Cox AD (Regulation of Rnd3 localization and function by protein kinase C alpha-mediated phosphorylation. Biochem J 424:153-161.2009).

Manser E, Leung T, Salihuddin H, Zhao ZS, Lim L (A brain serine/threonine protein kinase activated by Cdc42 and Rac1. Nature 367:40-46.1994).

Marcus RC, Mason CA (The first retinal axon growth in the mouse optic chiasm: axon patterning and the cellular environment. J Neurosci 15:6389-6402.1995).

Martiny-Baron G, Kazanietz MG, Mischak H, Blumberg PM, Kochs G, Hug H, Marme D, Schachtele C (Selective inhibition of protein kinase C isozymes by the indolocarbazole Go 6976. J Biol Chem 268:9194-9197.1993).

McCarthy RA, Barth JL, Chintalapudi MR, Knaak C, Argraves WS (Megalin functions as an endocytic sonic hedgehog receptor. J Biol Chem 277:25660-25667.2002).

Mehta D, Rahman A, Malik AB (Protein kinase C-alpha signals rho-guanine nucleotide dissociation inhibitor phosphorylation and rho activation and regulates the endothelial cell barrier function. J Biol Chem 276:22614-22620.2001).

Meier O, Boucke K, Hammer SV, Keller S, Stidwill RP, Hemmi S, Greber UF (Adenovirus triggers macropinocytosis and endosomal leakage together with its clathrin-mediated uptake. J Cell Biol 158:1119-1131.2002).

Mikule K, Sunpaweravong S, Gatlin JC, Pfenninger KH (Eicosanoid activation of protein kinase C epsilon: involvement in growth cone repellent signaling. J Biol Chem 278:21168-21177.2003).

Mills J, Digicaylioglu M, Legg AT, Young CE, Young SS, Barr AM, Fletcher L, O'Connor TP, Dedhar S (Role of integrin-linked kinase in nerve growth factor-stimulated neurite outgrowth. J Neurosci 23:1638-1648.2003).

Ming GL, Song HJ, Berninger B, Holt CE, Tessier-Lavigne M, Poo MM (cAMP-dependent growth cone guidance by netrin-1. Neuron 19:1225-1235.1997).

Mishima W, Suzuki A, Yamaji S, Yoshimi R, Ueda A, Kaneko T, Tanaka J, Miwa Y, Ohno S, Ishigatsubo Y (The first CH domain of affixin activates Cdc42 and Rac1

through alphaPIX, a Cdc42/Rac1-specific guanine nucleotide exchanging factor. Genes Cells 9:193-204.2004).

Mogami H, Zhang H, Suzuki Y, Urano T, Saito N, Kojima I, Petersen OH (Decoding of short-lived Ca2+ influx signals into long term substrate phosphorylation through activation of two distinct classes of protein kinase C. J Biol Chem 278:9896-9904.2003).

Montanez E, Wickstrom SA, Altstatter J, Chu H, Fassler R (Alpha-parvin controls vascular mural cell recruitment to vessel wall by regulating RhoA/ROCK signalling. EMBO J 28:3132-3144.2009).

Muranyi A, MacDonald JA, Deng JT, Wilson DP, Haystead TA, Walsh MP, Erdodi F, Kiss E, Wu Y, Hartshorne DJ (Phosphorylation of the myosin phosphatase target subunit by integrin-linked kinase. Biochem J 366:211-216.2002).

Nakagawa S, Brennan C, Johnson KG, Shewan D, Harris WA, Holt CE (Ephrin-B regulates the Ipsilateral routing of retinal axons at the optic chiasm. Neuron 25:599-610.2000).

Newton AC (Protein kinase C: structure, function, and regulation. J Biol Chem 270:28495-28498.1995).

Nishiyama M, Hoshino A, Tsai L, Henley JR, Goshima Y, Tessier-Lavigne M, Poo MM, Hong K (Cyclic AMP/GMP-dependent modulation of Ca2+ channels sets the polarity of nerve growth-cone turning. Nature 423:990-995.2003).

Nybakken K, Perrimon N (Hedgehog signal transduction: recent findings. Curr Opin Genet Dev 12:503-511.2002).

O'Donnell M, Chance RK, Bashaw GJ (Axon growth and guidance: receptor regulation and signal transduction. Annu Rev Neurosci 32:383-412.2009).

O'Leary DM, Gerfen CR, Cowan WM (The development and restriction of the ipsilateral retinofugal projection in the chick. Brain Research 312:93-109.1983).

Oancea E, Meyer T (Protein kinase C as a molecular machine for decoding calcium and diacylglycerol signals. Cell 95:307-318.1998).

Ohno S, Konno Y, Akita Y, Yano A, Suzuki K (A point mutation at the putative ATP-binding site of protein kinase C alpha abolishes the kinase activity and renders it down-regulation-insensitive. A molecular link between autophosphorylation and down-regulation. J Biol Chem 265:6296-6300.1990).

Oinuma I, Katoh H, Negishi M (R-Ras controls axon specification upstream of glycogen synthase kinase-3beta through integrin-linked kinase. J Biol Chem 282:303-318.2007).

Okada A, Charron F, Morin S, Shin DS, Wong K, Fabre PJ, Tessier-Lavigne M, McConnell SK (Boc is a receptor for sonic hedgehog in the guidance of commissural axons. Nature 444:369-373.2006).

Osawa H, Ohnishi H, Takano K, Noguti T, Mashima H, Hoshino H, Kita H, Sato K, Matsui H, Sugano K (Sonic hedgehog stimulates the proliferation of rat gastric mucosal cells through ERK activation by elevating intracellular calcium concentration. Biochem Biophys Res Commun 344:680-687.2006).

Pang H, Bitar KN (Direct association of RhoA with specific domains of PKC-alpha. Am J Physiol Cell Physiol 289:C982-993.2005).

Patten I, Placzek M (The role of Sonic hedgehog in neural tube patterning. Cell Mol Life Sci 57:1695-1708.2000).

Persad S, Attwell S, Gray V, Mawji N, Deng JT, Leung D, Yan J, Sanghera J, Walsh MP, Dedhar S (Regulation of protein kinase B/Akt-serine 473 phosphorylation by integrin-linked kinase: critical roles for kinase activity and amino acids arginine 211 and serine 343. J Biol Chem 276:27462-27469.2001).

Petros TJ, Bryson JB, Mason C (Ephrin-B2 elicits differential growth cone collapse and axon retraction in retinal ganglion cells from distinct retinal regions. Dev Neurobiol 70:781-794.2010).

Pike LJ (The challenge of lipid rafts. J Lipid Res 50 Suppl:S323-328.2009).

Plump AS, Erskine L, Sabatier C, Brose K, Epstein CJ, Goodman CS, Mason CA, Tessier-Lavigne M (Slit1 and Slit2 cooperate to prevent premature midline crossing of retinal axons in the mouse visual system. Neuron 33:219-232.2002).

Prada C, Puga J, Perez-Mendez L, Lopez, Ramirez G (Spatial and Temporal Patterns of Neurogenesis in the Chick Retina. Eur J Neurosci 3:1187.1991).

Qian Y, Zhong X, Flynn DC, Zheng JZ, Qiao M, Wu C, Dedhar S, Shi X, Jiang BH (ILK mediates actin filament rearrangements and cell migration and invasion through PI3K/Akt/Rac1 signaling. Oncogene 24:3154-3165.2005).

Raftopoulou M, Hall A (Cell migration: Rho GTPases lead the way. Dev Biol 265:23-32.2004).

Renault MA, Roncalli J, Tongers J, Thorne T, Klyachko E, Misener S, Volpert OV, Mehta S, Burg A, Luedemann C, Qin G, Kishore R, Losordo DW (Sonic hedgehog induces angiogenesis via Rho kinase-dependent signaling in endothelial cells. J Mol Cell Cardiol 49:490-498.2010).

Ribes V, Briscoe J (Establishing and interpreting graded Sonic Hedgehog signaling during vertebrate neural tube patterning: the role of negative feedback. Cold Spring Harb Perspect Biol 1:a002014.2009).

Ridley AJ (Rho GTPases and cell migration. J Cell Sci 114:2713-2722.2001).

Riobo NA, Haines GM, Emerson CP, Jr. (Protein kinase C-delta and mitogen-activated protein/extracellular signal-regulated kinase-1 control GLI activation in hedgehog signaling. Cancer Res 66:839-845.2006a).

Riobo NA, Lu K, Ai X, Haines GM, Emerson CP, Jr. (Phosphoinositide 3-kinase and Akt are essential for Sonic Hedgehog signaling. Proc Natl Acad Sci U S A 103:4505-4510.2006b).

Rohatgi R, Ma L, Miki H, Lopez M, Kirchhausen T, Takenawa T, Kirschner MW (The interaction between N-WASP and the Arp2/3 complex links Cdc42-dependent signals to actin assembly. Cell 97:221-231.1999).

Ron D, Luo J, Mochly-Rosen D (C2 region-derived peptides inhibit translocation and function of beta protein kinase C in vivo. J Biol Chem 270:24180-24187.1995).

Rosse C, Linch M, Kermorgant S, Cameron AJ, Boeckeler K, Parker PJ (PKC and the control of localized signal dynamics. Nat Rev Mol Cell Biol 11:103-112.2010).

Sakai JA, Halloran MC (Semaphorin 3d guides laterality of retinal ganglion cell projections in zebrafish. Development 133:1035-1044.2006).

Sakai T, Li S, Docheva D, Grashoff C, Sakai K, Kostka G, Braun A, Pfeifer A, Yurchenco PD, Fassler R (Integrin-linked kinase (ILK) is required for polarizing the epiblast, cell adhesion, and controlling actin accumulation. Genes Dev 17:926-940.2003).

Sanchez-Camacho C, Bovolenta P (Autonomous and non-autonomous Shh signalling mediate the in vivo growth and guidance of mouse retinal ganglion cell axons. Development 135:3531-3541.2008).

Sanchez-Camacho C, Bovolenta P (Emerging mechanisms in morphogen-mediated axon guidance. Bioessays 31:1013-1025.2009).

Sanders LC, Matsumura F, Bokoch GM, de Lanerolle P (Inhibition of myosin light chain kinase by p21-activated kinase. Science 283:2083-2085.1999).

Sarkar K, Kruhlak MJ, Erlandsen SL, Shaw S (Selective inhibition by rottlerin of macropinocytosis in monocyte-derived dendritic cells. Immunology 116:513-524.2005).

Sculptoreanu A, Scheuer T, Catterall WA (Voltage-dependent potentiation of L-type Ca2+ channels due to phosphorylation by cAMP-dependent protein kinase. Nature 364:240-243.1993).

Sehr P, Joseph G, Genth H, Just I, Pick E, Aktories K (Glucosylation and ADP ribosylation of rho proteins: effects on nucleotide binding, GTPase activity, and effector coupling. Biochemistry 37:5296-5304.1998).

Shirai Y, Saito N (Activation mechanisms of protein kinase C: maturation, catalytic activation, and targeting. J Biochem 132:663-668.2002).

Slater SJ, Seiz JL, Stagliano BA, Stubbs CD (Interaction of protein kinase C isozymes with Rho GTPases. Biochemistry 40:4437-4445.2001).

Soh JW, Weinstein IB (Roles of specific isoforms of protein kinase C in the transcriptional control of cyclin D1 and related genes. J Biol Chem 278:34709-34716.2003).

Song H, Ming G, He Z, Lehmann M, McKerracher L, Tessier-Lavigne M, Poo M (Conversion of neuronal growth cone responses from repulsion to attraction by cyclic nucleotides. Science 281:1515-1518.1998).

Song HJ, Ming GL, Poo MM (cAMP-induced switching in turning direction of nerve growth cones. Nature 388:275-279.1997).

Steinberg SF (Structural basis of protein kinase C isoform function. Physiol Rev 88:1341-1378.2008).

Swanson JA (Shaping cups into phagosomes and macropinosomes. Nat Rev Mol Cell Biol 9:639-649.2008).

Tenzen T, Allen BL, Cole F, Kang JS, Krauss RS, McMahon AP (The cell surface membrane proteins Cdo and Boc are components and targets of the Hedgehog signaling pathway and feedback network in mice. Dev Cell 10:647-656.2006).

Tojima T, Akiyama H, Itofusa R, Li Y, Katayama H, Miyawaki A, Kamiguchi H (Attractive axon guidance involves asymmetric membrane transport and exocytosis in the growth cone. Nat Neurosci 10:58-66.2007).

Tojima T, Itofusa R, Kamiguchi H (Asymmetric clathrin-mediated endocytosis drives repulsive growth cone guidance. Neuron 66:370-377.2010).

Toyofuku T, Yoshida J, Sugimoto T, Zhang H, Kumanogoh A, Hori M, Kikutani H (FARP2 triggers signals for Sema3A-mediated axonal repulsion. Nat Neurosci 8:1712-1719.2005).

Trousse F, Marti E, Gruss P, Torres M, Bovolenta P (Control of retinal ganglion cell axon growth: a new role for Sonic hedgehog. Development 128:3927-3936.2001).

Van Vactor D (Adhesion and signaling in axonal fasciculation. Curr Opin Neurobiol 8:80-86.1998).

Vespa A, Darmon AJ, Turner CE, D'Souza SJ, Dagnino L (Ca2+-dependent localization of integrin-linked kinase to cell junctions in differentiating keratinocytes. J Biol Chem 278:11528-11535.2003).

Wahl S, Barth H, Ciossek T, Aktories K, Mueller BK (Ephrin-A5 induces collapse of growth cones by activating Rho and Rho kinase. J Cell Biol 149:263-270.2000).

Wickstrom SA, Lange A, Montanez E, Fassler R (The ILK/PINCH/parvin complex: the kinase is dead, long live the pseudokinase! EMBO J 29:281-291.2010).

Williams SE, Mann F, Erskine L, Sakurai T, Wei S, Rossi DJ, Gale NW, Holt CE, Mason CA, Henkemeyer M (Ephrin-B2 and EphB1 mediate retinal axon divergence at the optic chiasm. Neuron 39:919-935.2003).

Wolf AM, Lyuksyutova AI, Fenstermaker AG, Shafer B, Lo CG, Zou Y (Phosphatidylinositol-3-kinase-atypical protein kinase C signaling is required for Wnt attraction and anterior-posterior axon guidance. J Neurosci 28:3456-3467.2008).

Wong EV, Kerner JA, Jay DG (Convergent and divergent signaling mechanisms of growth cone collapse by ephrinA5 and slit2. J Neurobiol 59:66-81.2004).

Wong K, Ren XR, Huang YZ, Xie Y, Liu G, Saito H, Tang H, Wen L, Brady-Kalnay SM, Mei L, Wu JY, Xiong WC, Rao Y (Signal transduction in neuronal migration: roles of GTPase activating proteins and the small GTPase Cdc42 in the Slit-Robo pathway. Cell 107:209-221.2001).

Wu DY, Zheng JQ, McDonald MA, Chang B, Twiss JL (PKC isozymes in the enhanced regrowth of retinal neurites after optic nerve injury. Invest Ophthalmol Vis Sci 44:2783-2790.2003).

Xiang Y, Li Y, Zhang Z, Cui K, Wang S, Yuan XB, Wu CP, Poo MM, Duan S (Nerve growth cone guidance mediated by G protein-coupled receptors. Nat Neurosci 5:843-848.2002).

Xu L, Shen Y, Joseph T, Bryant A, Luo JQ, Frankel P, Rotunda T, Foster DA (Mitogenic phospholipase D activity is restricted to caveolin-enriched membrane microdomains. Biochem Biophys Res Commun 273:77-83.2000).

Yam PT, Langlois SD, Morin S, Charron F (Sonic hedgehog guides axons through a noncanonical, Src-family-kinase-dependent signaling pathway. Neuron 62:349-362.2009).

Yuan XB, Jin M, Xu X, Song YQ, Wu CP, Poo MM, Duan S (Signalling and crosstalk of Rho GTPases in mediating axon guidance. Nat Cell Biol 5:38-45.2003).

Yukawa K, Tanaka T, Bai T, Ueyama T, Owada-Makabe K, Tsubota Y, Maeda M, Suzuki K, Kikutani H, Kumanogoh A (Semaphorin 4A induces growth cone collapse of hippocampal neurons in a Rho/Rho-kinase-dependent manner. Int J Mol Med 16:115-118.2005).

Zervas CG, Gregory SL, Brown NH (Drosophila integrin-linked kinase is required at sites of integrin adhesion to link the cytoskeleton to the plasma membrane. J Cell Biol 152:1007-1018.2001).

Zhang J, Jin Z, Bao ZZ (Disruption of gradient expression of Zic3 resulted in abnormal intra-retinal axon projection. Development 131:1553-1562.2004).

Zhang W, Kang JS, Cole F, Yi MJ, Krauss RS (Cdo functions at multiple points in the Sonic Hedgehog pathway, and Cdo-deficient mice accurately model human holoprosencephaly. Dev Cell 10:657-665.2006).

Zheng JQ (Turning of nerve growth cones induced by localized increases in intracellular calcium ions. Nature 403:89-93.2000).

Zhou FQ, Cohan CS (Growth cone collapse through coincident loss of actin bundles and leading edge actin without actin depolymerization. J Cell Biol 153:1071-1084.2001).